UNIVERSITY OF NAPLES FEDERICO II

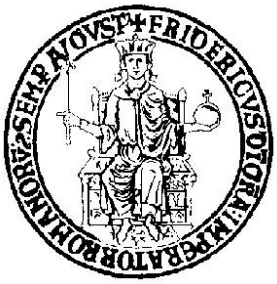

Doctoral School of Hydraulic, Transportation and Urban Planning Engineering

Doctoral Thesis

Driving behaviour for ADAS: theoretical and experimental analyses

Luigi Pariota

Dean of the doctoral school:
Prof. Arch. Elvira Petroncelli

Tutor:
Prof. Ing. Gennaro Nicola Bifulco

Acknowledgments

My first thought is dedicated to Cino, my supervisor. He has often left me free to follow my interests and ideas, as well as he has been ready to provide an authoritative and wise guidance in moments of uncertainty. Thank you for all!

I would also like to acknowledge members of my Department that have given me the possibility to discuss with them and to learn from them; in particular I would like to thank Francesco and Roberta.

I am also very grateful to people I met in Southampton! They gave me the possibility to live a great training time, they shared with me data, knowledge and experience. Brian, Eddie, Mark, Mike and Neville (strictly in alphabetical order!) thanks to all you!

I'll be eternally grateful to my parents that have given me the possibility to stay here now.

The final acknowledgment is for my wife, Anna. With her by my side I am a better man. Hers tenacity represents a reference point for me and being her husband makes me feel proud and motivated every day.

All the people I mentioned demonstrate to trust in me every day. I hope to always comply with of your expectations.

Overview

This thesis deals with the analysis and understanding of drivers' behaviours under car-following. The aim is to enhance the modelling tools toward the development of new ADAS (Advanced Driving Assistance System) logics, characterized by a more human-like behaviour. After having introduced the argument of the thesis (and motivated the work) and having recalled the state of the art most relevant in the field of car-following (as well as in the instruments for observing car-following in the real world), the thesis evolves toward three main sections: actual observation of real-world data and collection of the datasets to be employed for theoretical analysis; theoretical enhancements and propositions; applications to ACC (Adaptive Cruise Control), as a relevant field for ADAS.

The data employed in this work have been collected in three different field surveys, two of them carried out in Italy and the other in the United Kingdom. In all cases data have been collected by instrumented vehicles, equipped in such a way to observe and record car-following trajectories. Data have been framed into different theoretical paradigms in order to both validate each theory and to establish the links between these theories. Links have been established both in a formal way (through theoretical investigation) and in a data-driven way. The considered theoretical paradigm for modelling car-following follows different approaches: one is based on the psycho-physical approach and two others are based on an engineering-inspired approach. In particular, the considered psycho-physical approach has been the Action Point theory (Wiedemann, 1974); a revised version of the paradigm, more compliant with the original version of Barbosa (1961) and Todosoiev (1963) has been proposed and justified with reference to the collected data.

The first engineering paradigm has been based on a state-space approach. The proposed approach has been shown to be consistent with the Action Point theory. The parameters of the model have been estimated by means of the collected data and the obtained results have been discussed; they are consistent with observations and justify the adopted model. The other engineering model is based on a linear approximation (at any time t, in a discrete-time approach) of the response of the follower to the leader's stimuli. Also the linear model is shown to be a very good approximation of the observed data; moreover, it has been shown to lead to an harmonic oscillation around the desired spacing at steady-state. This oscillation is consistent with both the Action Point theory and (partially) with the proposed state-space approach. The linear model is particularly suitable for real-time ACC-oriented application; thus it is the model employed in section 4 of this work, where a fully-adaptive ACC system is developed, able to actuate a driving-style actually consistent with driver's expectations and preferences.

Index of Figures

Index of Tables

Table of contents

Introduction (and motivation)

Modelling driving behaviour represents a fundamental requirement in many transportation applications. Three main topics can particularly benefit from such studies: Accident Analysis and Prevention, Microscopic Simulation of Traffic and Intelligent Transportation Systems (ITS).

Accident analysis and prevention refers to methods and measures to reduce the risk of injury (or death) to road users, namely drivers, pedestrians, and private and public transport passengers. Road traffic safety conditions can be determined according to different approaches. One is based on statistical considerations and concerns identification of so-called *hotspots*, which are defined as accident-prone locations on the road, in the sense that a number of crashes higher than in other similar locations is observed there, probably due to local risk factors. Many methods have been set up to identify hotspots, several of which are compared by Montella (2010). The problem of such methods concerns the need to observe the "highest number of crashes", hence the need to identify the risk factors after several injuries or deaths have occurred. Another approach, based on statistical inference, analyses recurrent conditions in observed accidents in order to identify (un)safety factors related to various aspects, as the road geometry, road section, vehicle characteristics, the pavement, the weather (and other external) conditions and, of course, driving behaviour.

Safety evaluation can also be carried out by using so-called surrogate safety measures. The definition of such methods is somewhat vague, but basically the concept is that a surrogate measure should be based on an observable non-crash event, related predictably and reliably to crashes, which may in practice correspond to a crash frequency or severity (Tarko, 2009). In this context, the Time-to-Collision in a car-following process and observation of deceleration rates at intersections are examples of surrogate safety measures (Gettman and Head, 2003).

Microscopic models have been developed to improve the accuracy and quality of traffic flow studies, explicitly representing the interaction between single components of the traffic stream. Microscopic models can be defined with respect to any transportation system, but are probably most commonly found in the field of road transport. In these models the choices of each vehicle, in terms of spacing with respect to vehicles ahead, lane changing, gap-acceptance, etc., are modelled and driver and vehicle characteristics defined. In the previous context, the expression *driving behaviour* is very general, in the sense that observations of drivers' behaviours, needed to define drivers' characteristics, have to refer to several traffic situations, such as longitudinal driving, lane changing and behaviour at

intersections. A review of some of these models can be found in Toledo (2007), even if he asserted that, in the case of microscopic simulation models, calibrating models independently cannot capture interdependencies among decisions made by the same drivers over time and across decision dimensions; an attempt at a model that jointly explains acceleration decisions and lane-changing is provided in Toledo et al. (2009).

That said, it is common to focus research efforts on only a few components of driving behaviour that are believed to impact more upon the particular traffic analysis in hand or to be more affected by the dispersion of the behaviour or, also, that can be realistically studied with the available research tools. In particular, longitudinal driving is often divided into some sub-phases like free flow, approaching, car-following, emergency braking, and stop and go. Of these, the car-following process is believed in this thesis to be the most interesting sub-phase.

ITS are advanced applications that embody decision-making and/or operational intelligence in order to provide innovative services relating to different modes of transport and traffic management and allow users to make a safer, more efficient use of transport networks. The scientific community's interest in ITS has grown in recent years thanks to the increasing availability of information and communications technologies (ICT), both related to technological innovation and the decreasing cost of such technologies.

In the field of ITS, Advanced Driver Assistance Systems (ADAS) represent a real opportunity to both improve road safety and support efficient transportation systems, that are two often contrasting objectives able to induce economic and societal benefits. On the one hand, ADAS directly affect how vehicles interact with one another and thus, at a macroscopic level, may affect traffic flows and characteristics, while on the other hand, by directly controlling the driving task, driver errors can be reduced and reaction times shortened.

The development of these systems is not straightforward, and indeed many of the issues are now well known (see for example Van der Heijden and Marchau, 2005). Of great importance is to make sure that any proposed system considers driver expectation and behaviour and ensures there is a minimal mis-match between the system behaviour and the driver's normal behaviour, thus increasing driver acceptance. Indeed, an *ideal* ADAS system needs to be based on a good understanding of driver behaviour. At some driving tasks drivers are better than at others. For instance, they have relatively limited ability in perceiving the absolute value of longitudinal distances or absolute velocities, as well as in perceiving the absolute value of accelerations. Drivers are more able to perform good estimates of relative kinematics (spacing, relative velocity, etc.) with respect to other moving objects, thanks to their perception of visual angles subtended by objects and related

rates of change (Warren, 1995; Gray and Regan, 1998). An ideal ADAS should behave better than the driver in tasks in which he/she performs poorly and as well as the driver in tasks in which he/she performs better.

Of course, since driving behaviour is not always safe, an ADAS cannot simply reproduce it without controlling unsafe attitudes. The problem is addressed in Bonsall et al. (2005) with respect to several situations such as car following and lane changing. On the other hand, ADAS are in principle safer, although unsafe situations can still be caused by, for instance, Adaptive Cruise Control (ACC). Indeed, if vehicles cut in and there is sharp deceleration in the control system, one could induce a rear-end collision. Kesting (2008) describes this problem very well in his thesis. For these reasons, studies and models of driver behaviour under car following, as well as for other driving tasks, remain a crucial field of development in ADAS.

Several tools are available to observe driving behaviour and, as in many experimental fields, the proper choice of instrument should maximize the compromise between the aims, costs, feasibility and validity of the experiment. The first element that has to be taken into account regards the point of view from which the driver is observed during the experiment; drivers can be observed from *outside* and from *inside* the vehicle.

The first option refers to situations in which an unaware driver is monitored while driving on an instrumented site. Different technologies can be used for this purpose, even if the most suitable may well be the use of video cameras. Video cameras allow vehicles, via image processing algorithms, to be directly tracked. The whole trajectory of each vehicle of a traffic stream can be reconstructed. The accuracy of the obtained trajectories still is a debated issue. This method was recently employed in the Next Generation SIMulation program (NGSIM), which is a public-private project between the Federal Highway Administration of USA and several commercial micro-simulation software developers. The goal was to develop some driver behaviour models that would constitute the core background of commercial micro-simulation tools validated on the NGSIM dataset. The NGSIM data are public and available for all scientists from the project website (www.ngsim.fhwa.dot.gov).

An alternative approach to obtain motorway Individual Vehicle Data (IVD) was proposed in Wilson (2008). It is based on the use of data collected with an inductive loop detector. From loop detectors (especially double loops) it is possible to obtain an accurate estimate of vehicle speed, length and past time-instant. Loops are usually used in order to obtain averaged (the typical time interval is one minute) measures related to the traffic stream. In the approach proposed by Wilson, the main idea is not to average data but to record single detections. Using the speed

detected at an upstream double-loop detector, the arrival time of the vehicle at the downstream double-loop detector can be predicted; compatibly with the predicted arrival time at downstream the best-matching record is searched, using the detected vehicle's length to help matching. It is worth noting that the reliability of data is strictly related to the distance between detectors. The proposed method has been applied on data from the Motorway Incident Detection and Automatic Signalling (MIDAS), that consists of a distributed network of traffic sensors installed on several (highly congested) UK motorways. The main purpose of MIDAS is to enable mandatory variable speed limit signs as part of the controlled motorway scheme. In particular, the proposed IVD collecting method was applied for data from the M42 motorway near Birmingham, where the loops were installed in a very dense manner, that is with a nominal spacing of 100 m which decreases to 30 m in a 900 m section where queuing is common.

A great advantage of both the NGSIM and MIDAS cases concerns the huge amount of data that can be collected. The major disadvantage is that drivers can be observed only for a few seconds, on a limited portion of the instrumented site. Moreover, it is not possible to have information on the driver's characteristics and only combined drive-and-vehicle behaviour can be observed.

In order to obtain longer observations of drivers' behaviour, in addition to the possibility of benefiting from more flexible experimental conditions or making drivers execute manoeuvres of particular interest, it is possible to adopt the *inside* approach. In this case, the tools used have to focus more on the driver than on the infrastructure, and then the experimental point of view has to pass to a higher level of detail. Two instruments can be considered as optimal for these experiments, namely instrumented vehicles (IVs) and driving simulators (DSs). An instrumented vehicle, in a very simplistic definition, can be represented as a standard car whose kinematics is recorded in order to be analysed. Importantly, the possibility of observing only the kinematics of IVs can lead to a reduced understanding of driving behaviour, especially in situations where the drivers are largely influenced by the traffic. This is typical of car-following conditions, where the possibility of observing the relative kinematics of the IV with respect to the leader is a prerequisite. For this reason, IVs are usually equipped with a larger number of sensors, allowing detection of the surrounding traffic conditions, direct monitoring of the drivers and their interface with the car and on-board devices, and an improvement in the estimation of the kinematics of the IV itself. Of course, what is important in this framework is the ability to handle the previously large number of data and data-sources, including filtering and fusion techniques.

DSs have long been used by car manufacturers to test users' acceptability of on-board devices and human-vehicle interfaces. In recent years DSs have been

increasingly employed also in earlier conception phases, where the feasibility, effectiveness and safety of ADAS devices and solutions have to be assessed. Studies based on DSs provide a virtual experimental environment that replicates the test road conditions with realism. The use of simulation allows a wide range of test conditions to be prescribed and applied consistently. For example, in the real world the influence of weather, environmental lighting, etc., on driving conditions is unpredictable and can make testing difficult. Simulation permits almost any desired scenario to be created and to test drivers with timing and frequency that is not possible in the real world. The simulations are controlled and repeatable, as well as safe even in cases where (simulated) unsafe road conditions are deliberately induced for research purposes.

However, the main issue in using DSs for studying ADAS relates to their validation, by which we mean how to generalize the results obtained from the simulation context to the real world. In a very reductive way, the validation of a DS can be defined as a comparison between observed behaviours on the road and in the virtual environment of several drivers placed in similar conditions. Again, the ability to analyse and interpret drivers' behaviour in both the real and the simulated environment is a crucial requisite.

The main purpose of the research described in this PhD thesis was to study car-following behaviour so as to obtain better understanding of the phenomenon and supply suitable solutions for ADAS applications. Thus, the main objective was not to reproduce what drivers do, but what they would do consistently with a supposed behaviour, as interpreted by the ADAS. From this standpoint, the ADAS could also act in an anticipatory way or correct the actual kinematics of the vehicle if inconsistent with the wishes of the driver.

The studies were based on direct observations of field data and, for this purpose, analyses were carried out using data obtained from three different experimental campaigns carried out in two countries, Italy and United Kingdom, by means of instrumented vehicles. Importantly, the experimental campaigns were conducted independently, in the sense that the way in which data were collected and the requests that were made to the drivers were not the same, because the experiments were refined, in time, in order to focus on several specific behaviours and/or to disclose some (supposed) hidden phenomena. That said, the availability of a dataset which, as a whole, is very variegates represented a great advantage due to the large number of (different) analyses possible.

Operatively this thesis takes its cue from both theoretical and experimental evidence. At first, some analyses were carried out with respect to the Action Point paradigm (Wiedemann, 1974) and a revised version of the paradigm was suggested. A dynamic system for the car-following model was developed and its consistency

with the AP paradigm investigated; thirdly a general dynamic model for car-following was supplied in a linear (simplified) formulation in order to be applied in real time. The linear model, even if simpler from the analytical point of view, was empirically verified to be consistent and appropriate.

Finally, results of the theoretical studies were applied to develop a technological system aimed at improving its customer acceptability and market penetration. The goal there was to develop *fully-adaptive* cruise control, based on a learning machine approach The structure of the system was based on four layers and for one of these, *the* sampler, which represents the core model of the embedded control unit, the previously introduced linear model was used.

As a consequence, the thesis was organized with:

- a first section where a literature review is reported; the review covers mostly car-following models even if references to the use of car-following models in the development of Adaptive Cruise Control were reported;
- Section 2 presents the data used for the analyses, as well as more details about the three experiments for data collection;
- Section 3 explains the theoretical investigations on car-following models, presenting two topics addressed in two proper sub-sections (*Enhancing the car-following approach, A state space model for car following* behavior);
- Section 4 describes a linear car-following model explicitly developed for a fully-adaptive cruise control system; the model is shown to be consistent with the behavioural analyses in Section 3;
- finally the thesis concludes by summarising the work and by discussing the principal findings and weaknesses of these studies; opportunities for further developments are also introduced.

1 State of the art

A car-following model is a microscopic behaviour model that computes the kinematics of a following vehicle as a response to the stimuli of the leading one(s) within a traffic stream. These models are applicable under the hypothesis that the vehicle moves along the road adapting its speed to the vehicle(s) ahead, thus its dynamics can be described as a function of this(these) vehicle(s). Even if some models have been proposed with a look-ahead approach, that is based on the influence of more leading vehicles, the great part of the proposed approaches assume that the great part of the phenomenon can be explained in terms of one leading vehicle. In practice, in these models, each update of the follower's kinematic is obtained by considering its instantaneous position and speed and some kinematic variables of the vehicle directly ahead. The more significant variables considered in the literature are the spatial interspacing, the relative speed, the reaction time of the driver of the following vehicles.

The behavioral mechanism in car-following is generally complex, the car-following models aim at representing the results of this behavior by means of a formal framework as simple as possible. However the model has to be simple but not oversimplified and all elements that influence the phenomenon in the real world should be considered in order to reproduce in a timely, precise and specific way the behavior of the driver.

The car-following models are commonly used to analyze and process instant by instant the movement of each vehicle of a traffic stream, allowing to compute for each of them some variables such as position, speed and acceleration. Indeed, consistently with the previous way to use car-following models, considerable efforts have been devoted in the past to simulate with a microscopic approach traffic flow phenomena (e.g. Zhang, 1999), thereby supporting traffic engineers in both the theoretical analyses and the design and assessment of traffic schemes and policy strategies. A literature review of car-following models can be found in Brackstone and McDonald (1999), but here the car-following approaches will be rearranged in a different synoptic frame, with a greater specific consistency to the aim of this thesis. In particular, the scheme reported in Tripodi (2007) has been used also in this work where approaches to car-following have been classified, according to their basic philosophy, in:

- engineering-inspired formalisms, developed starting from mathematical assumptions that are based on what appears to be *common sense*;
- psycho-physical models, developed from human factors studies.

One of the first engineering approaches to car-following has been the stimulus-response one. It assumes that drivers choose their acceleration as a response to the stimuli coming from the leader.

The first model in this frame has been developed at the Road Research Laboratories of the General Motors and proposed by Chandler et al. in late 1958. The model was based on a simple linear function:

$$a_n(t) = c_1 \Delta v_n(t - \tau) \quad 1)$$

in which $a_n(t)$ is the response in term of acceleration of the *n*-vehicle observed at time *t*, Δv_n is the relative speed evaluated with respect the vehicle *n-1* (the vehicle immediately in front) at the time *t*- τ, where τ is the driver's reaction time; c_1 represents the sensitivity of the driver to the relative speed. The model proposed by Chandler does not depend on the spacing and then estimates the same accelerations at very different spacing values; this can lead, in particular at smaller spacing values, to un-realistic behaviours.

Helly (1959) introduced a second stimulus in the model as a function of the actual spacing Δx_n (evaluated at time *t*- τ) and of the so-called desired spacing $D_n(t)$, evaluated as a function of follower's speed and acceleration at time *t*- τ. The formulation was so changed as:

$$a_n(t) = c_1 \Delta v_n(t - \tau) + c_2(\Delta x_n(t - \tau) - D_n(t)) \quad 2)$$

$$D_n(t) = \alpha + \beta v_n(t - \tau) + \gamma a_n(t - \tau) \quad 3)$$

where again c_1 and c_2 represent two sensitivity parameters and α, β and γ parameters to be calibrated.

Gazis et al. (1959) carried out studies aimed at obtaining a macroscopic relationship between speed and flow. This led to another change in the original formulation of Chandler. The sensitivity term was substituted with a function of the follower's actual speed (evaluated at the time *t*) and of the $\Delta x_n(t - \tau)$. This model is the GHR, that is probably the most well-known car-following model:

$$a_n(t) = c \frac{v_n(t)^m}{\Delta x_n(t-\tau)^l} \Delta v_n(t - \tau) \quad 4)$$

in which *c*, *m* and *l* are parameters to be calibrated.

Brackstone and McDonald (1999) in their detailed review showed that several investigations with respect to the *m* and *l* parameters of the GHR model have been carried out in the years following the Gazis's model, leading to controversial results. Some of these results are re-called in the following *Table I*.

Table I - Calibration results of the GHR model (source: Brackstone and McDonald, 1999)

Source	***m***	***l***
Gazis et al. (1961)	0-2	1-2
May and Keller (1967)	0.8	2.8
Heyes and Ashworth (1972)	-0.8	1.2
Hoefs (1972) (dcn no brk/dcn brk/ acn)	1.5/0.2/0.6	0.9/0.9/3.2
Treiterer and Myers (1974) (dcn/acn)	0.7/0.2	2.5/1.6
Ceder and May (1976) (single regime)	0.6	2.4
Ceder and May (1976) (uncgd/cgd)	0/0	3/0-1
Aron (1988) (dcn/ss/acn)	2.5/2.7/2.5	0.7/0.3/0.1
Ozaki (1993) (dcn/acn)	0.9/-0.2	1/0.2

Key: dcn/acn: deceleration/acceleration; brk/no brk: deceleration with and without the use of brakes; uncgd/cgd: uncongested/congested; ss: steady state

The experiments reported have been carried out in different driving conditions; anyway, even in cases where experimental conditions are similar, the values of parameters appear to be quite dispersed. The lack of conclusive evidence as to the behaviour of this equation has lead to its general demise.

In parallel with Chandler, Kometani and Sasaki (1958 and 1959) proposed a model based on the concept of *safety-distance*. In practice, they argued that the follower chooses a distance and a speed that allows for safe breaking if the leader slows-down abruptly. Also this formulation puts in relationship quantities detected at time t with others detected at time $(t-\tau)$ and is here reported below as in its original form:

$$\Delta x_n(\mathrm{t}-\tau) = \alpha v_{n-1}^2(\mathrm{t}-\tau) + \beta_1 v_n^2(\mathrm{t}) + \beta v_n(t) + \beta_0 \qquad 5)$$

where τ, Δx_n, v_n and v_{n-1} have been already defined and α, β_1, β and β_0 are parameters that have to be calibrated. Values of parameters supplied by the authors of the formulation are here reported in Table 2. The first row refers to values obtained from an experiment which considered 22 test runs taken on a road section of about 200m, while the second row presents correction proposed to the parameters after another experiment which involved only 2 subjects.

Table II - The original parameters from Kometani and Sasaki

τ	α	β_1	β	β_0
0.5	-0.00028	0.00028	0.585	4.1
0.75	-	-0.0084	0.78	-

Gipps, in 1981, improved this model introducing limitations on both the vehicle and driver behavior for the calculation of the minimum and the maximum acceleration rates. In fact, the original formulation of Kometani and Sasaki yields in some traffic situations to unrealistic acceleration rates (of more than 1700 m/s^2). Constraints imposed by Gipps where: i) an acceleration constraint (assumed to depend on vehicle characteristics and driver comfort); ii) a safety constraint

(assumed to depend on the speed of the leading vehicle). The safety constraint imposes that at each time step the driver chooses a speed that, in case the leader decelerates abruptly, allows him/her, applying the maximum deceleration rate (b_n), to stop the vehicle at a distance that is not less than the actual length of the leading vehicle (*n-1*). Assuming that the deceleration rate of the leader is $\bar{b}_{n-1}$, that the follower acts after a time that is the sum of the reaction time τ, it is possible to compute the stop position of the leader (x^*_{n-1}) and the corresponding position reached at the same time by the follower (x^*_n). :

$$x^*_{n-1} = x_{n-1}(t) - \frac{v_{n-1}(t)^2}{2\bar{b}_{n-1}} \quad 6)$$

$$x^*_n = x_n\,(t) - \frac{v_n(t+\tau)^2}{2b_n} + \frac{[v_n(t)+v_n(t+\tau)]}{2}\tau \quad 7)$$

where the term

$$\frac{[v_n(t)+v_n(t+\tau)]}{2}\tau$$

represents (in a simplified manner) the position of the follower after the reaction time (before the reaction time the follower does not start to brake).

The Gipps' model for car-following is then obtained substituting the constraint that ensures the safety:

$$x^*_n = x^*_{n-1} - S_{n-1}$$

and deriving the $v_n(t+\tau)$:

$$v_n(t+\tau) = -b_n\frac{(\tau+\theta)}{2} + \sqrt{\left[b_n\frac{(\tau+\theta)}{2}\right]^2 + b_n\left[2\left[x_{n-1}(t) - x_n\,(t) - S_{n-1}\right] - \tau v_n(t) + \frac{v_{n-1}(t)^2}{2\bar{b}_{n-1}}\right]}$$

It is worth noting that in this formula an additive reaction time θ (to be added to τ) has been introduced.

Gipps didn't estimate any value of the model parameters, but his model has been broadly used anyway because its parameters can be fixed using common sense assumptions.

Many others *collision avoidance* models have been developed after the Gipps' one, but they have not been reported here explicitly because the core structure of the models have been left the same. Main differences were related to the formulation that leads to the evaluation of $v_n(t+\tau)$. For example, in Benekohal and Treiterer (1988) it is supposed that the driver has a constant acceleration (AXL) from *t* to $t+\tau$, this is chosen by the model depending on the surrounding conditions.

Other (most recent) approaches to car-following have been obtained from results of physics studies; they are known as *continuous-time* models and describe the complete dynamics of the vehicles by *ordinary differential equations*.

The most famous continuous-time models are the *Optimal Velocity Model* (OVM) (Bando et al. 1995) and the *Intelligent Driver Model* (IDM) (Treiber et al., 2000).

In the OVM the instantaneous acceleration of the follower is obtained as a function of the difference between an optimal velocity (V) and the actual velocity v_n^t:

$$\dot{v_n^t} = \alpha(V - v_n^t) \quad 8)$$

where α in this case represents a sensitivity parameter of the model. The optimal velocity is chosen taking into account the actual spacing Δx_n^t, by applying the formula:

$$V(\Delta x_n^t) = V_0\left[\tanh m(\Delta x_n^t - b_f) - \tanh m(b_c - b_f)\right] \quad 9)$$

Were the parameters V_0, m, b_c and b_f have to be calibrated from observed data. The optimal velocity grows as the actual spacing grows, and reaches the maximum speed V_{max} when the actual spacing is very high (in this way free flow conditions can be simulated):

$$V_{max} = V_0\left[1 - \tanh m(b_c - b_f)\right] \quad 10)$$

The optimal velocity becomes null when $\Delta x_n^t = b_c$; where b_c represents the spacing needed to avoid crashes (e.g. a value greater than the average length of the common vehicles). The model neglects the effect of the relative speed in the follower's behaviour and this can lead to unrealistic acceleration rates. Ward (2009) proposed to modify the original formulations adding a term that explicitly takes in account the relative speed; the model was renamed Optimal Velocity with Relative Velocity (OVRV) and is written as:

$$\dot{v_n^t} = \alpha(V - v_n^t) + \beta\Delta v_n^t \quad 11)$$

where $\beta > 0$ represents the tendency for drivers to brake-down when closing in on their predecessor and to speed-up when the gap is increasing.

Also Treiber et al., for the same reason, proposed in the IDM a different function for the acceleration, based on the actual speed of the follower (v_n^t) and on the relative velocity Δv_n^t and position Δx_n^t with respect to the leader:

$$\dot{v_n^t} = \alpha_0\left[1 - \left(\frac{v_n^t}{v_0}\right)^{\delta} - \left(\frac{\Delta x_0[v_n^t, \Delta v_n^t]}{\Delta x_n^t}\right)^2\right] \quad 12)$$

here:

- α_0 represents a basic acceleration;

- v_0 is the desired velocity;
- δ is a parameter to be calibrated;
- $\Delta x_0[v_n^t, \Delta v_n^t] = d_0 + d_1\sqrt{\frac{v_n^t}{v_0}} + \mathrm{T}v_n^t + \frac{v_n^t \Delta v_n^t}{2\sqrt{\alpha_0 b_0}}$ is a function of the desired spacing of the follower, with d_0, d_1, b_0 e T parameters to be calibrated.

One of the mayor criticisms to this model is that no reaction time is considered; for this Treiber et al. (2006) generalized the model with respect to finite reaction time, estimation errors, spatial anticipation (looking several vehicles ahead) and temporal anticipation.

The approaches re-called above give an overview of the most used and inspiring paradigms, but do not cover all the models proposed in the complex and partially unexplored field of car-following behaviour. Other ideas have been proposed in relatively recent years such as the lower order model proposed by Newell (2002) and the fuzzy-based logic introduced by Chakroborty and Kikuchi (1999). These approaches are not summarised here for sake of simplicity.

It is worth noting that almost every one of the models introduced previously can be framed into the general formalism given by Wilson (2008) without excessive approximations; thus, it can be considered a general paradigm. The formulation is the one reported below:

$$\dot{v_n^t} = f(\Delta x_n^t, \Delta v_n^t, v_n^t) \qquad 13)$$

where:

- $\dot{v}_n^t$ is the acceleration planned to be applied by the follower (driver/vehicle *n* of an unidirectional traffic stream) as a decision taken on the base of variables evaluated at time *t*;
- Δx_n^t is the spacing (spatial headway) between the follower and the leader (that is the driver/vehicle *n-1* of the unidirectional traffic stream) at time *t*;
- Δv_n^t is the relative speed between the leader and the follower;
- f(·) is the acceleration function, it formally represents the car-following paradigm.

Some simple consistency equations should be reported:

$$\dot{S}_n^t = v_n^t, \qquad \dot{v}_n^t = a_n^t, \qquad \Delta x_n^t = S_{n-1}^t - S_n^t, \qquad \Delta v_n^t = v_{n-1}^t - v_n^t, \qquad \dot{\Delta} x_n^t = \Delta v_n^t$$

where S_n^t is the absolute (unidirectional) position of the follower and a_n^t is its acceleration, while S_{n-1}^t is the absolute position of the leader and v_{n-1}^t its speed.

A different stream of car-following models is based on the psycho-physical approach. This has been developed from an analysis of the behaviour more focused on the human cognitive and decision-making mechanisms. Indeed, its development is due to the criticisms moved toward the rational representation of the driving behaviours at the base of the engineering models. Also in this case several parameters of the drivers are defined in order to model their behaviour (e.g. the desired speed, the reaction time, etc.), but these models try to use them in order to understand cognitive and perceptive activities of the humans in driving situations and to reproduce perception thresholds and/or rules from which result the observed behaviours.

Some first discussions about factors underlying the process from the psycho-physical point of view were given by Michaels (1963) that investigated on perceptual factors that influence drivers in three situations, approaching with a constant relative speed (Michaels defines the approaching situation as "simple overtaking"), steady-state following and response to acceleration of a leading vehicle. Michaels has shown that in all three cases the drivers respond to changes in the apparent size of the vehicle ahead, expressed in term of θ, the visual angle subtended. In particular, considering only the horizontal angle subtended to the lead vehicle, the rate at which that angle changes can be related to the actual speed and spacing using the formulation:

$$\frac{d\theta}{dt} = k\frac{\Delta v_n^t}{\left(\Delta x_n^t\right)^2} \qquad 14)$$

In Michaels the behaviour is described starting from the ideal approaching situation, where the driver is at a distance greater than that at which he can detect variation of the angular velocity; this means that the rate is almost zero. When the distance decreases and/or the relative speed increases (in absolute value), the driver becomes able to detect the angular velocity and then the actual motion of the leading vehicle. This point is identified in the Michaels' theory when the rate reaches a value of about $6 \times 10^{-4}\, rad/sec$. Once this threshold is exceeded, drivers decelerate, until the perceived relative velocity is null and the spacing is reduced, then the observed angular velocity remains very close to the threshold. This "overtaking" model is such that the driver tends to close on the leading vehicle with relative velocity becoming zero at a point where separation is zero. Of course, in order to maintain steering control the driver needs a minimum viewing distance that in car-following situation is reflected in a desired headway. This is the steady-state condition.

In steady state conditions, if the drivers have perfect control over the speed of their vehicles, the leader-follower pair proceeds with constant headway (as well as

constant spacing). However, it is more likely that in this close-following zone the drivers are not fully able to control the acceleration/deceleration of their vehicle due to the very fine adjustments required. Thus, the dynamics of the vehicle is governed by very small values of accelerations and decelerations, theoretically the same as in the Montroll's acceleration-noise concept (Montroll, 1959). As a result, small fluctuations in relative speed are observable. Moreover, once in steady state (angular velocity below the threshold and small relative speed) drivers can perceive changes in motion only through the spacing. Of course, not all changes in spacing are perceivable; spacing must at least change by a Just Noticeable Distance (JND) that is related to the Weber's Law; this typically implies changes in the visual angle in the magnitude of 10-12%. Thus small relative speed differences are perceived if the distance separations increases or decreases by an amount equal to the JND. In practice, JNDs define two reaction thresholds with which is possible to describe the responses of the drivers to these small changes in relative velocity. Once perceived the relative speed change, drivers react by applying an acceleration and by changing their own speed until another JND is detected. The modelling framework assumes that the acceleration is kept as constant from one threshold to the other, since any change in the conditions is perceived.

As a consequence of the studies of Michaels some researches were carried out in order to quantify the values of these thresholds. A review of past analyses on this topic was reported by Evans and Rothery (1977). They showed that the wide body of research conducted on this topic during the seventies were all consistent from a statistical point of view. As an example of the methods used in these analyses, passengers in test vehicles were asked to judge, after an exposure time from 1 to 4 seconds to a known and controlled manoeuvre, whether the gap between themselves and the leading vehicle was opening or closing.

A particular relevance should be given to the extensive measurements and investigations carried out by Barbosa (1961) and Todosoiev (1963) through the use of driving simulators.

Barbosa, studying GHR and other engineering models, found only a limited fit of these equations with observed data. He started to study the car-following behaviour by means of the so called *phase plane* trajectories, using data obtained from steady state experiments. Given a dynamic system, a *phase plane* is a Cartesian plane in which different states (or phases) of the physical system are mapped. In the phase plane representation the y-axis is used to be the time-derivative of the state variable, represented on the x-axis. Barbosa adopted the spacing as representative of the state of the system, then the phase trajectories (also called *phase portrait*) represented the relative speed (the time-derivative of the spacing) on the y-axis, against the spacing (the state variable) on the x-axis. The

results of plotting in these charts observed car-following data are the well-known *car-following spirals* (see Figure 1 below obtained by on-the-road observation, smoothed according to the technique discussed in *Appendix A – Information fusion for car-following data*), to which are used all the analysts of car-following phenomena.

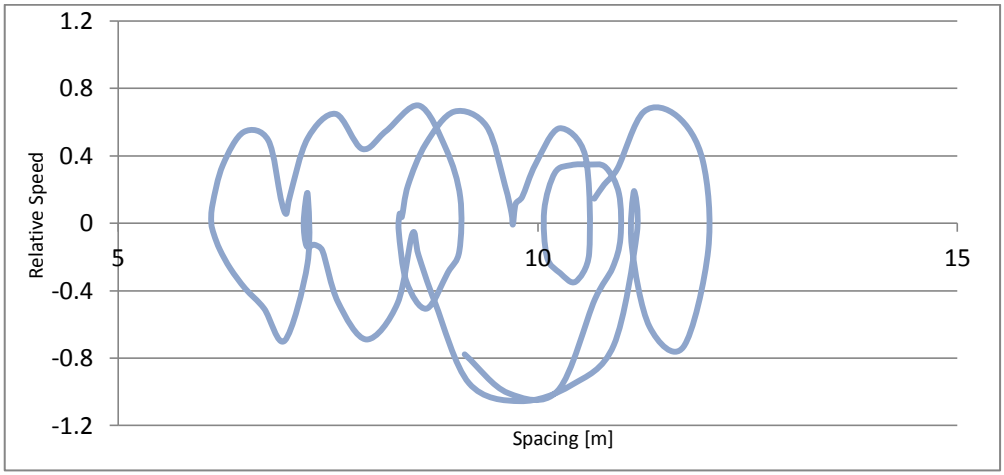

Figure 1 - An example of phase plane where a real trajectory is depicted

Barbosa also observed that certain portion of the trajectories were approximately parabolic. This approximation is depicted in Figure 2 below.

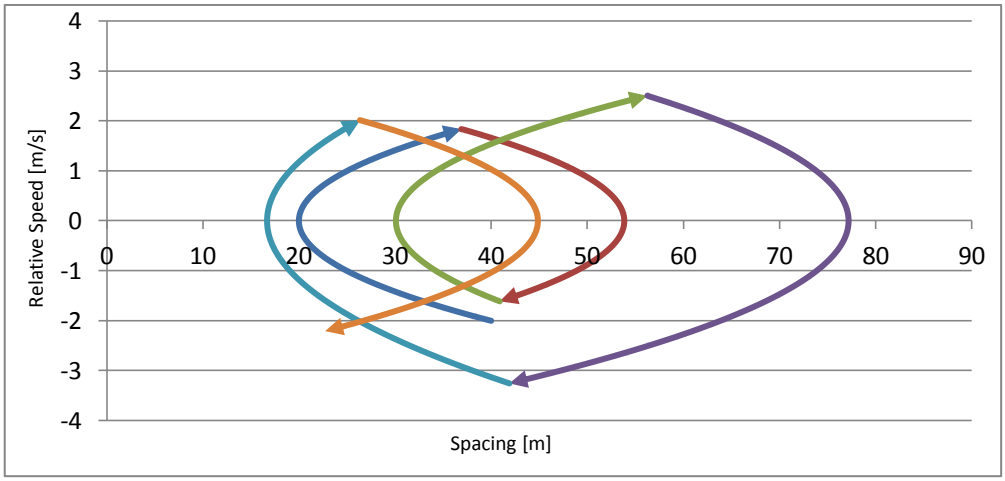

Figure 2 – The approximated interpretation of the phase portrait by Barbosa, the different portions of the depicted trajectory are parabolic curves

The approximation implies that the second derivative of the spacing with respect to the relative speed is piecewise constant. Taking into account that the acceleration of the leading vehicle is assumed as constant in the car-following theory, the second-derivative coincides with the follower's acceleration (provided that the sign is changed). If real data are plotted in terms of follower's acceleration

versus relative speed (see Figure 3 below), the approximation can be considered as acceptable. It is worth noting that the real data of Figure 3 should be compared with the theoretical plot in Figure 4.

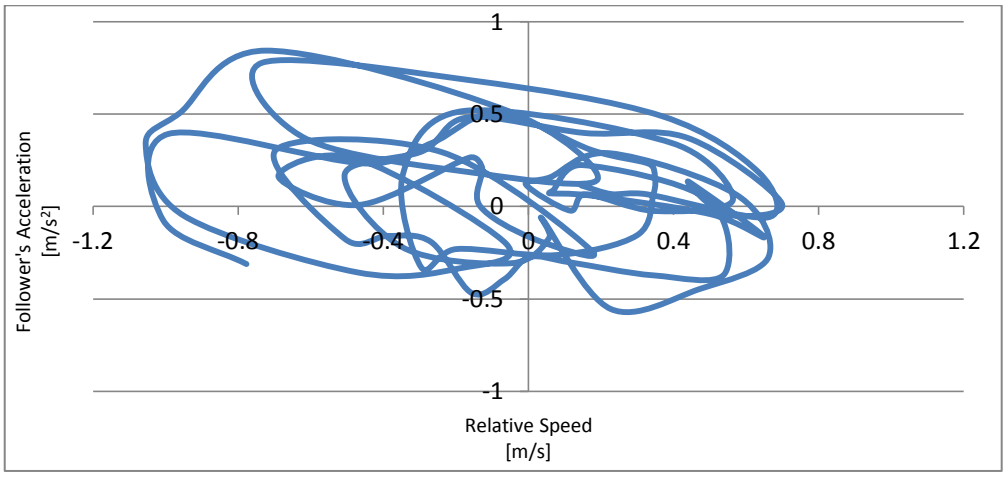

Figure 3 - The follower's acceleration plot with respect to relative speed for the same portion of real trajectory observed in the previous Figure

On the basis of the previous approximation and on plots similar to Figure 4 below, Barbosa proposed the *decision point model*, according to which, in close-following conditions, the driver make decisions to accelerate/decelerate at a constant acceleration/deceleration rate; this actions produce trajectories that oscillate around the approximate equilibrium points.

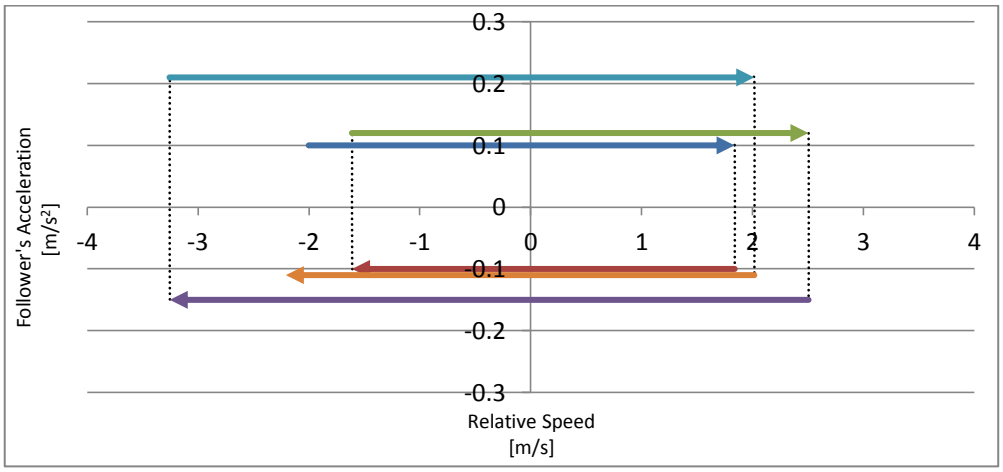

Figure 4 - The Action Point model presented by Todosoiev: the horizontal portions of trajectory represent the parabolic curves of previous Figure, while vertical tracts are Action Points where the acceleration is instantaneously changed

Studies by Barbosa inspired those by Todosoiev (1963) who studied the car-following process in the relative acceleration vs. relative speed plane, that he defined as the *second order phase plane*. As already stated, parabolic trajectories obtained with the model proposed by Barbosa correspond to rectangular trajectories

in the second order phase plane. It is worth noting that the trajectories abruptly change sign (from constant deceleration to constant acceleration and vice-versa, with infinite jerk, due to the parabolic approximation for spacing); these discontinuity points are evident in Figure 4. Todosoiev was the first analysts that called these point *action points* and the associated model *action point model*.

Starting from the analyses by Todosoiev, Wiedemann (1974) established his own (well known) Action Point model and used in the simulation tool MISSION, developed at the Institute for Transportation of the University of Karlsruhe in Germany (Wiedemann and Reiter, 1992).

Wiedemann discussed the possibility to distinguish different longitudinal driving conditions: vehicle not influenced by any front vehicle; vehicle consciously influenced because the driver perceives a slower vehicle ahead; vehicle unconsciously influenced by the vehicle ahead and in steady state car-following conditions; emergency situation. Wiedemann developed an analytical formulation for each of the previous conditions, as well as conditions for the evaluation of transition thresholds between the different conditions. In particular Wiedemann defined:

- SDV: the perception threshold of speed difference at long distances; it marks the point at which the driver consciously realizes that he is closing in a slower vehicle and reacts reducing his own speed;
- CLDV: the perceptual threshold for recognizing small speed differences at short, decreasing distances; in following a lead vehicle the driver perceives he is closing too much the gap and decelerates in order to avoid accidents;
- OPDV: the perceptual threshold for recognizing small speed differences at short, increasing distances; in following a lead vehicle the driver perceives he is opening too much the gap and accelerates;
- AX: the desired distance between the front sides of two successive vehicles in a standing queue, that consists of the length of the leader vehicle added with the desired (front to rear) distance of follower;
- ABX: the desired minimum following at low speed differences, that consists of AX added with an additional term that depends on the speed;
- SDX: the perception threshold to model the maximum following distance (typically 1.5-2.5 times ABX); it describes that the driver consciously recognizes he is leaving the following process and reacts accelerating;

In practice in the scheme of Weidemann, as shown in the next Figure, the follower vehicle drives uninfluenced until the SDV thresholds is reached, then the

driver consciously starts to decelerate because of the perceived slower vehicle; as in Michaels scheme he tries to maintain a certain headway and a null relative speed, but, unconsciously, he oscillates between the four thresholds CLDV, ABX, OPDV and SDX; then the car-following condition is defined in terms of spacing and relative speed as:

$$\begin{cases} \text{CLDV} < \Delta v_n^t < OPDV \\ ABX < \Delta x_n^t < SDX \end{cases}$$

In this condition the driver applies small positive and negative accelerations that were parameterized by Wiedemann with a parameter named *bnull*, that hash the magnitude of the Montroll's Noise.

However, the driver behaves in this way indefinitely unless an emergency braking (e.g. the leader decelerates abruptly) occurs.

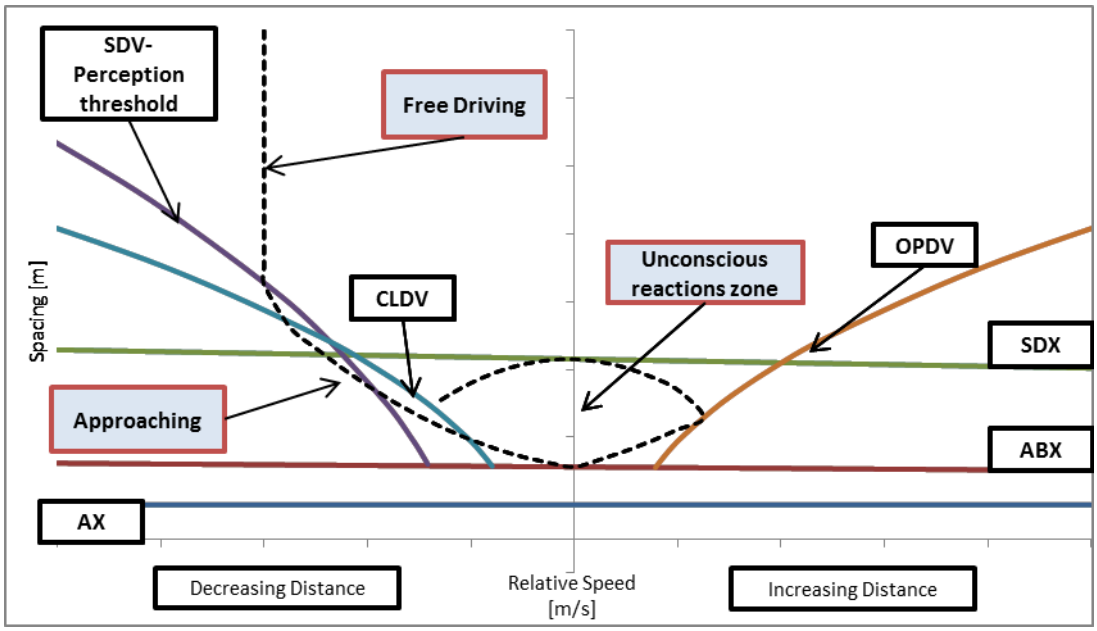

Figure 5 - An example of the modelling scheme given by Wiedemann: the follower is in free-driving condition until the perception threshold is reached, then after an approaching maneuver, the close-following condition is reached

The same approach can be found in another model presented by Fritzsche (1994) that used different thresholds (with different formulations for them), but similarly to Wiedemann he described the longitudinal driving behaviour as a combination of behaviours realized in each region; again a *bnull* value of acceleration is used (0.2 m/s^2) to model the inadequacy of driver to control the vehicle.

The models by Wiedemann and Fritzsche are at the bases of the longitudinal driving behaviour implemented in the micro-simulation models Vissim and Paramics.

Fancher and Bareket (1998) proposed a model based on action points, but their basic assumption was that the perception thresholds for relative speed can be evaluated using the *looming effect* theory; it stated that given the visual angle θ for an object wide ω placed at a distance Δ, it is valid the relation:

$$\omega = \Delta \times \theta$$

Differentiating with respect to time:

$$0 = \frac{d\Delta}{dt} \times \theta + \frac{d\theta}{dt} \times \Delta$$

and replacing in it $\theta = \frac{\omega}{\Delta}$, it is obtained:

$$\frac{d\theta}{dt} = -\omega \frac{\frac{d\Delta}{dt}}{\Delta^2}$$

It is worth noting that $\frac{d\Delta}{dt}$ is the relative speed.

This relationship was used to obtain information about the first threshold described in the Michaels' model. In fact, using results of Hoffmann and Mortimer (1996) they evaluated a perception limit for $\frac{d\theta}{dt}$ of about $3 \times 10^{-3}\, rad/sec$ (5 times bigger than the ones given in Michaels) and then, for a fixed value of ω, e.g. $\omega = 1.8$ m, the driver perceives the relative speed only when the distance is lower than:

$$\Delta = \sqrt{\frac{\frac{d\Delta}{dt}}{0.00164}}$$

The model proposed by Fancher and Bakeret is explained, as well as the other described previously, using perception thresholds in the phase-plane.

It is difficult to prove or refuse the validity of these models because experiments related to the calibration of individual thresholds are difficult to be carried out. Nevertheless, the hypotheses upon they are built are sound and seem to be realistic. For this reason attempts aimed at a better understanding of their usability are still in course, as in Hoogendoorn et al. (2011) where, using empirical data, regions are defined in the phase-plane in which the driver is likely to perform an action (in the sense that is likely to decrease or increase the acceleration) and then a cumulative probability distribution functions of the action points is given.

Moreover, another interesting approach is the one introduced by Wagner (2011), where a car-following model based on a dynamic system is calibrated taking into account observed action points, selected empirically by reasonable arbitrary conditions from on-field observed data. This approach is interesting because it allow to obtain engineering inspired models consistent with psycho-physical ones. This issue will be addressed in this thesis too.

Driving behaviour studies and car-following models (both engineeristic and psycho-physical) have been very often embedded into microscopic traffic simulation tools. Another use of these models is for ADAS and this is also the aim of this thesis. In particular, the aim here is to obtain ADAS characterised by an improved acceptability and the efficiency. Indeed, at the end of this thesis one of the developed models will be applied to an Human-Like Adaptive Cruise Control (ACC) system, designed in order to not only ensure safety but also produce trajectories consistent with observed drivers' behaviours. In other words, the proposed human-like ACC is able to apply the most *natural* driving behaviour among all those consistent with safety.

ACC systems have been actively developed and introduced into the consumer market by vehicle manufacturers in the past decade. They extend earlier systems (CCC – Conventional Cruise Control) to cases when driving at a fixed constant speed is not possible because of traffic conditions. Human likeness contributes to identify a *fully-adaptive* system, able to adapt not only to actual traffic conditions but also to driver's actual attitudes and preferences. This has been often recognised in the literature as a key feature, given that, in order to earn acceptance from drivers, ACCs should be perceived as a sort of co-pilot. In Kesting et al. (2008) for instance, even if the analysis is mainly oriented to the effects of ACC on traffic stability and performance (a topic not covered in this work), it is recognised that the system should be able to apply different driving behaviours in different traffic conditions, exactly as a human driver would have done. This point is confirmed in Viti et al. (2008), where frequent deactivations of ACCs are observed during a field operational test in the Netherlands. User acceptance is not only important for vehicle manufacturers (market penetration) but also crucial from a social perspective (actual adoption of the system).

The importance of fully adaptive systems has long been recognized in the scientific literature and efforts have been made to identify drivers' preferences through suitable parameters (see for example Reichart et al., 1997; Fancher et al., 1998). However, most of the applications propose only traffic adaptation, without dynamic adaptation also to drivers' attitudes and preferences. The parameters of the models (and characteristics of the drivers) are often proposed according to values determined statistically off-line (Marsden et al., 2001; Yi and Moon 2004; Zheng and McDonald, 2005; Moon and Yi, 2008). In most practical implementations, the approach by vehicle manufacturers is to ask for manual selection of a driving style among a set of predefined values. However, the application of a (predefined) set of parameters cannot take into account the complexity and the great heterogeneity of drivers' preferences, skills and attitudes, nor the fact that these can vary for a given driver, depending on trip context, purpose and duration or on other trip-specific

conditions, often very difficult to be fully understood. Heterogeneity and adaptation are confirmed in several works, both directly oriented to ACCs (Ervin, 2005) and traffic simulation (Wu et al., 2003; Ranjitkar et al., 2004; Punzo and Simonelli, 2005; Brockfeld et al., 2005). A performance-based benchmarking of car-following models in representing observed driving behaviours was carried out by Ranjitkar et al (2005); it was found that the same models performed differently from driver to driver and that interpersonal variation was higher than inter-model variation. The same result was found by Ossen and Hoogendoorn (2010).

1.1 Beyond the state of the art

The progresses of this thesis with respect to the current state of the art have been summarized in the next points:

- using different approaches and perspectives a better insights of actual driving behaviour have been researched;
- some step toward a unification of different approaches to the longitudinal driving behaviour (in car-following conditions) have been moved;
- simple formulations for driving behaviour, dependent on few parameters, consistent with observed behaviours, but effective enough for on-line uses have been developed;
- a driving behaviour model has been specialised for ADAS application in order to enlarge the field of application from the traditional microscopic traffic simulation issues.

2 Observation of driving behaviour and data collection

Car-following models have to be compared with observed car-following trajectories, both in order to validate different theories and to estimate modelling parameters for practical applications. As already discussed, one of the way to obtain car-following data is to observe fixed road sections, generally by means of optical sensors. Some example for this technique has already been discussed in the introduction, where the NGSIM (Next Generation SIMulation) project (US Department of Transportation FHWA, 2009) has been introduced. The project collects data using digital video cameras allowing the identification and tracking of each vehicle in the traffic stream of the observed section (typically 0.5 to 1 Km in length) every tenth of a second. While this data represents a valuable source of information, it has restricted applicability to studies of the form reported in this thesis due to the short nature of the observed trajectories. Moreover, errors and noise in observed data have been revealed in some previous studies such as those by Hamdar and Mahmassani (2008) and Thiemann et al. (2008).

The best choice in this case is represented by the direct collection of driving data and, in the research community, two main approaches have been identified as the most appropriate, one based on the use of Instrumented Vehicles (IVs), another on Driving Simulators (DSs). Both instruments offer important opportunities to researchers and stakeholders, albeit with their specific strengths and weaknesses.

DSs have long been used by car manufacturers to test users' acceptability of on-board devices and human-vehicle interfaces. In recent years DSs have been increasingly employed also in earlier conception phases, where the feasibility, effectiveness and safety of ADAS devices and solutions have to be assessed. Studies based on DSs provide a virtual experimental environment that replicates the test road conditions with realism. The use of simulation allows a wide range of test conditions to be prescribed and applied consistently. For example, in the real world the influence of weather, environmental lighting, etc. on driving conditions is unpredictable and can make testing difficult. Simulation permits researchers to create almost any desired scenario and to test drivers with timing and frequency that is not possible in the real world. The simulations are controlled and repeatable, as well as safe even in cases where (simulated) unsafe road conditions are deliberately induced for research purposes.

However, the main issue in using DSs for studying ADAS relates to their validation, by which it is meant how to generalize the results obtained from the simulation context to the real world.

IVs consist of commercial vehicles modified for research purposes by adding extensive instrumentation and sensors. This allows observation and assessment of on-road driver performance and driving styles. Several researches have been based on IVs, aimed at analyzing and modeling driving behavior or the interaction between vehicles in terms of car-following and/or lane-changing (Boyce and Geller, 2001). The dispersion of driving styles with respect to different personal characteristics, such as age, gender and driving experience, represents the target of an increasing number of IV-based studies, such as that of Ranjitkar et al. (2004). Moreover, IVs have been used for psychophysical analyses about the state of drivers, with main reference to fatigue or mental workload (Harms and Patten, 2003). Other studies have employed IVs in order to analyze drivers' responses to route guidance systems (Oh et al., 2009). IVs have also allowed for the analysis of drivers' behavior in the absence of interaction with other vehicles but with respect to different geometric features of the roads (Perez Zuriaga et al., 2000). From a broader perspective, Bishop provides an overview of the possible applications of instrumented vehicles in ITS, with particular reference to Intelligent Speed Adaptation (ISA) systems.

Of course, IVs can be used as observation tools mainly in order to gain insights into normal driving behavior. Critical behavior and/or unsafe situations may also be observed (hopefully rarely) (McLaughlin et al., 2008). However, these cannot be deliberately induced in road experiments, for evident ethical reasons. As a result, only surrogate measures of safety can be produced in most safety-related cases (Yan et al., 2008). This may not be sufficient, and direct observation of unsafe conditions could be required in some cases. Thus, different tools, such as DSs, have to be used.

For what concerns the technologies used in order to equip vehicles, very simple examples can be given, as in Gurusinghe et al. (2002), where vehicles have been equipped only with a GPS; however, some intrinsic difficulties have to be overcome in order to collect car-following data using this technique. In particular, at least two vehicles equipped with GPS are needed, one acting as the leader and the other (immediately to the rear) as the follower. Maintaining uninterrupted car following for suitable periods of time is not an easy experimental task in real contexts, and making an effort to do so could introduce some bias into the observed behaviour.

In practice, in recent years the more effective method for collecting car following data has been shown to be that of using instrumented vehicles. This technique has been applied, for instance, by Ma and Andreasson (2005) and the development of a top-end instrumented vehicle has been also discussed by McCall et al. (2004).

Moreover, instrumented vehicles can be used to collect data in active or/and passive modes (Brackstone et al., 2009). In active mode, the on-board sensors are used to obtain measures relative to the vehicle ahead, and the instrumented vehicle acts as the follower and its driver is the (aware) subject of a behavioural experiment. In passive mode, the sensors measure the relative kinematics with respect to a following vehicle and the (most probably unaware) subject of the experiment is the driver of the following vehicle. While active mode enables the recording of long sessions for the same subject (even involving several leading vehicles), the passive mode allows for the recording of shorter sessions but of many different subjects (with respect to the same leader).

2.1 The first Italian experiment

In this experiment car-following data were collected using (in active mode) the instrumented vehicle of the Department of Transportation Engineering of the University of Naples. The vehicle was a Fiat-Multipla equipped with data acquisition and video-recording devices. The real-time acquisition system was based on a central unit consisting of a notebook PC. The PC was equipped with a PCMCIA-CAN (with 2 ports) and a PCMCIA-DAQ card (allowing for 8 analog outputs, 8 digital outputs, 2 counter/timers). The vehicle was able to supply several data streams, including vehicle speed (with a maximum error of 2%), the position of the accelerator pedal, the brake and clutch positions, the rotation angle of the steering wheel. The vehicle was also equipped with two TRW Autocruise AC10 radars, able to collect information on relative speed (with an accuracy of 0.7 km/h) and relative spacing (with a maximum error less than 1 m for distances less than 20m, and less than 7% for distances greater than 20m) with respect to up to four vehicles ahead or behind. There was the possibility to collect data with a high frequency and the one employed in these studies was 10Hz. This value was consistent with similar experiments described in the literature (e.g. Wu et al., 2003), but higher values could be reached if needed. The video-capture system consisted of two cameras (rear and front); the overlay card (that was used to overlay information on absolute time, relative speed and relative spacing with respect to the vehicle ahead or behind), and a digital video recorder. All real-time acquisitions were synchronized and managed using a single software program developed in LabWindows. Finally, the vehicle was equipped with a GPS receiver and a data recorder, which could be employed for post-processing positioning with D-GPS and K-D-GPS techniques. Several images of the vehicle have been reported in Figures 6 and 7 below.

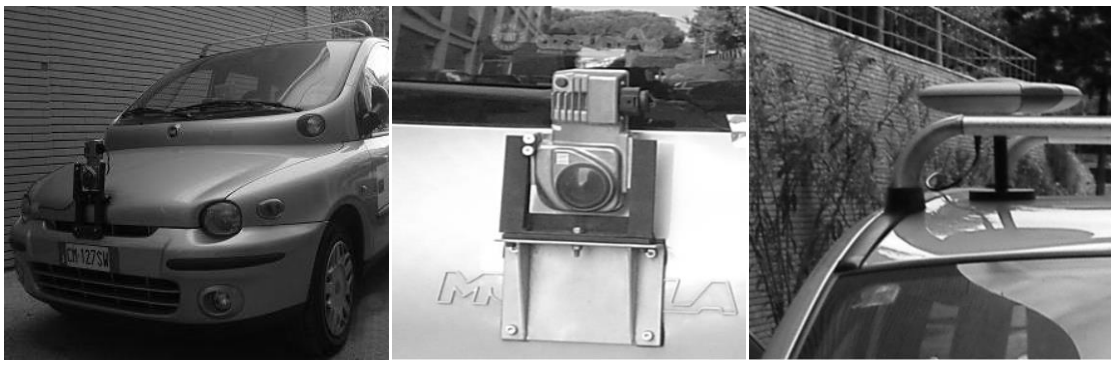

Figure 6 - The instrumented vehicle

Figure 7 - Pictures from a driving session

Using the instrumented vehicle, extensive car-following data were collected from 2008 to 2010 on two different routes near the city of Naples in southern Italy. The first was a National Highway (the ss. Quarter Domiziana) dual carriageway and two lanes for each direction of traffic, highway junctions and design speed interval of 60-120 km/h (speed limit 110 km/h). The second was a National Road (the ss. 268 "del Vesuvio") characterized by a single carriageway with one lane for each direction of traffic, at-grade intersections and design speed interval of 60-100 km/h (speed limit 90 km/h). Traffic conditions on the second route were more variable and lower speeds were observed. Trajectories were collected for twenty different drivers, each of them driving on one of the two routes as shown in *Table III* An example of an observed velocity trace is given in Figure 8. Each driver was allowed a short period of acclimatisation to the vehicle of ten minutes, which we considered enough given the familiarity and the simplicity of the task, and was then asked to follow a confederate car. The confederate car was instructed to drive for the great part of the time as the flow was driving; in few moment it was asked to increase its distance from the platoons ahead and to stimulate the instrumented vehicle with sudden accelerations and unexpected decelerations.

In this study we selected from each trajectory (which corresponds to each test run) the longest segment of contiguous car-following data observed in the driving session. From the twenty collected, only thirteen trajectories have been used, as seven of these presented too many fragmented sequences (typically shorter than 180 seconds). It was chosen to exclude them because it was retained that short sequences could not guarantee *pure* close following, with a danger of successive approaching conditions being observed instead. Additionally, data has been excluded where emergency braking or sudden accelerations/decelerations have occurred (greater than 1 m/s^2 in magnitude).

Table III - Drivers

Experimental context	Observed Drivers	Males	Females	Young (<30 years old)
Route 1	8	4 (50%)	4 (50%)	7 (87%)
Route 2	5	3 (60%)	2 (40%)	4 (80%)

Table IV - Driving sessions

Experimental context	Sessions with Good Weather	Length (km)			Average Speed (km/h)		Max Speed (km/h)		
		Total	Mean	St.Dev.	Mean	St.Dev.	Mean	St.Dev.	Max
Route 1	89%	59	7.4	2.51	63.7	7.09	113	16.16	130
Route 2	100%	29	5.7	1.20	47.2	2.87	99.33	21.55	120

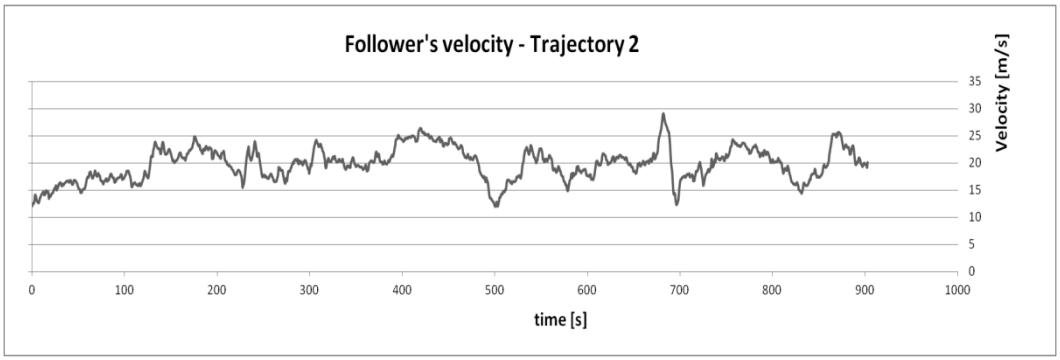

Figure 8 - An example of follower's velocity profile: trajectory 2

It is evident that, given the way the vehicle is instrumented, the complete (absolute and relative) kinematics of the following and leading vehicles can be directly recorded or easily estimated. The entities that we select in order to analyse the car following behaviour are the spacing between the vehicles, the velocity of the follower, the relative velocity and the velocity of the leader. We also computed the

time headway (TH) between the two vehicles (spacing over follower velocity) and the time-to-collision (TTC - the spacing over the relative speed). These quantities identify the safety margin and the time available to the driver to act if an immediate collision has to be avoided; these perceptual variables are argued (e.g. Goodrich et al., 1999) to play a role in decision making under car following, with, for example, Minderhoud and Bovy (2001) identifying a critical threshold of around 3.5 to 5 seconds as a level below which 'stable' car following cases, a figure confirmed in the main by Bevrani and Chung (2011) through examination of NGSIM data.

2.2 The English experiment

Data introduced in this section have been collected at the University of Southampton for the DIATS research project and have been supplied to the author during an Erasmus Exchange that started in September 2011 and ended in February 2012. Data of the DIATS project were obtained from three experimental surveys, carried out in three different countries (U.K., Germany and France) from 1997 to 1998 with an instrumented vehicle used in passive mode (the radar was rear-mounted in order to collect data on random following vehicles). In this thesis only data from the experiments conducted in U.K. have been used.

The instrumented vehicle used in this research has been described in several past papers (McDonald et al., 1999; Marsden et al., 2003). The vehicle concerned was a UK car, right hand drive with UK number plates equipped with:

i) an Optical Speedometer, accurate to <±0.02 m/s at typical motorway speeds;
ii) a radar Rangefinder, fitted to the rear of the vehicle to measure the distance to, and relative speed between the follower and the lead (test) vehicles; the unit had a measured accuracy of ±0.2 m in range and ±0.4 m/s in relative speed;
iii) a video-audio monitoring system allowing a permanent visual record of each experiment to be made, useful for an analysis of 'macroscopic features', apparent to the driver but not detectable to the sensors (eg. lane, visual conditions etc.).

Information from each of the sensors were sent to a controller PC at a rate of 10Hz (~3.5 Kb/sec.) and recorded in five minute blocks. After each experimental session the logged data were directly transferred to a removable 1Gb cartridge and taken for analysis.

The U.K. part of the database was collected on the M3 3-lane motorway, just to the Southwest of London. Data were collected during three morning peak periods,

with laps of a test course between junctions 2 and 4a (a total of 22 Km in each direction), yielding data on 30 drivers, averaging a little under four minutes each.

The aim of the DIATS project was to compare driving behaviours, then the experiment was to capture a random sample of following sequences on the three different test sites. For this reason the equipment was mounted on board the lead vehicle of the leader-follower pair and the driver following was unaware that data was being logged. This meant that the location of the following sequence was random (along the given area of road being examined) as well as its duration. Each following sequence captured only a short period of following for every driver and no details were available of the age, sex and driving history characteristics of the drivers. The same driver was used for the instrumented vehicle at all times. The following events were always undertaken in conditions where other traffic was in close proximity, both on near-side lanes and preceding the instrumented vehicle. In this way, the vehicle formed part of an 'enclosed' traffic event and was not blocking progress of the rear vehicle.

Table V - Main characteristics of the UK dataset

Dataset	Drivers		Driving sessions					
	Female (%)	Young (%)	Tot Trajectories	Tot Length (km)	Time (s)			Average Speed (Km/h)
					Mean	Max	Min	
UK	20 est.	80 est.	41	134	178.7	62	0.6	66

Ref: McDonald et al., 1999; Marsden et al., 2003

2.3 The second Italian experiment

The experiment described in this Section has been carried out during the DriveIn[2] (*DRIVE*r monitoring: technologies, methodologies, and *IN*-vehicle *IN*novative systems) research project that focuses on defining methodologies, technologies and solutions aimed at capturing driving behaviors (Bifulco et al., 2012). The research project is currently carried forward at Department of Transportation Engineering of the University of Naples and experimental sessions have lasted from September to November 2012. It is out of the scope of this thesis to describe in details the research project, anyway, it has implied the observation of:

- a sample of 100 drivers;
- each driver has driven the same scenario in two experimental environments, a virtual reality scenario (using for this a static driving simulator) and a road-field one, where an instrumented vehicle has been used;
- the scenario comprises a single loop over three roads near Naples: National Highways A1 and A30, and State Highway 268; the loop is 78

km long and can be travelled in about 1 hour. The scenario was conceived so that each experiment allows to collect data of:

i. a first motorway section of about 14 km (from B to D in Figure 9) where the driver is immersed in a traffic stream that moves at about 100 km/h; this allows to obtain "natural" car-following data, in the sense that no specific instructions were given to the driver;

ii. a second motorway section of about 30 km (from E to G in Figure 9) where the driver interacts with a corporate vehicle that carries out several standard maneuvers; in particular are asked to perform three approaching maneuvers with the leader at a constant speed of 80, 100 and 120 km/h;

iii. a third national roadway section of about 16 km (from I to K in Figure 9) where the driver is immersed again in a traffic stream, this time with lower speed; also in this case "natural" car-following data are obtained.

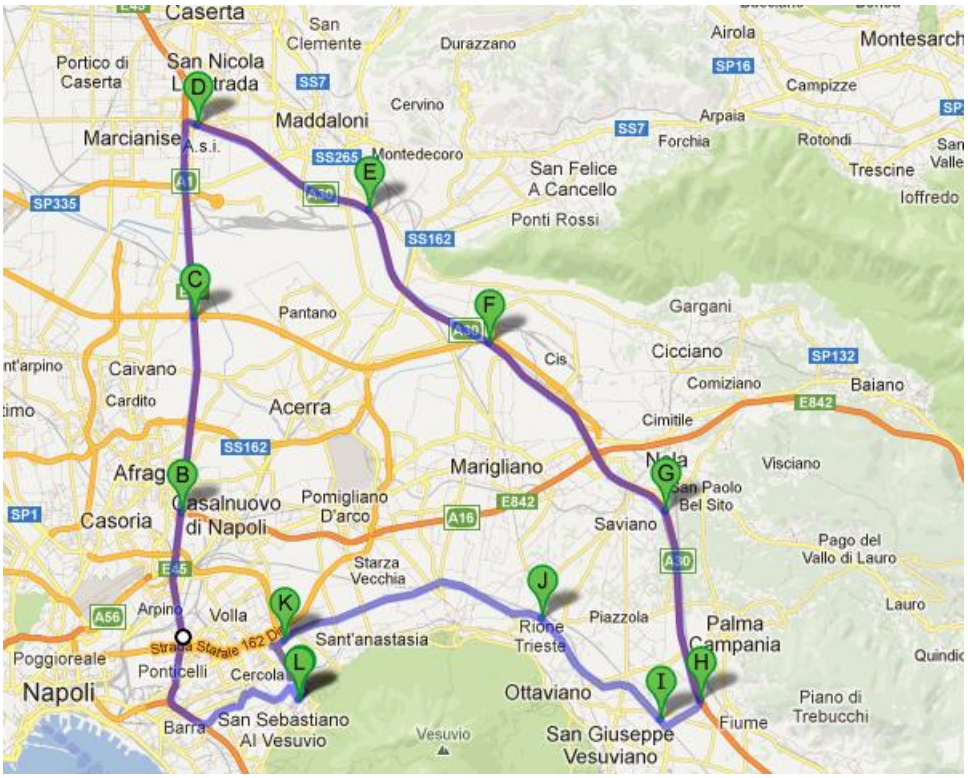

Figure 9 - The experiment road-field scenario

Among other things, the project allowed a strong upgrade of the instrumented vehicle, that is the same introduced in Section 0. Anyway, actually the core of the system is an NI CompactDAQ chassis, a modular data acquisition system for

gigabit ethernet with eight measurement-specific modules. CompactDAQ is the data acquisition device for all the sensors in the vehicle, except the video cameras. It receives digital and analog signals, as well as data and communications via the CAN. It is connected to a PC controller with an Intel Pentium I7 six-core processor. It has 32 GB of RAM, two 500 GB SSDs and three 1TB HDDs. The synchronization and acquisition software is based on LabVIEW. The on-board power supply is partly in direct current (from 5V to 24V depending on the device) and partly in 220V AC. Alternating current is supplied by a 500W inverter. The energy is supplied by two 12V (100Ah) service batteries able to provide safe, uninterrupted power for up to 5 hours. In order to allow for longer experimental sessions, the batteries are recharged while the vehicle runs by means of a Sterling Power active power split charger. The Topcon Global Positioning System (GPS) with a Differential GPS antenna still supplies positioning and kinematic data, but currently in this task it is integrated with a dead-reckoning technique based on an Xsense MTi-G Accelerometer. This is actually a MEMS Inertial Measurement Unit (IMU), in turn aided by another internal GPS. The radars have been changed with two TRW Autocruise AC20 radars mounted, hidden behind the bumper, on the front and on the back of the vehicle to enable collection of headway data (relative distance and speed of maximum five surrounding vehicles for each radar). Three potentiometers are used to collect data on the position of the brake pedal, the gas pedal and clutch pedal. The steering wheel angle is measured by a draw-wire displacement sensor and the angular velocity by a gyroscope (in addition to the Xsense IMU). Video data are collected by four Basler industrial cameras: 170 degree color giga-ethernet acA1300-30. The cameras have a resolution of 1294 x 964 pixels and a frame rate of 30 fps. Two cameras are oriented forward and backward outside the vehicle. One camera points toward the driver inside the vehicle. The last camera is positioned so that the lateral lane position of the vehicle can be detected. The front and rear cameras record the behavior of the surrounding traffic and the characteristics of the road environment. The presence of video cameras accounts for the large amount of storage space in the control PC. Video and data acquisition (from all sensors) are synchronized by an external trigger signal. The equipment is completed by a touch-screen panel PC allowing data acquisition to be managed and monitored and workload tests to be performed while driving.

Clearly the amount of data collected for the project allows the possibility to perform several analyses and comparisons in relationship to the dispersion of behaviours between drivers (as well as that of model parameters), but, for what concerns the topic of this thesis, the main contribution provided by this dataset regards the possibility to test developed models (and the underlying hypothesis) in

some specific and rarely observed (with the most commonly used research tools) situations. Therefore only data from several road-field trajectories (randomly chosen among those available) have been showed in the thesis and, for each of them, only data of the ii and iii experimental sections used.

Figure 10 - The renewed Instrumented Vehicle of the Department of Transportation Engineering of Naples

3 Theoretical analyses and developments

Theoretical analyses carried out in this thesis concern both psycho-physical approaches and engineering ones. In particular the starting point of this thesis has been the Action Point model proposed by Wiedemann (and described in Section 1. Data presented in previous Section 2 (in particular for those of experiment described in Section 2.1) have been analysed with reference to the Wiedemann's thresholds related to the area of unconscious reaction (ABX, SDX, CLDV and OPDV). These analyses and some considerations on pre-Wiedemann studies on psycho-physical models lead to a re-visitation of the paradigm. Moreover, some typical patterns for the car-following phenomenon are evidenced by studying the Action Points (APs) of the revised version of the model with respect to Time-To-Collision (TTC) and inverse-TTC (iTTC).

Then an engineering model is presented and theoretical conditions for the identification of APs demonstrated, thus establishing a relationship between the engineeristic and the psycho-physical approach. Parameters of the theoretical model are evaluated by using experiments described in Section 2 and the availability of both data from Italy and U.K. allows for a partial comparison. APs of the revised paradigm are shown to be suitable for the identification of the follower's desired steady-state spacing in car-following, which is one the key behavioural parameters of the model. As a result, this behavioural parameter can be employed in an engineeristic approach after being computed from on-field data in a way that is consistent with the psycho-physical approach.

The procedure for Action Point identification applied to all collected data used in this thesis has been drawn from Brackstone et al. (2002). The complete procedure has been reported in the *Appendix B – Empirical procedure for APs* , to which the reader can refer to for more information. Briefly speaking, in the procedure, each time an action point is identified the current leader and follower velocities are recorded for future use, as well as the current accelerations of both the vehicles, the actual spacing and the actual time instant.

Before entering the description of the analyses, for the reader convenience, hereafter are recalled the symbols that will be used in the following in order to describe the relevant variables of the problem:

- the follower vehicle has been indicated as *n*-vehicle, then his/her actual kinematic (in an unidirectional traffic stream) has been indicated with S_n^t, v_n^t and a_n^t respectively for his/her absolute position, speed and acceleration; consistency equations between the variables can be given

$\dot{S}_n^t = v_n^t$, $\dot{v}_n^t = a_n^t$, where Newton notation for time-differentiation has been used;

- the same variables have been defined for the leader vehicle, indicated as the *n-1* vehicle (S_{n-1}^t, v_{n-1}^t, a_{n-1}^t);
- the relative quantities have been defined from leader to follower, then the spacing is evaluated as $\Delta x_n^t = S_{n-1}^t - S_n^t$, as well as the others relative quantities; consistency equations can be given also in this case, that are $\dot{\Delta} x_n^t = \Delta v_n^t$ and $\dot{\Delta} v_n^t = \Delta a_n^t$.

3.1 Enhancing the car-following approach

In next sections the car-following paradigm is analysed and described in an enhanced way. First of all the AP paradigm is revisited in order to identify the key features to be modelled and the main figures related to APs and to other variables. Then an engineering approach to car-following is proposed, based on a state-space representation of the phenomenon. The relationship of the state-space approach with the AP one is discussed.

3.1.1 Revisiting the model

The Action Point model has often been considered as one of the soundest paradigms in car following, able to explain many of the commonly observed driving behaviours and consistent with the frequently observed so-called *car following spirals*. These are described by observed data once plotted in the spacing vs. relative speed plane (that also is the phase-plane or phase portrait already introduced in section 2).

An example of a following spiral where action points are evidenced is shown in Figure 11 below, based on one of the thirteen experimental trajectories obtained from the experiment described in Section 2.1. Similar charts can be plotted using different real-world observations (see for instance Brackstone et al, 2002 or Brackstone et al., 2009).

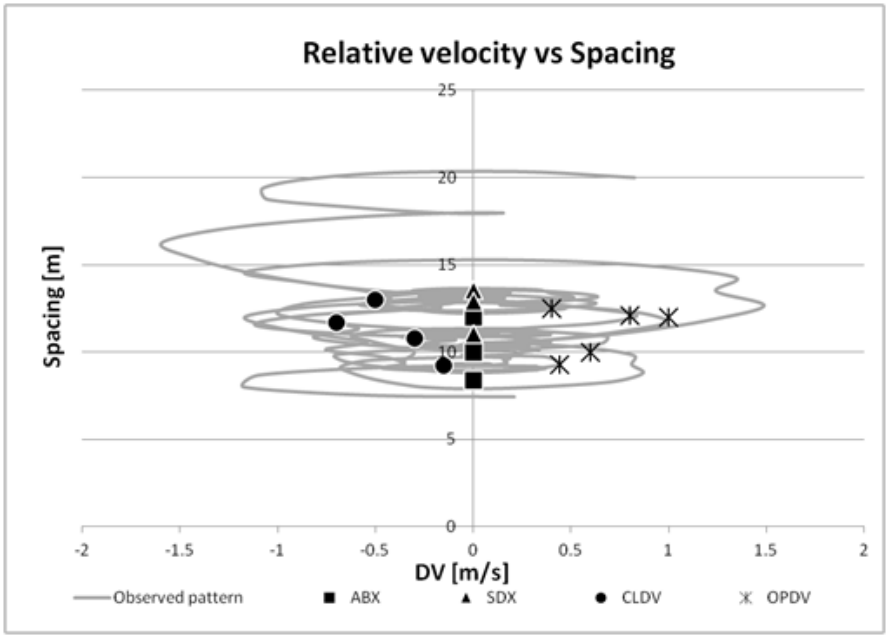

Figure 11 - Typical experimental car following spiral, in accordance with the Action Point paradigm (ground velocity of the order of 100 Km/h).

In this section the sounding Action Point paradigm will be re-interpreted with reference to its basic features, aiming at a both simpler and easier understanding, as well as at an easier calibration. Only action points associated with the relative velocity thresholds (OPDV and CLDV) are considered in the revised paradigm as true action points. In order to discuss this reinterpretation, Figure 11 is here conveniently stylized as Figure 12 below.

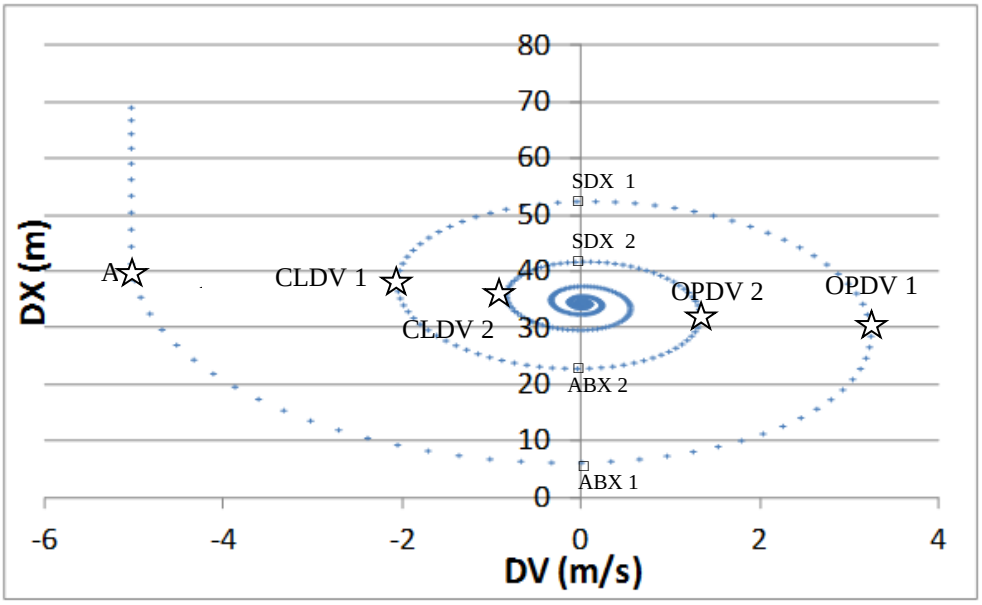

Figure 12 - Stylized car following spiral (synthetic data)

In this revisited action point paradigm, the follower cruises at her/his constant desired velocity, until she/he perceives the vehicle in-front as slower (point A). Starting from point A, the follower brakes in order to adapt the velocity to the one of the leader. From then onwards his/her goal is to follow the leader at both a desired spacing and a null relative velocity, and these conditions have to hold simultaneously for *steady-state* car-following conditions. The steady state is represented by the centre of the spiral. Small oscillations around the steady state are defined as *close-following* conditions.

In moving from point A to the desired steady state condition, the follower passes point ABX1. However, in the revised theory this is not a point in which the follower takes any action, thus it is not an action point. It is just a point when the decelerating process (started from action point A) leads to a null relative velocity (but not the desired spacing). Where this point is located on the vertical axis of Figure 12 depends on the deceleration that has been applied at point A and is not interpretable from a direct behavioural point of view. It can just be argued that point ABX1 is likely to correspond to a spacing very close to the steady state one if the driver is very skilled. The spiral continues with no action until point OPDV1 is reached. Here the follower perceives that the applied deceleration has lead to a positive relative velocity and that he/she is moving from the steady state condition (moreover with an absolute velocity significantly lower than both the desired and the leader's one). Thus, the action of accelerating is started. In the acceleration process from OPDV1, the car following spiral passes the point SDX1. Once again, this is just a point where the relative velocity is null but where the accelerating action continues without modification. At point CLDV1 the follower perceives a relative speed that is incompatible both with the steady state condition and safety and, as a consequence, a deceleration phase is started and the process moves toward points OPDV2, CLDV2, ..., OPDVi, CLDVi.

The process passes points ABX2, SDX2, ..., ABXi, SDXi which are not real action points, but kinematic consequences of the process between real action points; this does not mean that the ABXs and SDXs are not interesting, e.g. they can be selected in order to understand the width of the area of unconscious reactions, but because no action is taken at that points, they cannot be considered as action points. Then from this moment ABX, SDX, CLDV and OPDV will be named *Interesting Points* (IPs) and, between them, only OPDV and CLDV will be considered as *Action Points*.

It is worth noting that this re-visitation of the AP-paradigm is not so new, in the sense that considering real action points only these were an accelerating/decelerating action is taken is consistent with the original studies of Barbosa and Todosoiev presented in Section 1.

At each successive loop, the circle is closer to the steady-state point because of two phenomena. On one hand, the driver refines his/her perceptions and, on the other hand, the current condition is closer to the steady state one so that less vehicle control skills are required. Clearly, the spiral plotted in Figure 12 is not the unique pattern that can be argued as being produced by the revised paradigm, indeed the greater the driving skill, the more rapidly the radius of the spiral decreases, see for example the candidate spiral for a highly skilled driver, as in Figure 13.

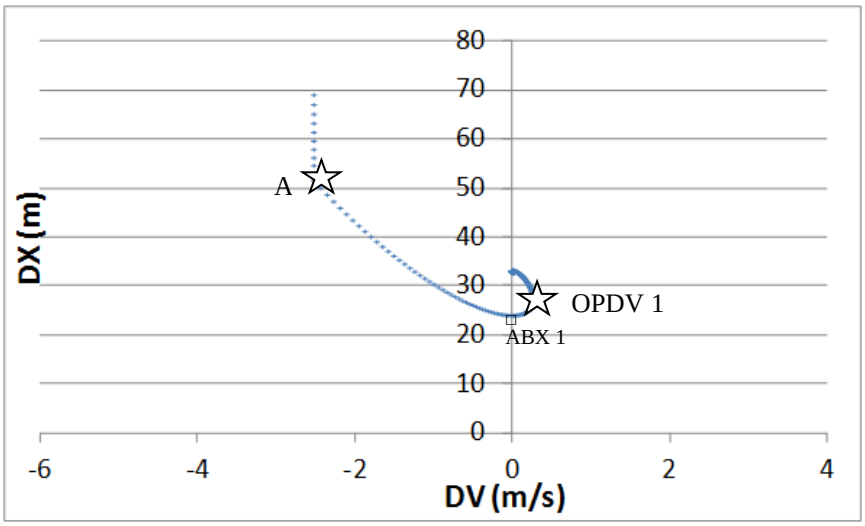

Figure 13 - Car following spiral by a skilled driver – further oscillation around the steady state are small but exist.

Real world observations are likely to deviate somewhat from this stylised example. For example, there may not be any convergence toward the steady state, nor do the loops become progressively smaller and closer. This may be due to the drivers' concentration and management of the driving task not being constant (even professional drivers are not able to perfectly control the kinematics of the vehicle). Moreover, for sure the leader does not cruise at a perfectly constant speed, thus the adaptation process has to be locally restarted many times depending on the leader's oscillations (this has also been indicated by Montroll 1959 through as *Acceleration Noise*).

If the stylized spiral of Figure 12, is re-drawn using time-headway with respect to relative velocity, similar spirals will occur (see Figure 14 upper part). A different plot is obtained if the rate $-\frac{\Delta v_n^t}{\Delta x_n^t}$ is used as the dependent variable (Figure 14 down part, where for negative relative velocity the rate represents the iTTC – inverse of the time-to-collision). In the obtained plot, the closing and opening phases of the follower with respect to the leader, are repeated in the form of successive *waves*,

according to the stylised spiral, which progressively tend to an asymptotic positive infinite value for TTC and then to a null value of -DV/DX.

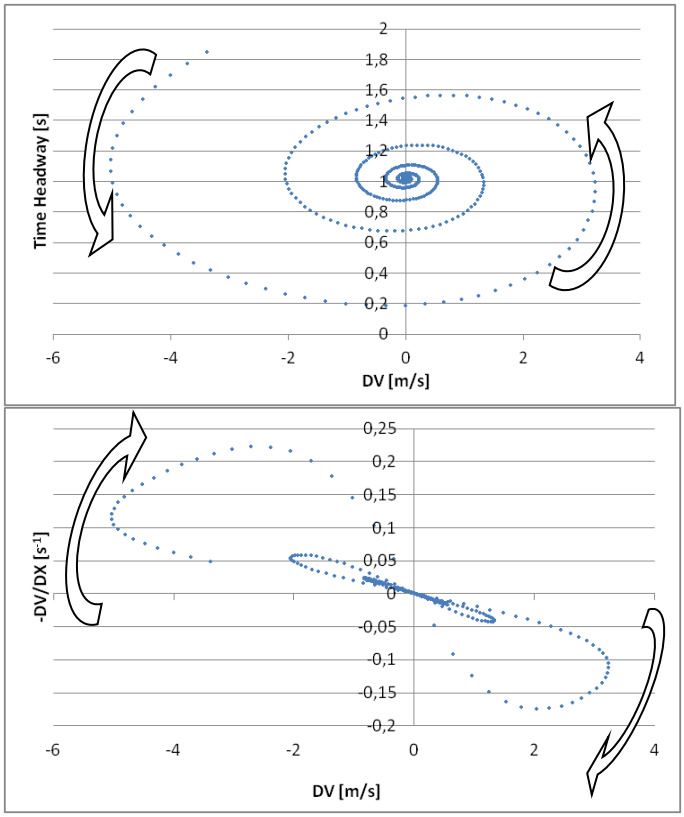

Figure 14 - Time-headway and inverse of TTC (synthetic data)

A zoom on the waves related to closing and opening situations have been depicted in Figure 15 (upper left and upper right). It is worth noting that, for each wave, the point with the largest value, in absolute terms, of relative velocity represents an action point.

A pattern can be identified for both closing and opening, whereby, when the relative speed decreases in successive opening processes, the opening (-DV/DX) index tends to a null value the associated action points follow a linear pattern. The same happens in the closing processes, but in this case, due to the inverse relationship between the two indexes, the distribution fits a rectangular hyperbola.

If the distribution of the action points associated with the opening process is prolonged also for negative relative speeds, the resulting linear pattern passes for the action points associated with the closing process. Similarly, if the hyperbola associated with the action points of the closing process is plotted also for positive relative velocities, the action points of the opening process are encountered.

The resulting whole charts (refer to Figure 16) are defined here, as the *opening chart* and the *closing chart* respectively. It is worth noting that strictly speaking the

opening index is defined only for negative relative velocities and that the closing index is defined only for positive relative velocities.

This explains why, in the following, both the opening and closing index have been plot for all APs depending on the reader convenience; in fact the opening and the closing charts give the same kind of information and can be arbitrarily chosen in order to describe the pattern of action points.

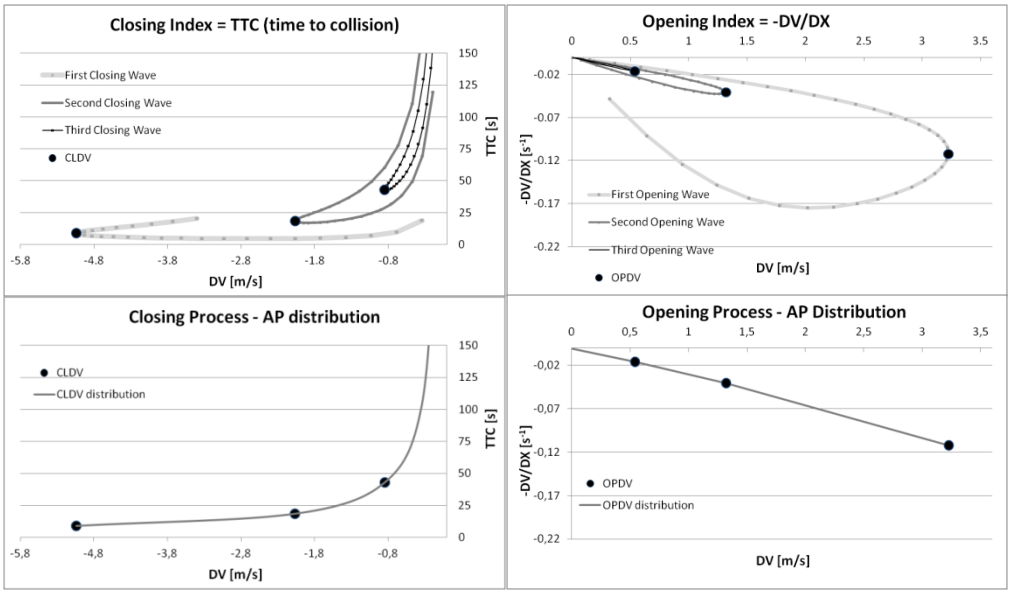

Figure 15 - Closing and opening waves (synthetic data) and distribution of the action points

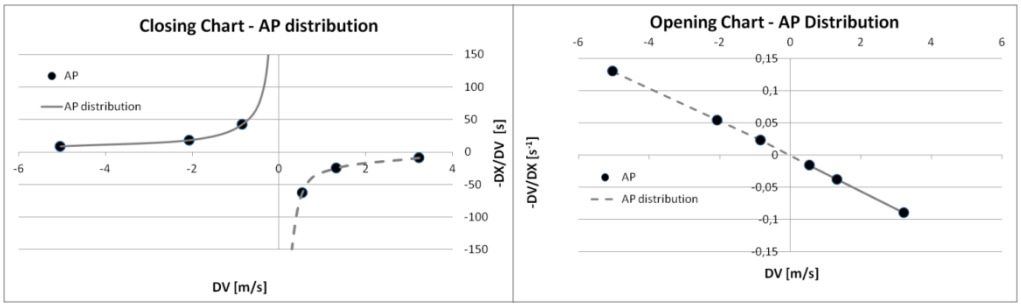

Figure 16 - Closing and opening charts (synthetic data) and distribution of the action point

3.1.2 The revised paradigm with respect to observed data

Analyses of these Section have been referred only to data obtained from the experiment described in Section 2.

For information completeness, Car-following models have to be compared with observed car-following trajectories, both in order to validate different theories and

to estimate modelling parameters for practical applications. As already discussed, one of the way to obtain car-following data is to observe fixed road sections, generally by means of optical sensors. Some example for this technique has already been discussed in the introduction, where the NGSIM (Next Generation SIMulation) project (US Department of Transportation FHWA, 2009) has been introduced. The project collects data using digital video cameras allowing the identification and tracking of each vehicle in the traffic stream of the observed section (typically 0.5 to 1 Km in length) every tenth of a second. While this data represents a valuable source of information, it has restricted applicability to studies of the form reported in this thesis due to the short nature of the observed trajectories. Moreover, errors and noise in observed data have been revealed in some previous studies such as those by Hamdar and Mahmassani (2008) and Thiemann et al. (2008).

The best choice in this case is represented by the direct collection of driving data and, in the research community, two main approaches have been identified as the most appropriate, one based on the use of Instrumented Vehicles (IVs), another on Driving Simulators (DSs). Both instruments offer important opportunities to researchers and stakeholders, albeit with their specific strengths and weaknesses.

DSs have long been used by car manufacturers to test users' acceptability of on-board devices and human-vehicle interfaces. In recent years DSs have been increasingly employed also in earlier conception phases, where the feasibility, effectiveness and safety of ADAS devices and solutions have to be assessed. Studies based on DSs provide a virtual experimental environment that replicates the test road conditions with realism. The use of simulation allows a wide range of test conditions to be prescribed and applied consistently. For example, in the real world the influence of weather, environmental lighting, etc. on driving conditions is unpredictable and can make testing difficult. Simulation permits researchers to create almost any desired scenario and to test drivers with timing and frequency that is not possible in the real world. The simulations are controlled and repeatable, as well as safe even in cases where (simulated) unsafe road conditions are deliberately induced for research purposes.

However, the main issue in using DSs for studying ADAS relates to their validation, by which it is meant how to generalize the results obtained from the simulation context to the real world.

IVs consist of commercial vehicles modified for research purposes by adding extensive instrumentation and sensors. This allows observation and assessment of on-road driver performance and driving styles. Several researches have been based on IVs, aimed at analyzing and modeling driving behavior or the interaction

between vehicles in terms of car-following and/or lane-changing (Boyce and Geller, 2001). The dispersion of driving styles with respect to different personal characteristics, such as age, gender and driving experience, represents the target of an increasing number of IV-based studies, such as that of Ranjitkar et al. (2004). Moreover, IVs have been used for psychophysical analyses about the state of drivers, with main reference to fatigue or mental workload (Harms and Patten, 2003). Other studies have employed IVs in order to analyze drivers' responses to route guidance systems (Oh et al., 2009). IVs have also allowed for the analysis of drivers' behavior in the absence of interaction with other vehicles but with respect to different geometric features of the roads (Perez Zuriaga et al., 2000). From a broader perspective, Bishop provides an overview of the possible applications of instrumented vehicles in ITS, with particular reference to Intelligent Speed Adaptation (ISA) systems.

Of course, IVs can be used as observation tools mainly in order to gain insights into normal driving behavior. Critical behavior and/or unsafe situations may also be observed (hopefully rarely) (McLaughlin et al., 2008). However, these cannot be deliberately induced in road experiments, for evident ethical reasons. As a result, only surrogate measures of safety can be produced in most safety-related cases (Yan et al., 2008). This may not be sufficient, and direct observation of unsafe conditions could be required in some cases. Thus, different tools, such as DSs, have to be used.

For what concerns the technologies used in order to equip vehicles, very simple examples can be given, as in Gurusinghe et al. (2002), where vehicles have been equipped only with a GPS; however, some intrinsic difficulties have to be overcome in order to collect car-following data using this technique. In particular, at least two vehicles equipped with GPS are needed, one acting as the leader and the other (immediately to the rear) as the follower. Maintaining uninterrupted car following for suitable periods of time is not an easy experimental task in real contexts, and making an effort to do so could introduce some bias into the observed behaviour.

In practice, in recent years the more effective method for collecting car following data has been shown to be that of using instrumented vehicles. This technique has been applied, for instance, by Ma and Andreasson (2005) and the development of a top-end instrumented vehicle has been also discussed by McCall et al. (2004).

Moreover, instrumented vehicles can be used to collect data in active or/and passive modes (Brackstone et al., 2009). In active mode, the on-board sensors are used to obtain measures relative to the vehicle ahead, and the instrumented vehicle acts as the follower and its driver is the (aware) subject of a behavioural experiment. In passive mode, the sensors measure the relative kinematics with

respect to a following vehicle and the (most probably unaware) subject of the experiment is the driver of the following vehicle. While active mode enables the recording of long sessions for the same subject (even involving several leading vehicles), the passive mode allows for the recording of shorter sessions but of many different subjects (with respect to the same leader).

The first Italian experiment all the relevant points (CLDV, OPDV, ABX and SDX) selected from the observed data have been reported hereafter. In particular, both kind of APs (OPDV/CLDV and ABX/SDX, Figure 17 up and down) have been plotted versus the current follower's velocity at which they have been detected. It is encouraging that these figures are very similar to those reported in Brackstone et al. (2002) which used data obtained from a totally different experiment carried out in England.

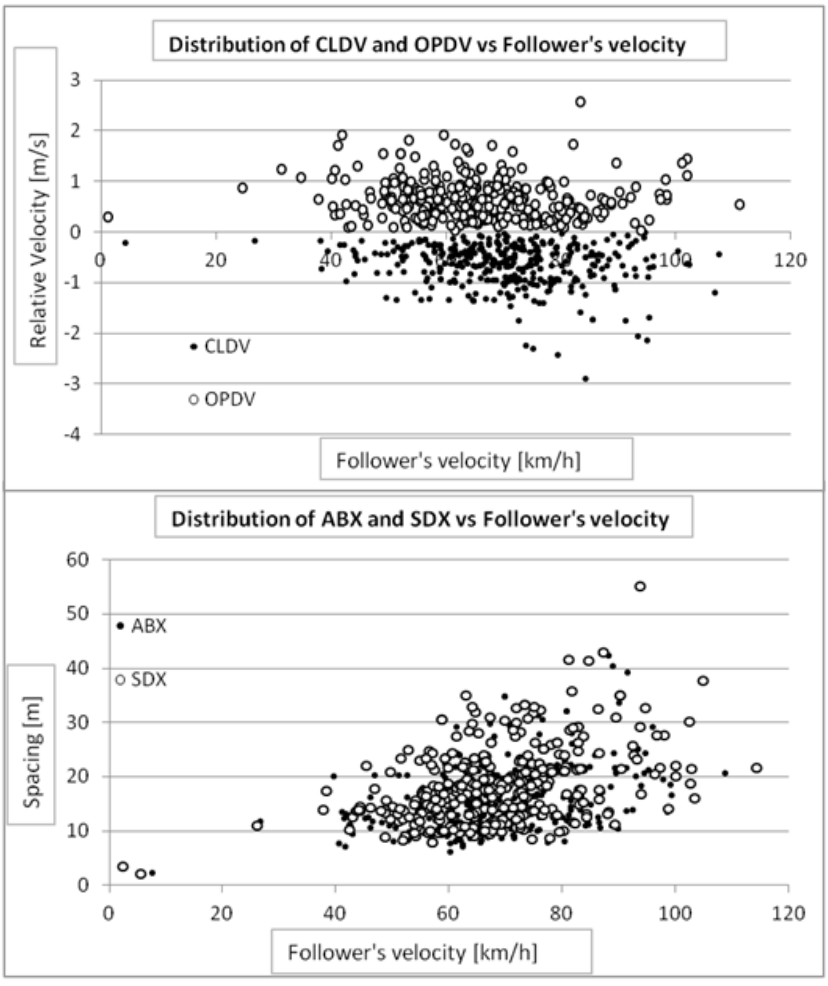

Figure 17 - Action Points identified in the First Italian Experiment

The analysis of observed data has been carried out focusing the interest on the *closing* and *opening* indexes and with respect to patterns identifiable in the *closing* and *opening* charts.

Observed data would seem to fit the revised theoretical framework, although this is confounded by the fact that the lead vehicle never maintains a constant speed. As a consequence, while closing and opening waves can be identified, their evolution is less ordered due to a degree of overlapping through additional and unpredictable adjustments. An example is shown in Figure 18 where the closing and opening waves observed in driving session 4 have been plotted.

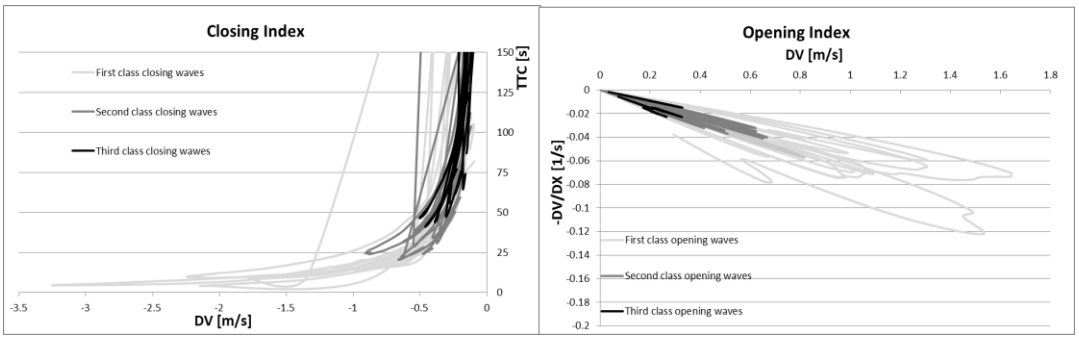

Figure 18 - Closing and opening waves (trajectory 4 of the considered experimental session)

Figure 18 shows the total of 12 different *clips* (around 300 seconds in total, each around 25 seconds long and consisting of several waves), with each clip re-starting the evolutionary process toward the steady state. The number of observed waves likely depends on the driver's skill and on the driver's power of concentration that is not constant during long driving sessions. It is worth noting also, that while in theory each successive wave should give rise to a 'smaller' action point, this is unlikely to be observed in practice, not only because of fluctuations of the lead vehicle speed, but also because the car-following processes may not necessarily start from the basis of an approach to the lead vehicle, but for example from a lane change. Waves should however be considered together with other characteristics of driving.

As an example, a zoom on a small part of driving session 2, where 3 clips can be identified, is shown in next figures.

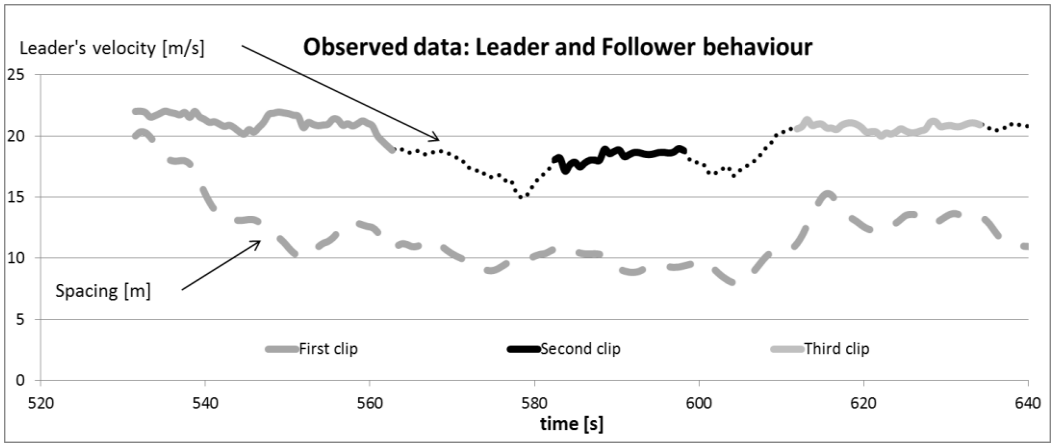

Figure 19 - An observed pattern: leader's Velocity and Spacing vs. time, section of driving session 2

In the clips used in the previous example, the leader has a more or less constant speed (smoother in the third clip) and the follower tries to reach a close–following condition. In the first clip, after an approach phase, the close-following condition is not reached because of the unstable behaviour of the leader and the associated velocity reduction. In Figure 20 below, points related to the first clip are easily identifiable. These points generate the closing and opening waves depicted at the first row of Figure 21. As the car-following process is disturbed, as are the waves and their sequences.

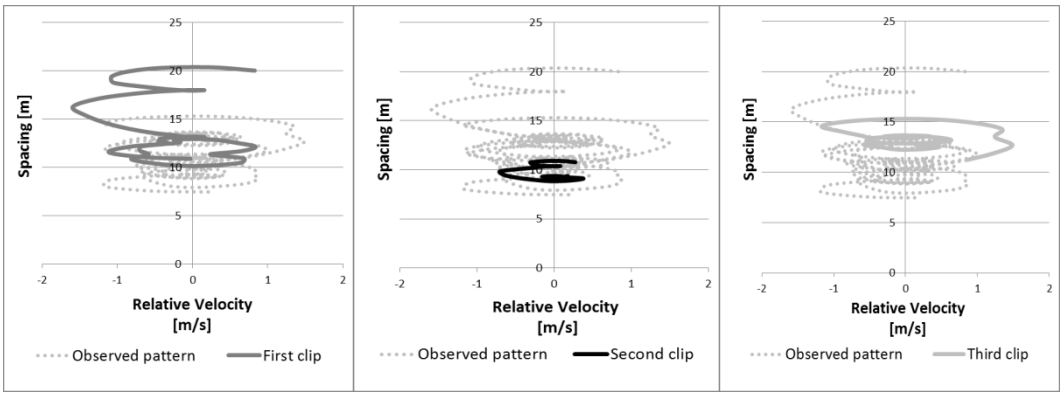

Figure 20 - Spacing vs. Relative velocity for the three clips

In the second clip the follower is quickly satisfied because he/she only adjusts the current spacing value, so the close-following condition is soon reached. In Figure 21 second row, the waves are consistent with a quick adjustment toward a close-following condition.

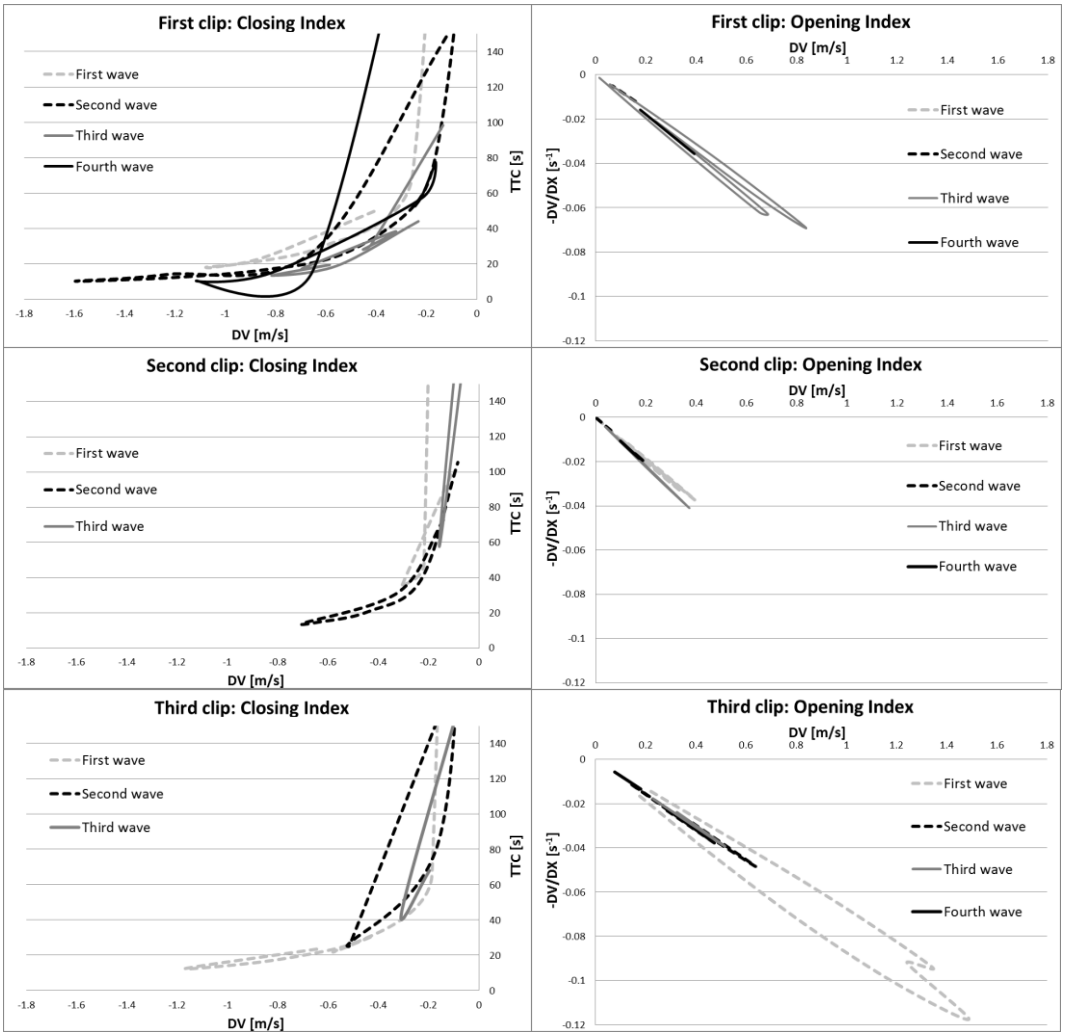

Figure 21 - Closing and Opening Indexes (observed data)

The third clip is probably the smoother. As a consequence of the increase of the leader's velocity the spacing grows, so an adjustment is required (it is not a proper approaching manoeuvre as, while the leader only slightly accelerates, the vehicles still are in car-following), but after a transient the close-following condition is reached. Waves in Figure 21, third row, are more evident than for clip 2.

A global analysis of the Action Points computed for all driving sessions of the considered experimental session (a total amount of more than 700 points) has also been carried out. The points have been framed in both the closing and opening chart, and, on aggregate, are in good accordance with the revised theory.

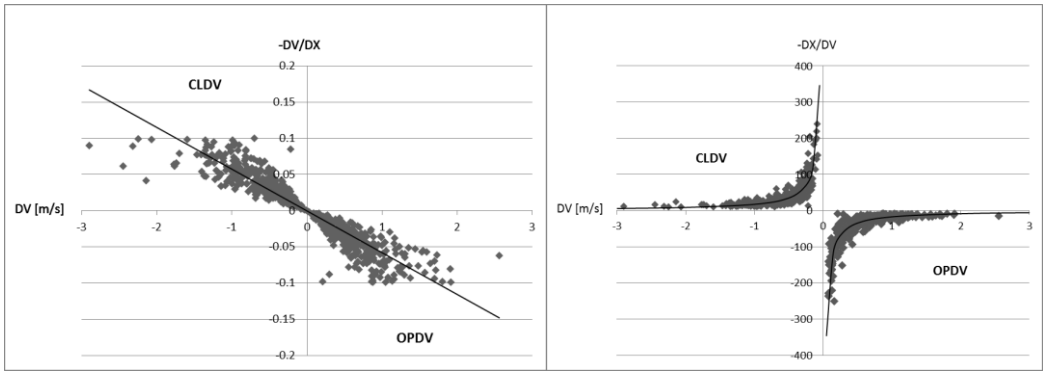

Figure 22 - The distribution of CLDV and OPDV (observed data) and the result of the least squares analysis

The same analysis has been carried out also considering each driving subject. This has been conduct using separate best fit curves in the opening chart, as shown in Table VI and in Figure 23.

Table VI - Results of the linear regression

	Regression Parameters		**Estimation Statistics**			
	Constant term (1/s)	Coefficient (1/m)	N	R-square	Fisher-F	error variance
All Action Points	-0.00072	-0.0579	745	0.874	5165.8	0.000273
Driving Session						
1	0.00059	-0.05968	148	0.936	2126.7	0.000142
2	-0.00203	-0.08530	120	0.960	2830.8	0.000123
3	-0.00380	-0.03837	52	0.874	346.60	0.000292
4	-0.00096	-0.05475	33	0.953	625.62	0.000110
5	-0.00039	-0.05475	25	0.912	237.27	0.000274
6	-0.00111	-0.05167	78	0.912	791.75	0.000113
7	-0.00038	-0.04127	16	0.962	357.12	0.000052
8	0.00191	-0.08407	38	0.969	1137.0	0.000066
9	-0.00527	-0.08407	28	0.827	124.137	0.000720
10	-0.00011	-0.06003	44	0.897	363.78	0.000189
11	-0.00096	-0.05363	94	0.915	986.83	0.000129
12	-0.00088	-0.05811	33	0.958	707.62	0.000082
13	0.00131	-0.05763	36	0.955	726.20	0.000100

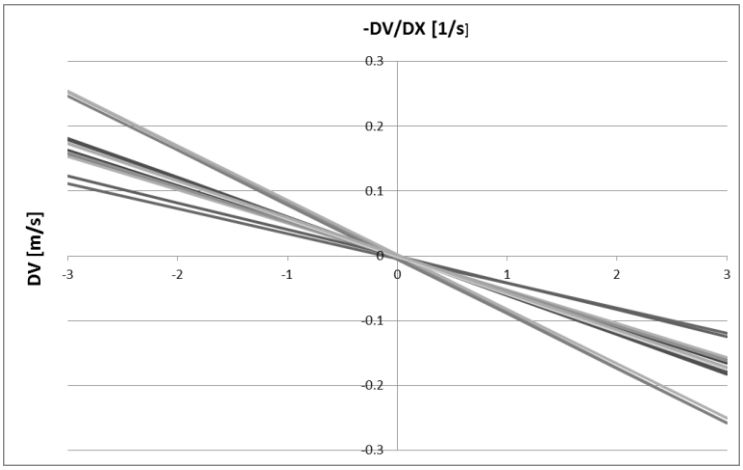

Figure 23 - Results of the least squares analysis for each driver depicted in the opening chart box

The accordance of the observed data with the stylized figures deriving from the revised Action Point theory seems to be encouraging and qualitatively validates the revised paradigm. In particular, for both opening and closing phases, the behavior is well explained using waves that, even if different in amplitude, are distributed according to identifiable patterns.

Hypothesis on the succession of waves in the car-following process have been partially verified; observed data also in this case well fit with the theoretical paradigm, even if a not negligible bias is induced by the variation of leader's behavior. This is mainly due to leader's non constant velocity, that is a topic addressed in a deeper way in next section. Also low order effects such as geometry, poor driving concentration or particular condition encountered during the driving session can induce some variation in follower's behavior, with unpredictable patterns.

3.2 A state space model for car following behavior

The AP paradigm, even in the revised version, allows a good understanding of the car-following phenomena but does not provide a complete, in analytical terms, description of the follower's dynamic (for example Wiedemann gives an extra-formulation to evaluate follower's acceleration in each zone).

At this scope an analytical tool, as those derived within the engineering approach, could represent the most appropriate solution. This Section is then aimed at presenting a continuous response car-following model placed in a state-space representation; as well as the AP model is assumed as a valid, coherent and significant paradigm, the consistency of the proposed model with this theory will be verified. The contemporary validity of the AP theory and of the state-space dynamic

model allows for a potential reciprocal estimation of the relevant parameters. The main advantages of this approach can be so resumed in:

- the possibility to model the car following driving behaviour as a response to different (and sometimes unknown) stimuli and to better understand the process through their explicit separation;
- the possibility to explicitly evaluate some relevant variables through the study of the performance characteristics of the model;
- the possibility to give, even if in certain conditions, an analytical solution for the identification of the APs on the basis of the parameter of the calibrated model.

The starting point for the development of the continuous response model is the general formula given by Wilson and already introduced in Section 1:

$$\dot{v}_n^t = f(\Delta x_n^t, \Delta v_n^t, v_n^t)$$

As already hypothesized in all previous sections, according to most of the car-following models, it is assumed that an equilibrium condition hold in which the leader and the follower cruise at the same speed and the spacing is the *equilibrium* one, that is a sort of preferred spacing for the follower that depends on the cruising speed. In analytical terms, the equilibrium point of the car-following process can be described as:

$$\dot{v}_n^* = 0 \qquad \Delta v_n^* = 0 \rightarrow v_n^* = v_{n-1}^* \qquad \Delta x_n^* = g(v_{n-1}^* = v_n^*)$$

Car following patterns where the equilibrium point exists and depends on the speed according with a g(·) function can be used to derive from the microscopic behaviour a macroscopic model consistent with the *fundamental diagram* paradigm. It can be assumed that when in car following the driver tries to control the vehicle and oscillates around the equilibrium point; in this event a Taylor's expansion in the vicinity of the equilibrium point can be assumed:

$$\dot{v}_n^t = \frac{\partial f(\cdot)}{\partial \Delta x_n}(\Delta x_n^t - \Delta x_n^*) + \frac{\partial f(\cdot)}{\partial \Delta v_n}(\Delta v_n^t - 0) + \frac{\partial f(\cdot)}{\partial v_n}(v_n^t - v_n^*) \qquad 15)$$

Now, given that , close the equilibrium, the current speed is not significantly different from the equilibrium speed, the term $\frac{\partial f(\cdot)}{\partial v_n}(v_n^t - v_n^*)$ can be neglected.

Moreover, let define:

$$\frac{\partial f(\cdot)}{\partial \Delta x_n} = \omega_N^2 \qquad \text{and} \qquad \frac{\partial f(\cdot)}{\partial \Delta v_n} = \omega_F \qquad 16)$$

As a result one obtains:

$$\dot{v}_n^t = \omega_N^2\ (\Delta x_n^t - \Delta x_n^*) + \omega_F\ \Delta v_n^t \qquad 17)$$

Given $\dot{v}_n^t = \dot{v}_{n-1}^t - \Delta\dot{v}_n^t$, it can be written that:

$$\Delta\dot{v}_n^t = -\omega_N^2 \Delta x_n^t - \omega_F \Delta v_n^t + \omega_N^2 \Delta x_n^* + \dot{v_{n-1}^t} \quad 18)$$

This form can be rearranged in a continuous state-space representation:

$$\begin{pmatrix} \Delta\dot{x}_n^t \\ \Delta\dot{v}_n^t \end{pmatrix} = \begin{bmatrix} 0 & 1 \\ -\omega_N^2 & -\omega_F \end{bmatrix} \begin{pmatrix} \Delta x_n^t \\ \Delta v_n^t \end{pmatrix} + \begin{bmatrix} 0 & 0 \\ \omega_N^2 & 1 \end{bmatrix} \begin{pmatrix} \Delta x_n^* \\ \dot{v_{n-1}^t} \end{pmatrix}$$

that can be rewritten, in a more compact formulation, as:

$\dot{\bar{x}}_n^t = \mathrm{A}\,\bar{x}_n^t + \mathrm{B}\,\bar{u}^t$

where:

$\mathrm{A} = \begin{bmatrix} 0 & 1 \\ -\omega_N^2 & -\omega_F \end{bmatrix}$ is the *state matrix*;

$\mathrm{B} = \begin{bmatrix} 0 & 0 \\ \omega_N^2 & 1 \end{bmatrix}$ is the *input matrix*;

$\bar{x}_n^t = \begin{pmatrix} \Delta x_n^t \\ \Delta v_n^t \end{pmatrix}$ is the *state vector*;

$\bar{u}^t = \begin{pmatrix} \Delta\dot{x}_n^* \\ \Delta\dot{v}_{n-1}^t \end{pmatrix}$ is the *input vector*;

$\dot{\bar{x}}_n^t = \frac{d}{dt}\bar{x}_n^t = \begin{pmatrix} \Delta\dot{x}_n^t \\ \Delta\dot{v}_n^t \end{pmatrix}$ is the first derivative of the status vector.

It is worth noting that for a rational driving behaviour drivers should increase their acceleration when there is an increase of the spacing (the actual spacing becomes greater than the desired one), and decrease it in the opposite situation. The same happens with respect to the relative speed. Thus it is reasonable to retain $\omega_F, \omega_N^2 \geq 0$.

The given *state space* representation is of the *linear time-invariant* type and has superposition property. Thus it allows to model the evolution of the car-following process as the sum of the *natural* and *forced* responses, this sum is commonly indicated as the *general* response of the model.

The natural response can be used to investigate stability properties of the model and, if the system is stable, is such that, if considered alone, the driver tends to close the gap ($\Delta x_n^t \to 0$). In fact, the presence and the analytical form of the considered stimuli condition only the form of the forced response (then also the general response of the model is conditioned by stimuli).

In particular in the adopted schematization two disturbances are considered:

- the existence of the desired (and safe) spacing that means the gap is closed until the desired one (Δx_n^*);

- the presence of the external disturbance coming from the leader's kinematics ($\dot{v}_{n-1}^{t}$).

Interestingly inputs of the system are qualitatively different because Δx_n^* hides a driver's preference, while $\dot{v}_{n-1}^{t}$ $v_{n-1}^{\dot{t}}$ summarizes the changes in the leader's behaviour, independent of the follower. In other terms, $v_{n-1}^{\dot{t}}$ can be seen as an actual disturbance to the desired gap-closing process.

The form of matrices A and B suggests that both the parameters ω_N^2 and ω_F influence the natural response while the forced one is influenced only by ω_N^2.

It is worth noting that this scheme allows to consider any type of disturbance considered relevant for car-following just adding the new terms to the input vector and formalising the expected effect in the B matrix.

3.2.1 Natural response and stability of the state-space model

Stability characteristics of the system can be studied from the eigenvalues of the state matrix A. In particular, the eigenvalues (λ_1 and λ_2) of the dynamic system are obtained solving the equation:

$$\lambda^2 + \omega_F \lambda + \omega_N^2 = 0$$

yielding the solutions:

$$\lambda_{1,2} = -\frac{1}{2}\omega_F \pm \frac{1}{2}\sqrt{\omega_F^2 - 4\omega_N^2}$$

It can be derived from previous equation that the stability of the model only depends on the sign of ω_F.

In particular, under the (already introduced) rational assumption that $\omega_N^2 > 0$, $\omega_F > 0$, the response of the system is stable (namely, the natural response tends to 0) and the analytical solution can be written as:

$$\overline{x_n^t} = e^{At}\overline{x_n^0}$$

in which:

- e^{At} is the matrix exponential;
- $\overline{x_n^0}$ is the vector of the initial conditions.

The matrix exponential can be expressed as:

$$e^{At} = Te^{Dt}T^{-1}$$

where:

- e^{Dt} is the diagonal matrix of eigenvalues, diag $\{e^{\lambda_1 t}, e^{\lambda_2 t}\}$;
- T is the full matrix of eigenvectors.

The most general case is that of under-damped solutions, where a particular expression may be obtained for e^{At} using Euler's formula; in fact the generic e^{ix} can be re-written as $\cos x + i \sin x$ (i being the imaginary unit). In this case the obtained eigenvalues can be re-written as $\lambda_{1,2} = a \pm ib$, where:

- a = $-\begin{bmatrix} 0 & 1 \\ -\omega_N^2 & -\omega_F \end{bmatrix} \frac{1}{2} \omega_F$ represents the real count-part of the solution;
- b = $\frac{1}{2}\sqrt{\omega_F^2 - 4\omega_N^2} = \sqrt{\frac{\omega_F^2}{4} - \omega_N^2}$

Given the eigenvalues, the eigenvectors can be computed solving the problem:

$$(A - \lambda I)\bar{v} = 0$$

where λ is one of the eigenvalues and $\bar{v}$ is the corresponding eigenvector.

Finally, the equation of each component of the state vector can be computed using the modal expansion of the dynamic system:

$$\overline{x^t} = c_1 e^{\lambda_1 t}\overline{v_1} + c_2 e^{\lambda_2 t}\overline{v_2}$$

where c_1 and c_2 depend on the initial conditions.

In the case in which eigenvalues have no complex part, the analytical form of each component of the natural response can be obtained as a linear combination of exponential functions which, if the system is stable, tend to zero when time increases. The analytical form of the response, in our case, is related to both ω_F and ω_N^2; in particular, it depends on the value of b (or better of the discriminant $\sqrt{\frac{\omega_F^2}{4} - \omega_N^2}$), as shown in next Figure 24, where the stability/instability regions of the dynamic problem have been summarized.

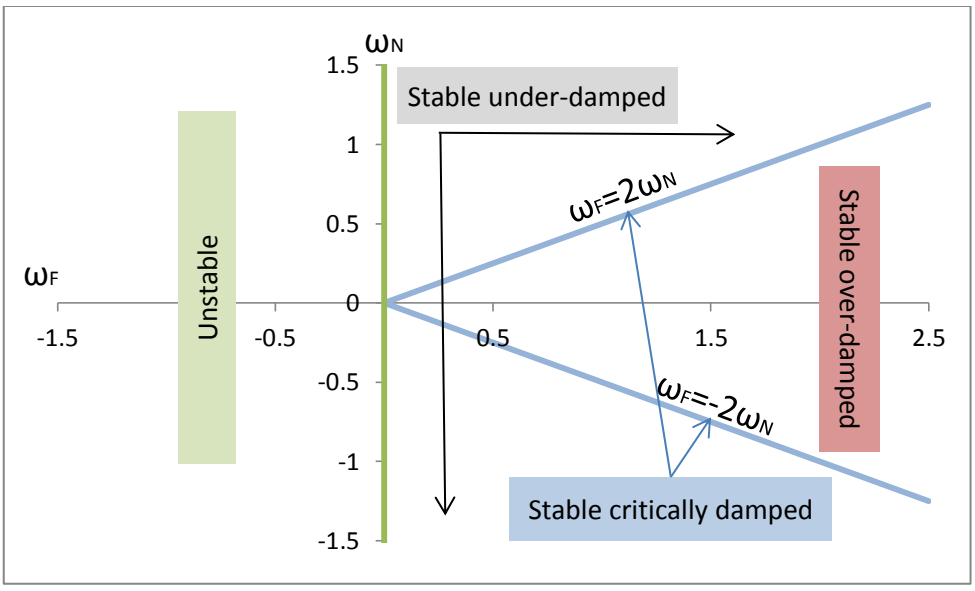

Figure 24 - Stability regions of the state-space model

For what concerns the speed of the convergence to zero of the exponential function, it depends on the real part of the eigenvalue. A time constant (τ) of each component of the dynamic system can be evaluated and, from that, the so-called settling-time (t_s):

$$\tau = -\frac{1}{a} = \frac{1}{\frac{1}{2}\omega_F} = \frac{2}{\omega_F}$$

$$t_s \approx 4.6\,\tau = \frac{9.2}{\omega_F}$$

In the case of under-damped solutions, using $t_s \approx 4.6\tau = \frac{9.2}{\omega_F} b$ (that represents the effective angular velocity) it is possible to evaluate the period, $T = \frac{2\pi}{b} T = \frac{2\pi}{b}$, and the frequency, $f = \frac{b}{2\pi} f = \frac{b}{2\pi}$, of the oscillations.

3.2.2 The general response of the state-space model

As already stated above, the general response of the model can be obtained as the sum of the natural response and of the forced one, evaluated through the convolution integral:

$$\overline{x_n^t} = e^{At}\overline{x_n^0} + \int_0^t e^{A(t-\mu)} B\overline{u(\mu)} d\mu \qquad 19)$$

The solution presented here before is the most general one, which can be particularized when inputs have a particular form.

For the study of the general response, in the first instance it is assumed that the leader has a constant speed during the process ($\dot{v}_{n-1}^t = 0$), such that only inputs related to the desired spacing are considered; in particular it is also hypothesized that the desired spacing is chosen at the beginning and does not change during the car-following process. In this way, the desired spacing can be modelled as a *step input*, and the evolution of the system can be expressed as a *step response*. The convolution integral is then simplified in:

$$\overline{x_n^t} = e^{At}\overline{x_n^0} + (e^{At} - I)A^{-1}B\overline{u^0} \qquad 20)$$

where:

- $\begin{bmatrix} 0 & 1 \\ -\omega_N^2 & -\omega_F \end{bmatrix}$ is the vector of the initial conditions;
- $\begin{bmatrix} 0 & 0 \\ \omega_N^2 & 1 \end{bmatrix}$ is the step input, dependent on the stimulus given by the desired spacing.

At the equilibrium condition, the equation that describes the states assumes the value:

$$\bar{x}_n^* = -A^{-1} B \bar{u}^0$$

Provided that:

$$-A^{-1} B = \begin{bmatrix} 1 & \frac{1}{\omega_N^2} \\ 0 & 0 \end{bmatrix}$$

It results that:

$$\bar{x}_n^* = \begin{pmatrix} \Delta x_n^* \\ 0 \end{pmatrix}$$

Besides being consistent with the genesis of the model, this proves that the equilibrium does not depend on any parameter of the dynamic process.

An example is reported below, where the values ω_F=0.1 and ω_N^2=0.0225 have been arbitrarily fixed for exemplification purposes:

$$\begin{pmatrix} \Delta\dot{x}_n^t \\ \Delta\dot{v}_n^t \end{pmatrix} = \begin{bmatrix} 0 & 1 \\ -0.0225 & -0.1 \end{bmatrix} \begin{pmatrix} \Delta x_n^t \\ \Delta v_n^t \end{pmatrix} + \begin{bmatrix} 0 & 0 \\ 0.0225 & 1 \end{bmatrix} \begin{pmatrix} 30 \\ 0 \end{pmatrix}$$

The chart representing the spacing (Δx_n^t) in the event of initial conditions $\begin{pmatrix} 70 \\ -3 \end{pmatrix}$ and desired equilibrium spacing $\Delta x_n^* = 30$ is depicted in the following Figure 25. The settling time ($t_s \approx 92$ seconds) that can be measured on the chart confirms the ones that can be computed from the theoretical equations.

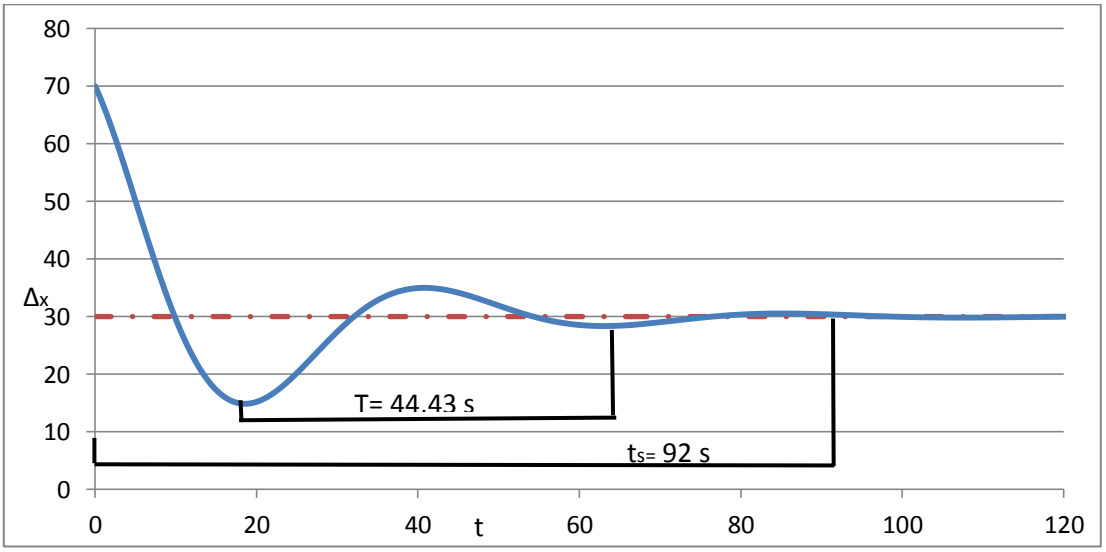

Figure 25 - Example for the dynamics of the state-space model

When the leader's kinematic is considered the analytical form of the response can't be defined *a priori*. Indeed, drivers (then leaders) performances are conditioned by distractions, variable skills in controlling the vehicle and unpredictable changes in the level of attention and, as a consequence, it is very hard to observe a trajectory in which the leader maintains a constant speed for a long time; moreover they usually do not follow a specific law while driving and for this reason any hypothesis can be done, when their accelerations are used as stimulus for the state-space model, in order to particularize the form of the input. An example of leader's generic trajectory collected on the road in Italy (trajectory 1 of the experiment described in Section 0) is reported in Figure 26 below. The trajectory refers to a *true* leader because it was not conditioned by the presence of other vehicles ahead.

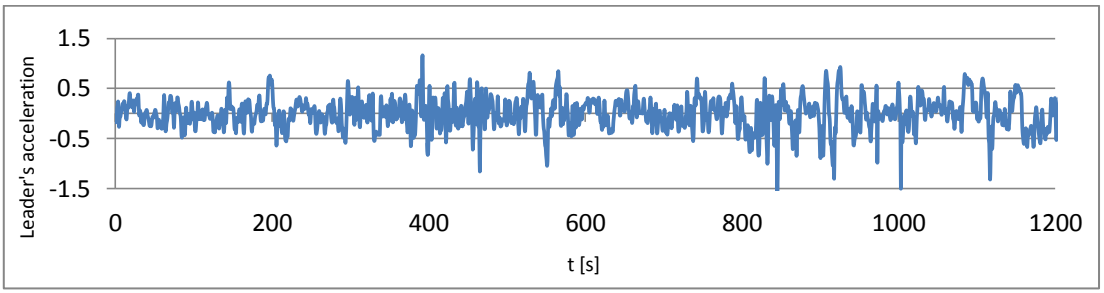

Figure 26 - Example for a leader's trajectory, smoothed as discussed in Appendix A

In correspondence to the previous leader's trajectory (with variable speed), the car-following process expressed by the state-space model used in Figure 25 results to be (with reference to the dynamics of the spacing) as in Figure 27 and Figure 28. It is worth noting that the follower tries to achieve the desired spacing Δx_n^* but the process is continuously un-stabilized by the leader. Interestingly, for the whole trajectory the stable condition is not reached at all. Of course this could be due not only to oscillation of the leader's speed around a stable value, but also on different values of the leader's speed (or even on different leaders during the trajectory).

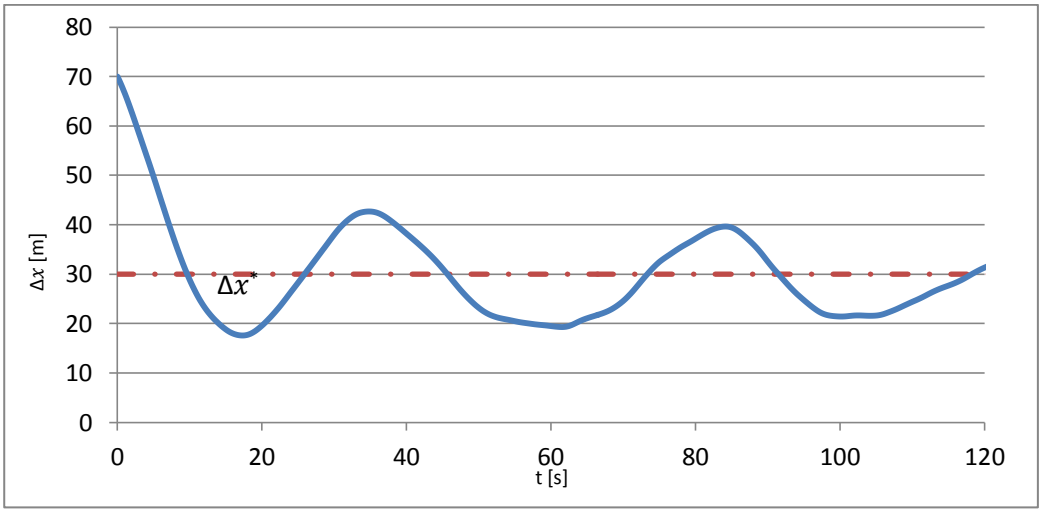

Figure 27 - Example of the dynamics of the state-space model as biased by a non-constant leader' speed in the same time interval of Figure 25

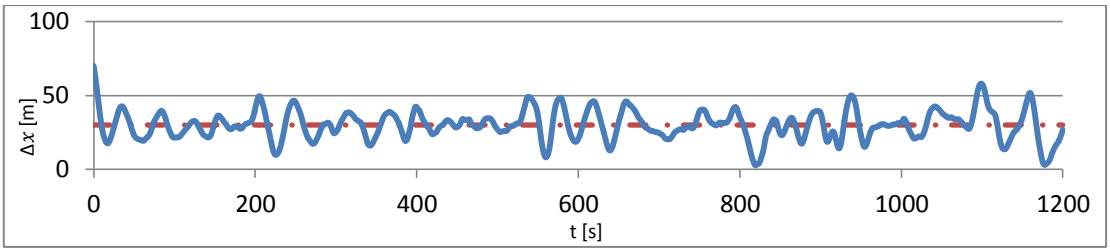

Figure 28 - Example of the dynamics of spacing (non-constant leader' speed), whole trajectory

3.2.3 Reinterpreting the AP model in view of the state-space model

As already introduced in Section 1 and also above in this section, the car following behaviour has been often studied using the so-called *car following spirals*. These spirals are described by observed data once depicted in the Cartesian plane Δx_n^t , Δv_n^t, as stylized again, for reader convenience, in next Figure 29.

The classical car-following spiral of the AP model is consistent with the state space model introduced in the previous. Actually, as already stated, in this representation it basically is the *phase portrait* of the state-space dynamic system.

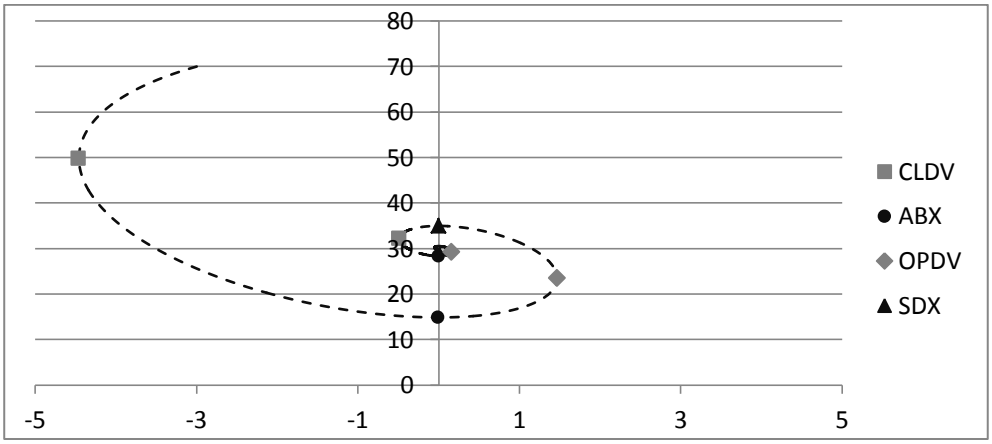

Figure 29 - Example of a car-following spirals

Now consider the next figure, where the same points have been identified on the plot in the time domain of Δx_n^t, Δv_n^t and $\Delta \dot{v}_n^t$:

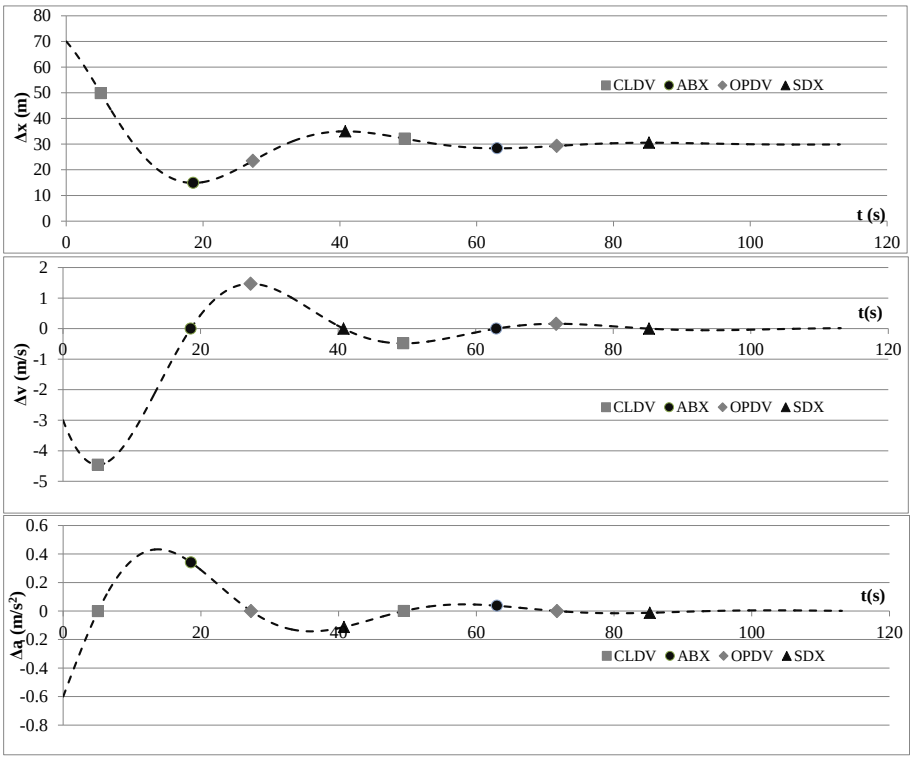

Figure 30 - Identification of ABX, SDX, CLDV and OPDV (IPs) in the time domain plots of spacing, relative speed and relative acceleration (leader's velocity is constant)

It is evident from Figure 30 that if the state-space model is used in order to interpret the car-following process, then the ABX, SDX, CLDV and OPDV points can be analytically identified by the following two conditions:

- ABXs and SDXs are points in which the function $\Delta\dot{x}_n^t = \Delta v_n^t$ assumes null values; in correspondence to ABXs the function $\Delta\dot{v}_n^t$ assumes a positive value, while it is negative for SDXs;
- CLDV and OPDV represent respectively the local minimum and maximum of the Δv_n^t, they are identifiable when the $\Delta\dot{v}_n^t$ assumes a null value.

In the event that the leader has a constant speed, then $\Delta\dot{v}_n^t = -\dot{v}_n^t$ and the analytical conditions for identifying the IPs depend only on the follower's behaviour. Moreover, the main parameters of the process are fully known and also the frequency of the IPs can be analytically identified. In fact, it should be noted that the functions Δv_n^t and $\Delta\dot{v}_n^t$ are continuous in the generic range [α,β], where α and β represent two consecutive points of local maximum/minimum of the functions, and they assume opposite sign in the extremes of the range. Hence they respect the hypothesis of Bolzano's theorem (Intermediate Value Theorem), that is exists at least one null value point. Moreover, as the functions in the same range are monotonically increasing/decreasing, there is only one point in which the functions assume a null value. In these events, the previous are necessary and sufficient analytical conditions for the identification of ABX, SDX, CLDV and OPDV points of the trajectory.

All the previous demonstrate that, under the proposed state-space interpretation of the car-following model, different experimental laws under the selected points do not exist, but they are all particular points of a single function; the calibration of only one model ensures the knowledge of the whole evolution of the phenomena.

3.2.4 The bias from non-constant leader's speed

Most of the previous analyses depend on the assumption that the leader cruises at a constant speed. As already shown in Section 3.2.2 (but also discussed, for the AP paradigm, in section 3.1.2), the process becomes less intelligible when the interference of the leader's behavior is relevant. The behavior can be still studied using the *phase portrait*, but some of the analytical properties introduced before are no more ensured.

In the previous example, the $\Delta\dot{v}_n^t$ function (and consequently the Δv_n^t) is monotonically increasing for any given $\dot{v}_{n-1}^t$, but if $\dot{v}_{n-1}^t$ is not constant the monotonicity of the functions is not ensured. As a consequence, said again α and β two consecutive points of local maximum/minimum of the functions, more than one null value can be observed; this means that the analytical conditions for identifying

the IPs are only necessary and not sufficient: also some false IPs could be identified in case of the application of the analytical conditions, because given conditions for ABX/SDX or CLDV/OPDV could be respected even in some points that are not IPs.

In practice the paradigm is still valid, but different practical tools have to be employed in order to estimate the main figures of the model (mainly, APs and desired spacing). Such a tool, at least for what concerns the identification of the APs, has been reported in the *Appendix B – Empirical procedure for APs* to which the reader can refer for any detail and has been verified, for what concerns the respect of necessary conditions in the *Appendix C – Validation of the empirical procedures for APs*. From this reason it will be used forward for any situation where sufficient conditions are not applicable.

3.2.5 Identification results and their discussion

The identification process has been carried out using the Matlab® System Identification Toolbox. It is out of the scope of this paper to describe the identification algorithm (for more information refer to Ljung, 1987), but some relevant information have to be known:

- the model introduced is a so-called *grey-box* model (the matrix A and B are known and only 2 parameters have to be estimated);
- the used procedure needs the knowledge of the inputs and outputs time-sequence;

Inputs and outputs can be obtained from observed data except for the desired spacing; then an estimation of the desired spacing (Δx_n^*) for the state-space model can be computed from APs as shown in *Appendix D – Estimation of the desired spacing by APs*. There, in order to validate the tool, the desired spacing is computed for a synthetic trajectory with known desired spacing (with leader's constant speed); the computation has been carried out both with reference to the analytic identification and by averaging APs. The comparison between the averaging estimate and the analytical result shows that the estimating heuristic performs very well. In the event of real data, only the averaging method can be used, being the analytical one unavailable because of the non-constant leader's speed. This methodology has been used also for the results of this Section.

The results of the identification procedure are presented in this Section from two points of view. First of all, the values of the estimated parameters are computed for two datasets, that are those obtained from experiments described in Section 2.1and 2.2; also the effects of the parameters on the process stability and on the analytical form of the natural response are discussed; the consistency with some

observations from the experiments described in Section 2.3 is discussed too. After this, the performance of the model in reproducing observed behaviors (again with reference to experiments described in Section 2.1and 2.2) is shown and discussed.

3.2.6 Results of the identification of the state-space model

In the next Table VII and Table VIII, the values of the estimated parameters for both datasets are presented. These have been obtained by using the Matlab® System Identification Toolbox already presented.

Table VII - Parameters evaluated in the First Italian experiment

Italian Dataset			
n	ω_N^2	ω_F	**Response**
1	0.096241	0.652196	stable over-damped
2	0.018555	0.86647	stable over-damped
3	0.031801	1.103089	stable over-damped
4	0.007628	0.512808	stable over-damped
5	0.017726	0.458321	stable over-damped
6	0.004557	0.300702	stable over-damped
7	0.01285	0.349806	stable over-damped
8	0.084112	1.215347	stable over-damped
9	0.022944	0.119139	stable under-damped
10	0.000818	0.779928	stable over-damped
11	0.097578	1.304557	stable over-damped
12	0.054844	0.407822	stable under-damped
13	0.022777	0.487586	stable over-damped

Table VIII - Parameters Evaluated in the English experiment

English Dataset			
n	ω_N^2	ω_F	**Response**
1	0,000081	0,170362	stable over-damped
2	1,07652E-07	0,723565	stable over-damped
3	0,000000	0,644559	stable over-damped
4	2,28693E+07	1,09543E+08	stable over-damped
5	0,014391	1,208078	stable over-damped
6	1,48439E+07	9,37809E+07	stable over-damped
7	0,030141	1,550133	stable over-damped
8	0,000000	0,621657	stable over-damped
9	0,008538	1,039101	stable over-damped
10	0,000922	0,897501	stable over-damped
11	1,46058E-07	0,980712	stable over-damped
12	0,011842	0,601806	stable over-damped
13	0,003788	0,887227	stable over-damped
14	7,62823E+07	4,71334E+08	stable over-damped
15	0,020687	0,239213	stable under-damped
16	9,24323E-08	0,621260	stable over-damped
17	0,104271	1,365767	stable over-damped
18	5,70374E-08	1,658468	stable over-damped
19	0,000065	0,913520	stable over-damped
20	1,33843E-07	0,901378	stable over-damped
21	1,72536E-07	1,208643	stable over-damped
22	0,009766	0,613243	stable over-damped
23	1,84467E+08	2,58331E+08	stable over-damped
24	0,000001	1,229436	stable over-damped
25	0,079398	1,193299	stable over-damped

26	1,82443E+07	1,02245E+08	stable over-damped
27	1,37098E+06	1,21527E+08	stable over-damped
28	0,018393	0,527545	stable over-damped
29	4,91762E+07	1,76881E+08	stable over-damped
30	0,000312	1,074471	stable over-damped
31	2,30612E+08	2,33423E+09	stable over-damped
32	0,567879	21,272505	stable over-damped
33	0,020224	0,663724	stable over-damped
34	0,000027	0,790337	stable over-damped
35	0,033283	0,528995	stable over-damped
36	6,48464E-08	0,435426	stable over-damped
37	0,001695	0,414457	stable over-damped
38	0,036235	1,387731	stable over-damped
39	0,002764	1,074494	stable over-damped
40	0,027301	0,691428	stable over-damped
41	0,018567	0,747872	stable over-damped

The first element to be noted is the sign of the parameters, that is always positive in both datasets. This confirms that the hypothesis of *rational* driving behavior introduced in Section 3.2 is realistic. Moreover it implies, for what concerns the stability of the state space model, that responses of the model are always stable. It is interesting to note that using conditions introduced in Section 3.2.1 an analysis of the analytical form of the response can be done; in particular in the Italian dataset in two cases the response has an under-damped form, while in the other 11 it is over-damped. Similarly in the English dataset only one trajectory (between the 41 considered) has an under-damped response.

Another interesting question to be addressed concerns the values of the parameters. In particular in the U.K. dataset, trajectories numbered 4, 6, 14, 23, 26, 27, 29, 31 and 32 present values exceptionally high; such values lead to an exceptionally rapid response. The rapidity of the response is confirmed by the observed data; however, the identified parameters are rather extreme.

In order to better analyze this phenomenon, it is preferable to focus on the corresponding eigenvalues, given that they give a more evident information with respect to the response of the model. Indeed, the trajectory of the system in the phase plot evolves in accordance with the direction of the eigenvectors, as it will be detailed in the following. The eigenvalues have been computed for all the trajectories of the English dataset by using the already introduce formula:

$$\lambda_{1,2} = -\frac{1}{2}\omega_F \pm \frac{1}{2}\sqrt{\omega_F^2 - 4\omega_N^2}$$

Computed values are reported in Table IX.

For sake of simplicity, the analyses is here continued by only referring to the case of over-damped solutions (real and distinct eigenvalues) which are almost the generality of the English parameters and can be interpreted in an easier way by using the phase portraits.

Given the structure of A, the eigenvectors can be obtained as:

$\bar{v}_1 = \begin{pmatrix} p \\ p\lambda_1 \end{pmatrix}$ and $\bar{v}_2 = \begin{pmatrix} p \\ p\lambda_2 \end{pmatrix}$, where p is an arbitrary constant to be chosen.

Eigenvalues and eigenvectors give information with respect to the trajectory of the dynamic system in the phase-plane, in particular the eigenvectors can be used to understand the direction of the field (they represent straight lines in the phase-plane), while the eigenvalues give information related to the speed of the response in each direction. In stable systems, the smaller is the eigenvalue, the faster is the response in the direction of the associated eigenvectors.

Table IX – Eigenvalues computed in the English experiment

English Dataset			
n	λ_1	λ_2	**Response**
1	-0,00048	-0,16988	stable over-damped
2	-1,5E-07	-0,72357	stable over-damped
3	-1,5E-07	-0,64456	stable over-damped
4	-0,20877	-1,1E+08	stable over-damped
5	-0,01203	-1,19605	stable over-damped
6	-0,15828	-9,4E+07	stable over-damped
7	-0,01969	-1,53044	stable over-damped
8	-1,5E-07	-0,62166	stable over-damped
9	-0,00828	-1,03082	stable over-damped
10	-0,00103	-0,89647	stable over-damped
11	-1,5E-07	-0,98071	stable over-damped
12	-0,02037	-0,58144	stable over-damped
13	-0,00429	-0,88294	stable over-damped
14	-0,16184	-4,7E+08	stable over-damped
15	-0,1196+0.08i	-0,1196-0.08i	stable under-damped
16	-1,5E-07	-0,62126	stable over-damped
17	-0,08117	-1,2846	stable over-damped
18	-3,4E-08	-1,65847	stable over-damped
19	-7,1E-05	-0,91345	stable over-damped
20	-1,5E-07	-0,90138	stable over-damped
21	-1,4E-07	-1,20864	stable over-damped
22	-0,01636	-0,59688	stable over-damped
23	-0,71407	-2,6E+08	stable over-damped
24	-8,2E-07	-1,22944	stable over-damped
25	-0,07073	-1,12257	stable over-damped
26	-0,17844	-1E+08	stable over-damped
27	-0,01128	-1,2E+08	stable over-damped
28	-0,03754	-0,49001	stable over-damped
29	-0,27802	-1,8E+08	stable over-damped
30	-0,00029	-1,07418	stable over-damped
31	-0,0988	-2,3E+09	stable over-damped
32	-0,02673	-21,2458	stable over-damped
33	-0,03202	-0,63171	stable over-damped
34	-3,5E-05	-0,7903	stable over-damped
35	-0,07299	-0,45601	stable over-damped
36	-1,5E-07	-0,43543	stable over-damped
37	-0,00413	-0,41032	stable over-damped
38	-0,02662	-1,36111	stable over-damped
39	-0,00258	-1,07192	stable over-damped
40	-0,04204	-0,64939	stable over-damped
41	-0,02571	-0,72216	stable over-damped

In summary, given the value of the two parameters , it is possible to compute: the A matrix, the eigenvalues and the eigenvectors. Thus, a qualitative trend of the natural response of the model in the phase plane can be obtained depending on different initial conditions. An example is reported in the next Figure 31 where ω_F=1.2 and ω_N^2=0.2 have been arbitrary chosen.

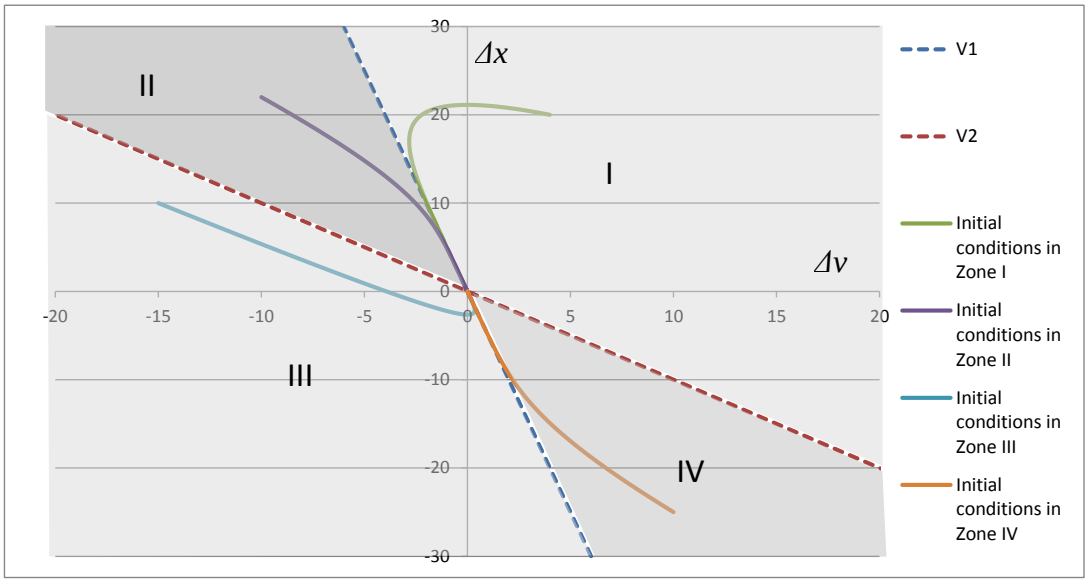

Figure 31 - Qualitative trends of the natural response, depending on eigenvectors and for different initial conditions

From the previous Figure can be also noted that patterns obtained from initial conditions that fall in the I and III zones are more consistent with our observation of how car-following spirals evolve, the others evolve in a somehow unusual direction. It is worth noting that the width of the four zones depend on eigenvalues.

As it can be noted from Table IX, consistently with the exceptionally high values of the parameters, trajectories labeled with the numbers 4, 6, 14, 23, 26, 27, 29, 31 and 32 present one of the eigenvalues with an exceptionally low value. An immediate consequence of this can be found in the position of the second eigenvector that becomes almost horizontal in our representation. From the analysis of Figure 31, an horizontal eigenvector is associated with an horizontal direction of the initial part of the trajectory and thus with an high value of the initial relative acceleration.

Figure 31 is particularized in the following, with reference to the English trajectories with extreme parameters and with reference to their actual initial conditions, as depicted in Figure 32 below.

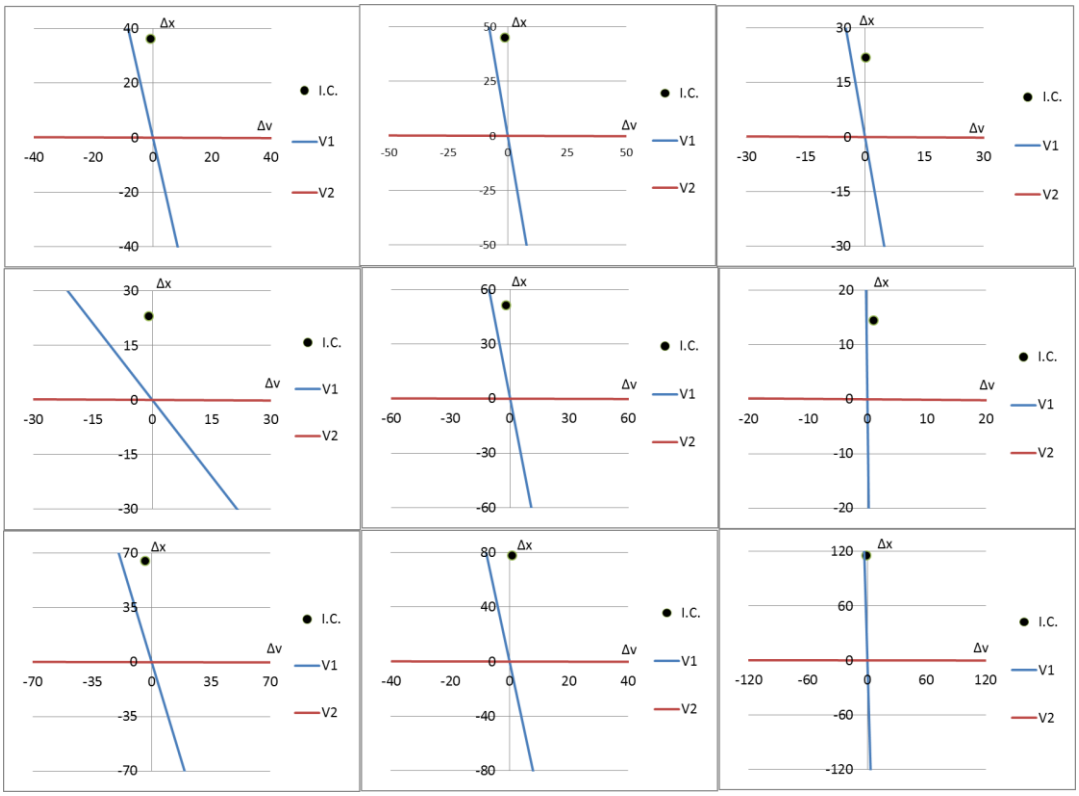

Figure 32 - The initial conditions of the nine trajectories depicted with respect to eigenvectors

Independently from the eigenvectors (and then from the width of the four zones) the initial conditions fall for all the considered cases in the zone which has been previously indicated as I.

As stated in the previous Section, given the initial conditions and the value of the parameters of the model, an analytical solution for the state of the model can be given using the modal expansion. In particular in next equations Δx_n^t, Δv_n^t and $\Delta \dot{v}_n^t$ have been reported ($\Delta \dot{v}_n^t$ has been obtained computing the time derivative of the Δv_n^t):

$$\Delta x_n^t = c_1 e^{\lambda_1 t} + c_2 e^{\lambda_2 t}$$
$$\Delta v_n^t = \lambda_1 c_1 e^{\lambda_1 t} + \lambda_2 c_2 e^{\lambda_2 t}$$
$$\Delta \dot{v}_n^t = {\lambda_1}^2 c_1 e^{\lambda_1 t} + {\lambda_2}^2 c_2 e^{\lambda_2 t}$$

Thus, the consequence of the exceptionally high parameters can be evaluated in terms of initial value of the relative acceleration imposed by the model. Actually, the parameters lead to unfeasible values of relative acceleration, as reported in next Table X.

Table X - The initial value of relative acceleration computed in the case of extremely high values of the parameters

English Dataset			
n	Δx_n^0	Δv_n^0	$\Delta \dot{v}_n^0$
4	36,35	-0,69	-1,10E+08
6	45,01	-1,1	-9,38E+07
14	21,94	0,24	-4,71E+08
23	23,07	-0,89	-2,58E+08
26	51,41	-2,03	-1,02E+08
27	14,43	1,06	-1,22E+08
29	64,95	-3,92	-1,77E+08
31	77,95	0,78	-2,33E+09
32	115,27	-0,98	-2,12E+01

The reason of these unfeasible values comes from numerical troubles of the optimization algorithm used for the identification of the model; a standard algorithm has been used and it is not one of the major focuses of this work.

The numerical nature of the troubles are evidenced by the fact that the most extreme of the eigenvalues can be bounded without actually changing the fitting properties with observed data. Indeed, if new bounded values are computed, such as the maximum initial value of the relative deceleration is not greater than an arbitrary threshold (fixed at - 4 m/sec^2), then the actual trajectory of the resulting dynamic system is not really different from the unbounded case. The value of the constraining deceleration is high enough; however, it is feasible and it should be considered that the main reason of the extreme values identified by the algorithm is related to the high relative deceleration observed.

Actually, it is also possible to see for any of the trajectories that if the eigenvalue λ_2 varies, given the initial conditions and λ_1, then the trajectories tend to become undistinguishable. An example is reported for the natural response of our state space model in the next Figure 33 where the evolution of the state variables with respect to the time have been plot with respect to different values of λ_2, given the initial conditions and λ_1 that have been fixed respectively to Δx_n^0=25, Δv_n^0=-2 and λ_1=-0.15.

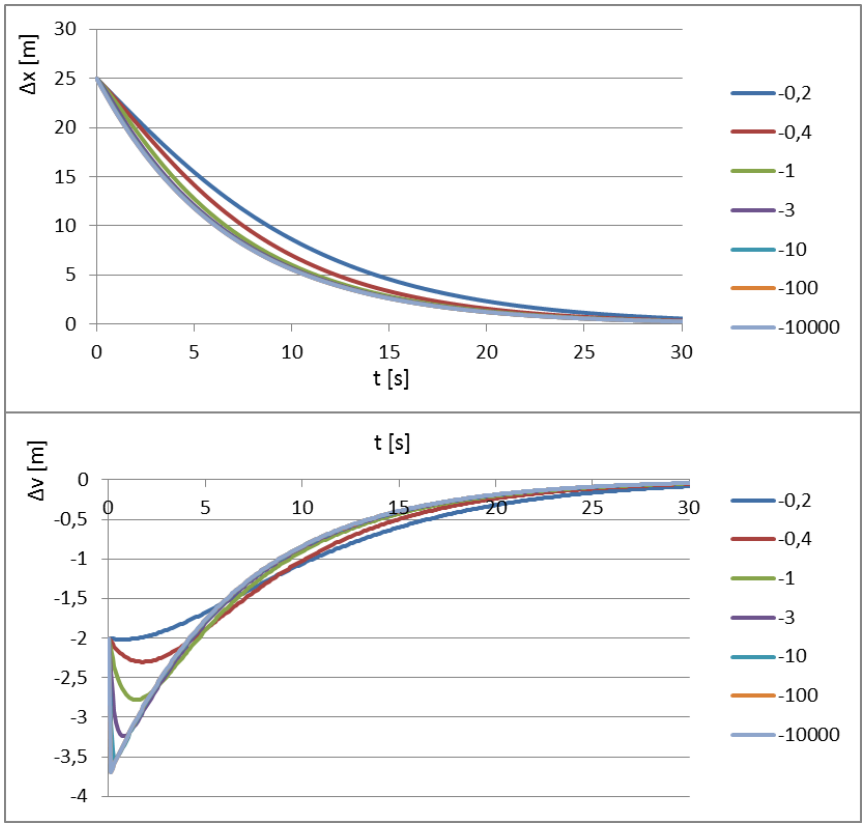

Figure 33 - The evolution of the state variables computed from different values of one of the eigenvalues

The effect of bounding the initial relative acceleration is evaluated in the following by applying to all the trajectories with extreme parameters the procedure described below.

The values of the parameters obtained for the trajectories indicated in Table X are recomputed in order to obtain a similar pattern for the state variables as well as a feasible value for the initial condition of the relative acceleration. Operatively, for these trajectories:

- an arbitrary threshold value of the initial relative deceleration imposed by the model has been chosen (in this case $\dot{\Delta v}_n^0 = -4\ m/sec^2$);
- the eigenvalue λ_1 has been left the same, while λ_2 has been changed in order to obtain a value of the initial deceleration that is not greater of the chosen threshold;
- the values of ω_F and ω_N^2 have been updated with respect the bounded value of λ_2.

The consequences of this process have been reported in the next Table XI

Table XI - The fixed values obtained as a consequence of the imposed threshold

English Dataset				
n	λ_1	λ_2	ω_N^2	ω_F
4	-0,20877	-0,60	0.1253	0.8088
6	-0,15828	-0.69	0.1092	0.8483
14	-0,16184	-1.04	0.1683	1.2018
23	-0,71407	-0,88	0.2200	1.1300
26	-0,17844	-0.61	0.1088	0.7884
27	-0,01128	-3.25	0.0367	3.2613
29	-0,27802	-0.562	0.1000	0.7400
31	-0,0988	-0.46	0.0454	0.5588
32	-0,02673	-1.89	0.0505	1.9167

The constraint on the values of the parameters neither has actually changed the trend of the response of the model (the initial conditions still fall in the zone I, Figure 34), nor the evolution of the state variables (in particular with reference to spacing, Figure 35).

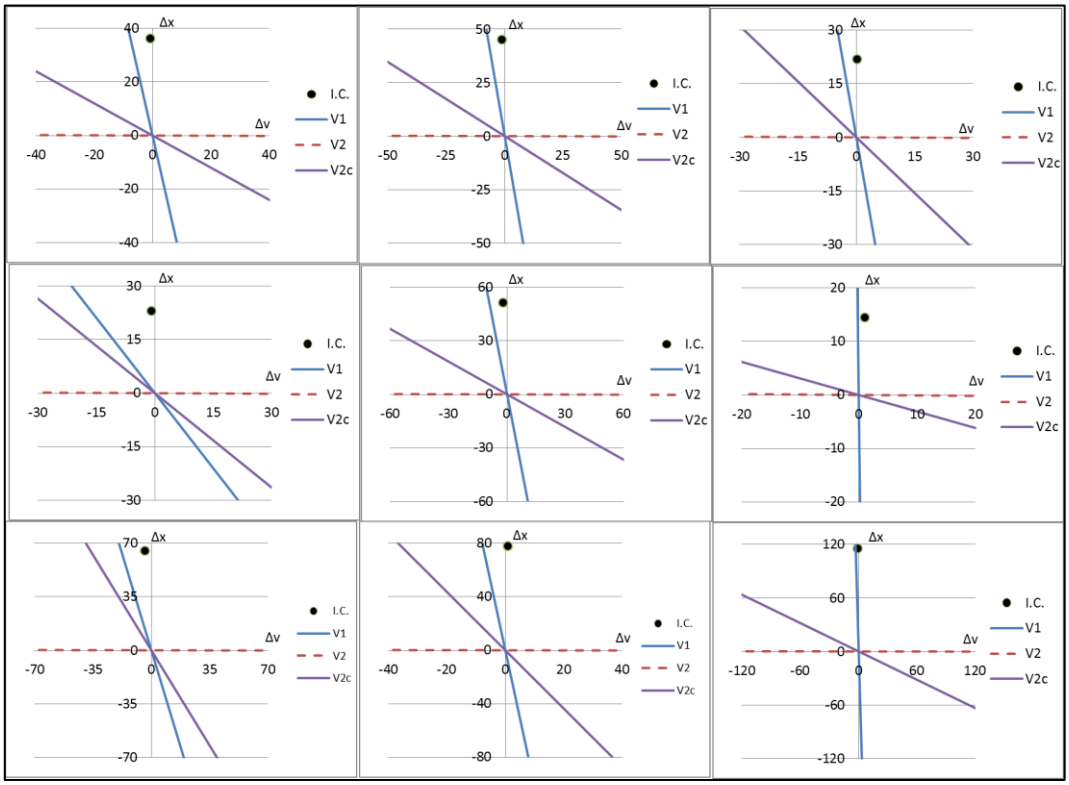

Figure 34 - The effect of the constraints on the slope of eigenvectors and the new width of the four zones

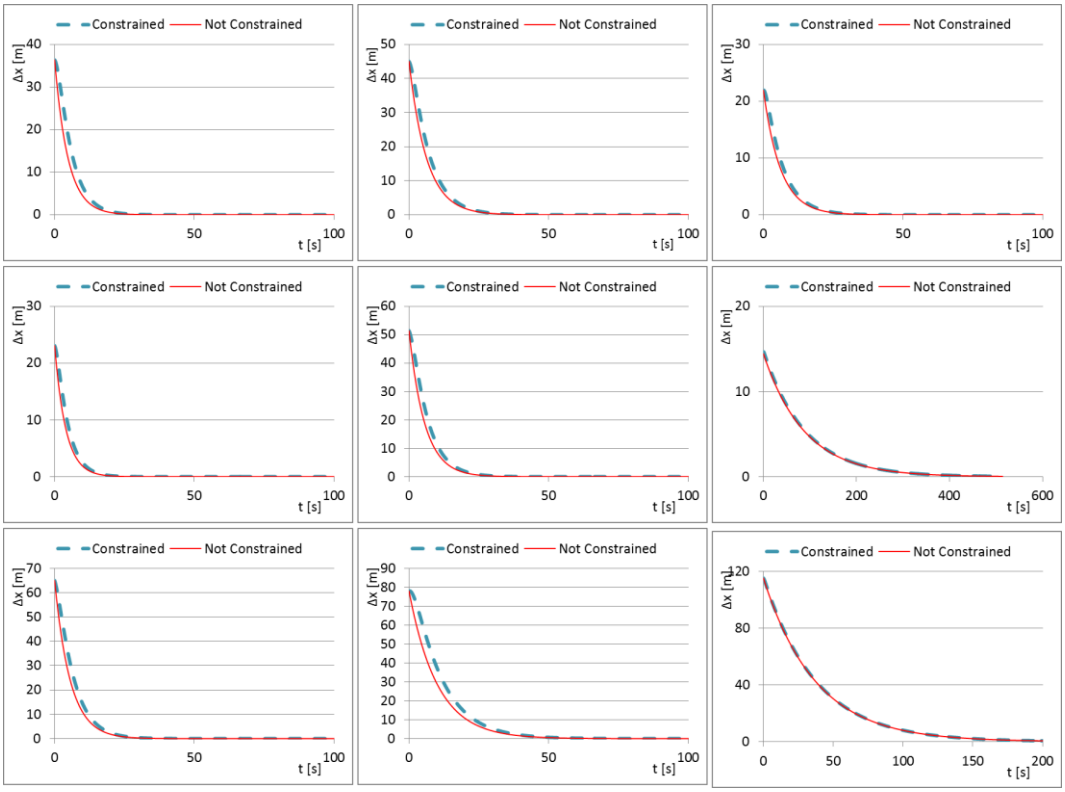

Figure 35 - The comparison between the spacing evolution using unconstrained and constrained value of the parameters

Apart of numerical troubles due to the algorithm, the extreme values are also due to high relative deceleration that the model has to impose in order to fit the observed driving behavior. The occurrence of the extreme values in the UK dataset could be not due to differences in driving style but, rather, to differences in observed stimuli. In fact, the presence of trajectories with relatively poor stimuli (in the sense of almost null leader's acceleration) helps a quick stability and so more evident exponential patterns, mathematically produced by higher values of the parameters. It should be noted anyway that so fast and stable responses could be not so common to be observed, but for sure are not un-realistic. To validate the previous statement, consider next Figure 36 where some trajectories obtained from the experiment described in Section 2.3 (point ii) have been plot.

In particular the three rows of Figure 36, show patterns observed respectively at 80, 100 and 120 km/h. It is worth noting that the approaching process started for each pattern from different initial conditions (this depends on the actual position of the two vehicles when the maneuvers started that were conditioned by local/random traffic conditions). Moreover the gap-closing processes last differently between experiments; this depends on the leader's speed (approaching to a faster leader requires a more challenging control of the vehicle), but also on driver's preferences. In particular in the left side of the figure faster maneuvers have been depicted.

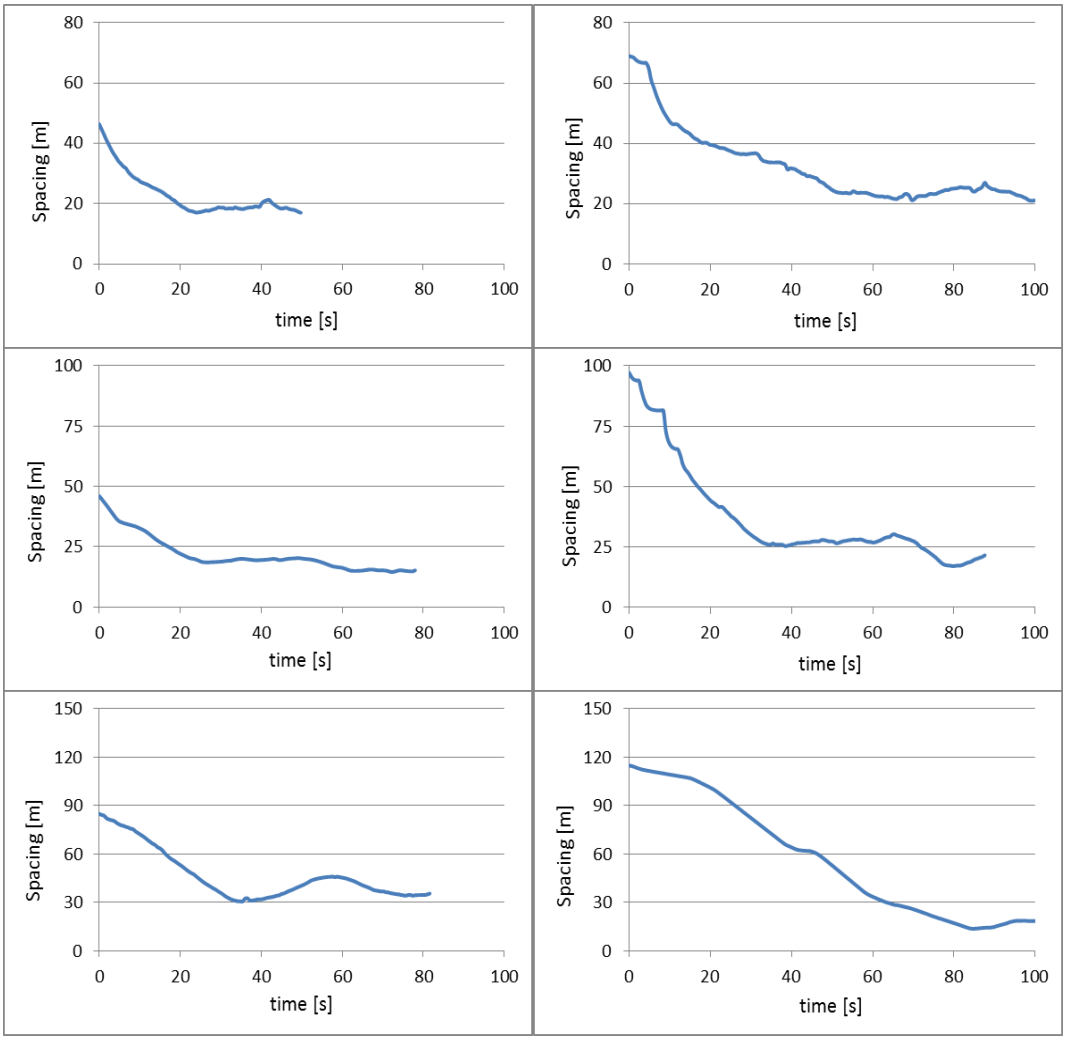

Figure 36 - Observed responses from a leader with a constant speed; the speed of the leader is respectively 80km/h (first row), 100 km/h (second row) and 120 km/h (third row).

Results of the identification procedure applied for experimental cases similar to those depicted in Figure 36 give again exceptionally high parameters of the model As an example, the parameters identified in three maneuvers of five drivers (randomly selected from the participants) as well as an example of model response have been reported respectively in the following Table XII and Figure 37

Table XII - Identification parameters from five randomly chosen drivers of the Second Italian Experiment

Leader's Speed	ω_N^2	ω_F
80	9,57E+07	6,29E+08
	1,97E+07	7,45E+07
	6,09E+07	4,21E+08
	1E+08	5,53E+08
	3,34E+13	3,7771E+14
100	5,39E+08	1,56E+09
	2,44E+08	2,65E+09
	1,28E+04	9,86E+04
	1,23E+07	2,03E+08
	3,8E+13	4,45E+14
120	3,71E+13	2,99E+14
	4,10E+07	2,71E+08
	3,8E+13	4,45E+14
	7,03E+07	2,84E+08
	1,9E+08	1,29E+09

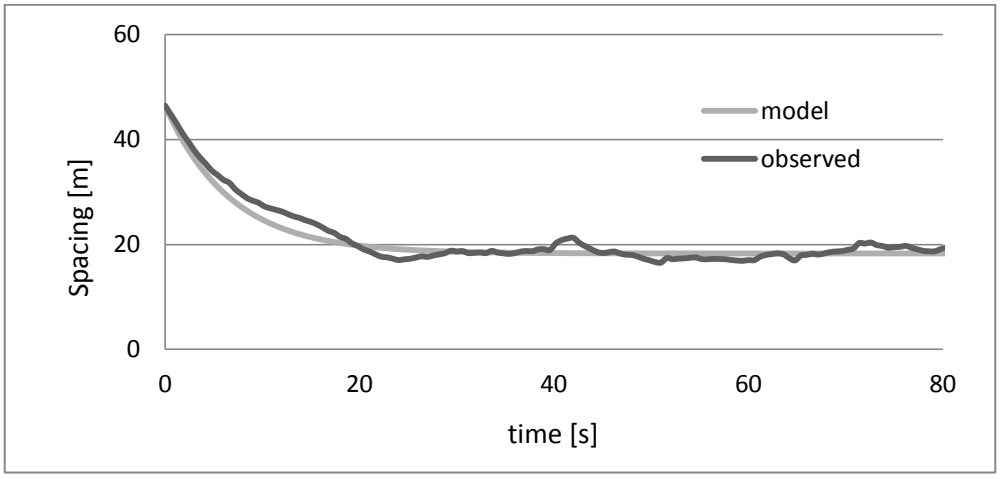

Figure 37 - The comparison between observed pattern and response of the model; the speed of the leader is 80 km/h

Again values extremely high of the parameters are obtained and then, also in this case, they should be treated in the same way as those obtained in the UK dataset.

It is worth noting that the discussed situation is independent from the length of the observed trajectory (unless the fact that a longer trajectory can conduct to observe more stimuli), in fact similar parameters (and consequent responses of the model) can be obtained also in longer observations.

To confirm this, a new ad-hoc car-following trajectory has been collected in Italy on the A30 Motorway. Once again the instrumented vehicle has been used in an active mode, following a confederate vehicle cruising at 100 km/h. In this experiment the confederate vehicle was equipped with a conventional cruise control; this allows to consider practically negligible the input of the state-space model corresponding to the leader's acceleration, because the constant-speed of the leader was maintained for several kilometres. The results of the identification

procedure (see Figure 38 below) show that the desired equilibrium spacing is 27.8 meters, the parameters of the state space model are ω_N^2=6.08E+07 and ω_F=2.09E+08, which are quite *extreme* values, typical of a trajectory that very quickly reaches stable equilibrium.

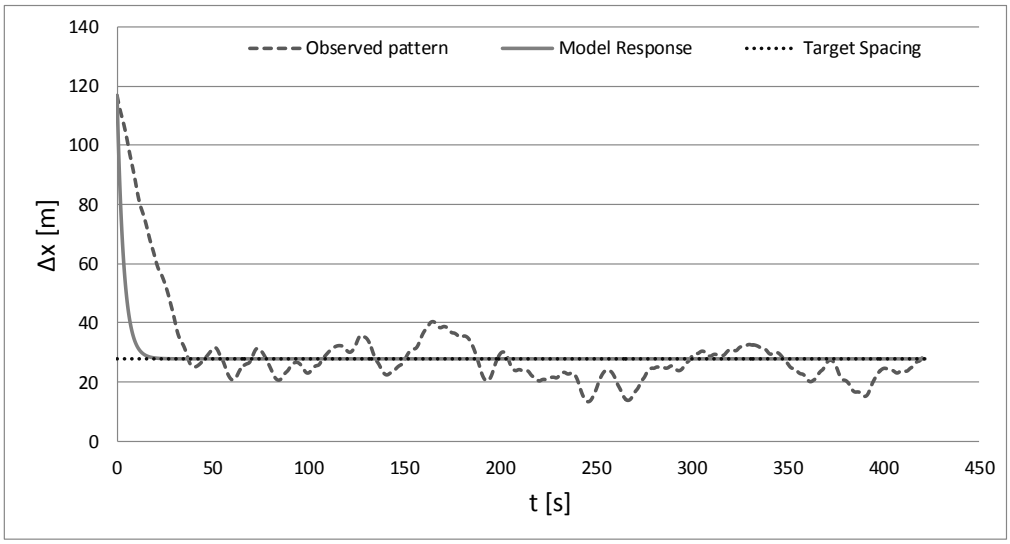

Figure 38 - Ad-hoc experiment in Italy

Ultimately exceptionally high parameters values have been obtained also in less controlled experiment in which any corporate vehicle has been used and then driver has followed a random leader. This situation has occurred some times in the last part of the experiment described in Section 2.3 (point iii) where the drivers have gone across the national roadway s.s.268. An example for this has been reported in the next Figure; there the observed spacing, the response of the model (parameters are respectively ω_N^2=1.96E+07 and ω_F=7.45E+08) and the observed leader's speed have been reported; it can be noted that also in this case the acceleration of the leader is not negligible nor particularly high.

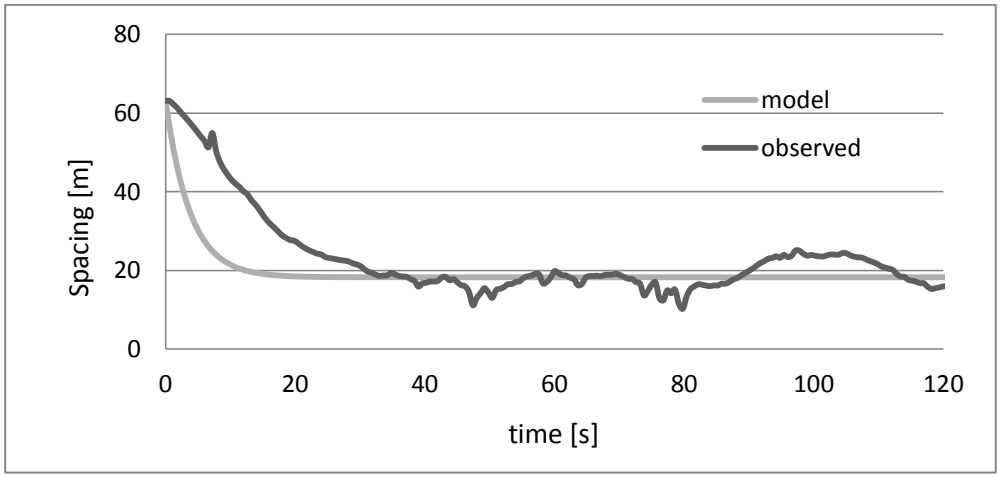

Figure 39 - Results of the identification procedure in an un-controlled car-following process

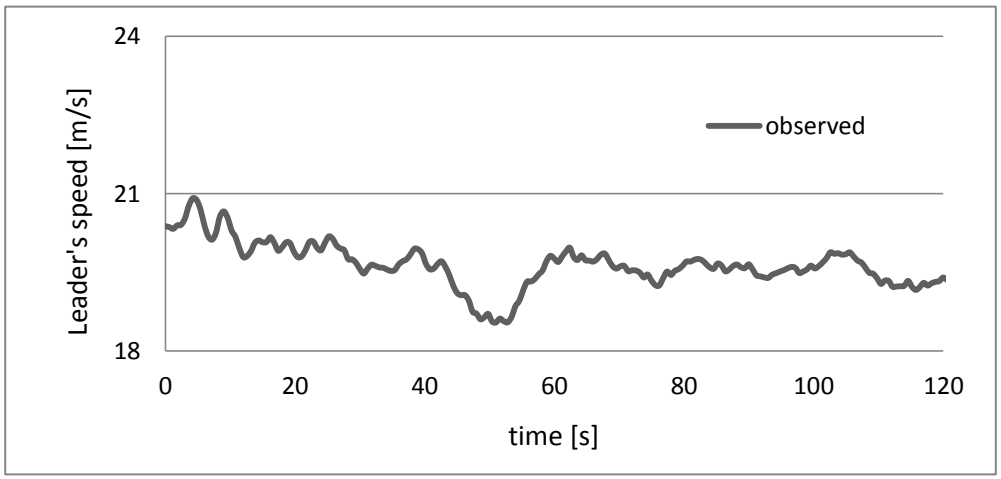

Figure 40 - Leader's speed in an un-controlled car-following process

Thus the typical conditions encountered in the UK dataset for short trajectories and for UK drivers were effectively replicated for longer trajectories.

This shows that parameters typical of the UK dataset are also obtained for Italian driving behaviours, in the event that the car-following process is characterised by very uniform driving contexts. In other terms, it is not a matter of driving style, rather the combination of a partially ineffective identification algorithm, combined with particular leaders' stimuli.

Table XIII - Some statistics on parameter computed in the considered datasets

	Italian Dataset		**English Dataset**	
	ω_N^2	ω_F	ω_N^2	ω_F
mean	0.0363	0.6583	0,0138	0,8627
st. dev.	0.0336	0.3709	0,0232	0,3594
max	0.0976	1.3046	0,1043	1,6585
min	0.0008	0.1191	5,704E-08	0,1704

Anyway, without considering these trajectories (4, 6, 14, 23, 26, 27, 29, 31 and 32), statistics on the parameters computed in the two datasets have been given in the Tables below; also a boxplot is given in the next Figure 41.

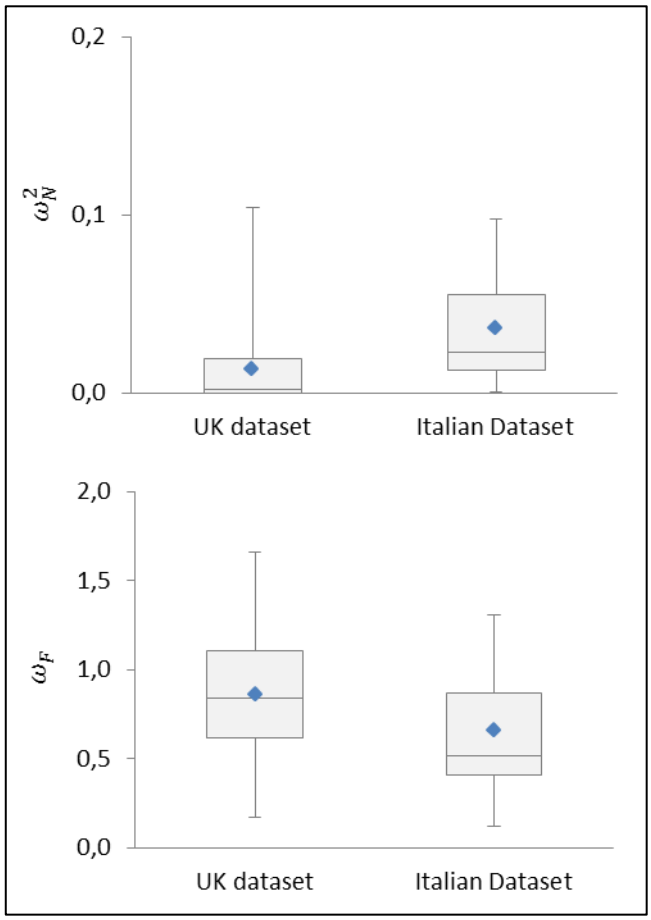

Figure 41 - The box-and-whisker plot for the two parameters evaluated with respect to the UK and Italian datasets

Another ad-hoc trajectory, observed in Italy with the same characteristic as that previously discussed, but produced by another driver, is shown in Figure 42. Also in this case, identification of the model (with an estimated desired spacing of 35 metres) gives ω_1=0.3113 and ω_2=5.768, that are similar in magnitude to the values found for the UK dataset, even if not extreme as in the previous cases. However, Figure 42 shows that the desired spacing was erroneously identified, since two different parts of the trajectory could be identified, one with desired spacing of about 45 metres and another (starting around at second 350) with a desired spacing of about 25 meters. Likely, the driver has adapted his desired spacing during the car-following session. At first he adopted a larger spacing and after some time (about 6 minutes) he accepted a shorter spacing, likely without external stimulus but

also because more at ease with driving. The procedure described in *Appendix D – Estimation of the desired spacing by APs* is not able to deal with such a phenomenon and a sort of averaged desired spacing has been estimated.

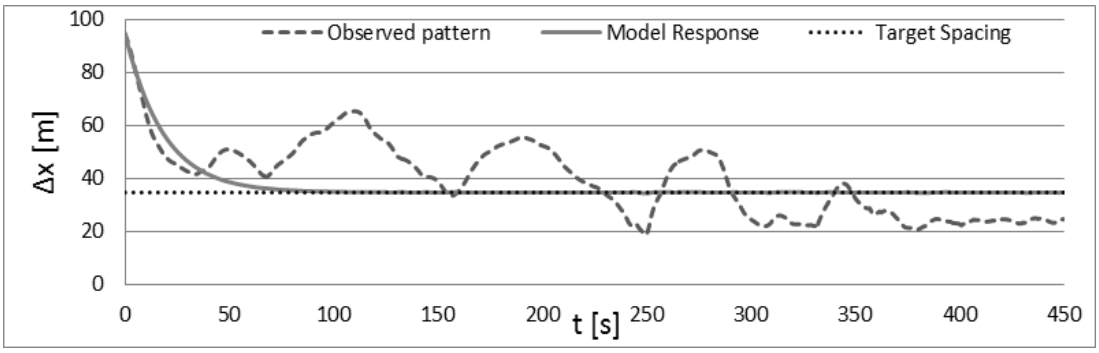

Figure 42 - Erroneous identification of the desired equilibrium spacing

This likely affects the whole response of the model with respect to the observed trajectory, as well as the values of the identified parameters. It is worth noting that this does not represent a problem of the state space model, but a limit of the methodology used for the evaluation of the target spacing.

These circumstances are likely to have occurred in 5 cases in the UK dataset, as it could be argued by next Figure 43, where model performances are shown.

The presence of those *multiple equilibrium-spacing* conditions in one trajectory is reflected in particular on the value of the parameter ω_1. Indeed the parameter represents the *weight* the model gives to the target spacing; the greater the dispersion of the equilibrium conditions observed in the trajectory, the less is the role the model has to assign to the unique (averaged) imposed equilibrium condition.

The performance of the models have also been evaluated comparing the observed data with the ones reproduced after the identification process. In particular, the output of a state-space model can be computed as a combination of states and inputs by appropriately setting matrix C and D in the following formula:

$$\bar{y}^t = C\bar{x}^t + D\bar{u}^t \qquad 21)$$

In this case, the two matrices are set as:

$C = \begin{bmatrix} 1 & 0 \\ 0 & 0 \end{bmatrix}$;

$D = \begin{bmatrix} 0 & 0 \\ 0 & 0 \end{bmatrix}$;

then the model output has been computed in terms of reproduced spacing.

The difference between the observed data and the model can be shown by means of the cumulative error distributions, where the error is defined as:

$$e = \frac{|\Delta x_m^t - \Delta x_{ob}^t|}{\Delta x_{ob}^t} \quad 22)$$

The distributions for both the IT and UK datasets have been shown hereafter:

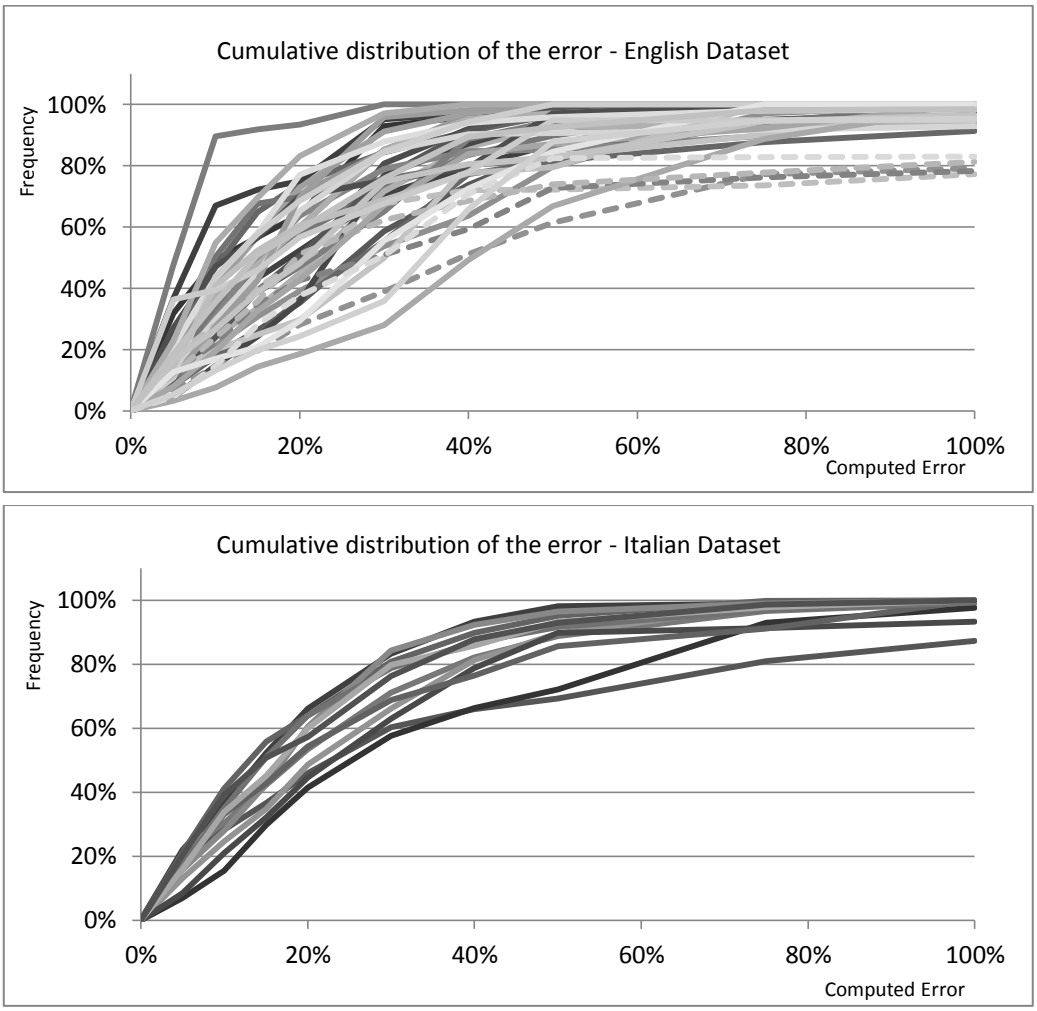

Figure 43 - The performance of the model with respect to the two datasets considered

For what concerns the evaluation of the error distribution, dashed trajectories of the English dataset represent the already mentioned cases where it is possible to argue that a wrong target spacing is reached. The results of the model in the two datasets are not so different. In the best case of the Italian dataset the error is lower than 40% in 93% of cases while in the worst case it is greater than 100% in 12% of cases. Similarly in the best case of the English dataset the error is lower than 30% in 100% of cases while in the worst case is greater than 100% in 8% of cases, in this the dashed trajectories of the UK dataset have not been considered.

3.2.7 Discussion of the state-space model with respect to literature

The use of dynamic systems in order to describe a car following process can be considered as a consolidated practice. Many of the approaches introduced in Section 1 represent de facto several (in discrete or continuous form) particularizations of the equation given by Wilson that has constituted the starting point of this model. The relevant point of the proposed approach is suited in the attempt to separate stimuli in order to obtain the *general* response as the sum of different, and more simply identifiable, effects on the driver. It is worth noting that other stimuli can be introduced inside the model inputs, if retained relevant, without changing its structure and stability condition. This is one of the main strong points of the proposed approach.

Another relevant point to be addressed regards the consistency between the model based on dynamic system and AP theory. The issue has been also addressed by Wagner (as already discussed in Section 1) with a similar approach, even if in that case APs have been used in order to reconstruct the dynamical equations governing the system dynamic. Selection of the APs has been based on analytical conditions similar to those introduced given in Section 3.2.3, but those conditions have been used also with some leader's trajectories with variable speed. Although a discussion of Wagner's findings lies beyond the scope of this thesis, it is worth noting that:

- he admits that the methodology to select APs does not guarantee to yield correctly all the APs;
- values of the estimated parameters lead him to model the car following behaviour using an harmonic oscillator that is completely equivalent (in its deterministic part) to the one presented in Section 3.2 if the distance of the follower from the equilibrium condition is defined as $d = \Delta x_n^t - \Delta x_n^*$, for which easily results, by applying trivial consistency conditions, that $\dot{d} = \Delta \dot{x}_n^t - \Delta \dot{x}_n^* = \Delta v_n^t$ and $\ddot{d} = \Delta \dot{v}_n^t$.

In the model proposed in this thesis, another point to be addressed concerns the model dependency from follower's speed. In particular, the model has been derived using a Taylor expansion around the equilibrium conditions, but has been applied also far from that. This leads to think that the dependency from follower's speed of a car-following process is not so strong, or (better) that the follower's speed affects the process only through the target spacing Δx_n^*. Moreover, for what concerns the target spacing, circumstances discussed in the previous Sections and shown in Figures 36 and 37 suggest that a dependence from time of the Δx_n^* can exist (that is

usually neglected in short trajectories). So a slight revised version of the general model given by Wilson can be proposed (but dealt with):

$$\dot{v_n^t} = f(\Delta x_n^t, \Delta v_n^t, \Delta x_n^*(v_n^t, t))$$

Unfortunately the revised formulation has not an immediate practical applicability because the function $\Delta x_n^*(v_n^t, t)$ represent an un-answered question for transportation analysts.

4 Application of car-following behaviour to ACC

Car-following models are components of several microscopic traffic simulation models. For instance, the Gazis' model is at the basis of MitsimLab, Gipps' model is at the basis of Aimsun, the model by Wiedemann is at the basis of the tool Vissim, while the (similar) one by Fritzsche at the basis of Paramics. Less attention has been devoted to the application of car-following paradigm in ITS and, in particular for ACC (Adaptive Cruise Control), even if car-following is the key condition for which ACC has been developed.

A better understanding and modelling of car-following is required from the particular point of view of ITS, where specific needs have to be addressed. One of the most important of these is to ensure that any proposed system considers driver expectation and behaviour and ensures there is a minimal mis-match between the system behaviour and the drivers normal behaviour, thus increasing driver acceptance.

In this section, a specific car-following model is presented. It is based on a linear approximation (at any time t, in a discrete-time approach) of the response of the follower to the leader's stimuli. The model is shown to be a very good approximation of the observed data; moreover, it is shown to lead to an harmonic oscillation around the desired spacing at steady-state . This oscillation is consistent with both the revised Action Point theory (section 3.1) and (partially) with the proposed state-space approach (3.2). The linear model is particularly suitable for real-time ACC-oriented application; thus it is here employed, where a fully-adaptive ACC system is developed, able to actuate a driving-style actually consistent with driver's expectations and preferences.

4.1 The ACC-oriented parametric model

The main scope of this thesis has been to obtain a better understanding and modelling of car-following behaviour, but also to enhance the modelling tools for the development of more driver-compliant ADAS. Here it is developed an ACC-oriented model that is specific for on-board application; the core idea is to develop a model consistent with observed properties of driver behaviour, but with a simpler model formulation.

4.1.1 Model development

Even in this case, the starting point is the Wilson's general formula, already introduced in Section 1 and 3.2:

$$\dot{v}_n^t = f(\Delta x_n^t, \Delta v_n^t, v_n^t)$$

In this model the leader's acceleration is not taken explicitly into account. However, in case of ACC, where the model has to be applied in real-time and with the purpose of control for safety aims, it has to be considered that, even if null on average, a small leader's acceleration can be applied at any time instant *t*. Because of this, the Wilson's formula is here modified in order to explicitly take into account the instantaneous (small) acceleration of the leader:

$$\dot{v}_n^t = f(\Delta x_n^t, \Delta v_n^t, v_n^t, \dot{v}_{n-1}^t)$$

Now a completely arbitrary form of the $f(\cdot)$ is proposed (it will be verified later on in this thesis):

$$\dot{v}_n^t = -\frac{2}{\tau^2}[k_0 + k_1 \Delta x_n^t + (k_2 - \tau)\Delta v_n^t + k_3 v_n^t] + \dot{v}_{n-1}^t \qquad 23)$$

Where τ is the length of time for which the acceleration identified by the driver at time t is actually applied, k_0, k_1, k_2 and k_3 are parameters to be calibrated.

From the previous formulation it can be obtained:

$$\tau \Delta v_n^t + \left(\dot{v}_{n-1}^t - \dot{v}_n^t\right)\frac{\tau^2}{2} = k_0 + k_1 \Delta x_n^t + k_2 \Delta v_n^t + k_3 v_n^t \qquad 24)$$

Under the approximated hypothesis that from *t* to *t*+τ the accelerations of the leader and of the follower are constant, the left-side of equation 24 is the variation of spacing between the two vehicles. As a consequence, the main equation of the model is:

$$\Delta\xi_n^{t,t+\tau} = k_0 + k_1 \Delta x_n^t + k_2 \Delta v_n^t + k_3 v_n^t \qquad 25)$$

where $\Delta\xi_n^{t,t+\tau}$ is the target variation of spacing (inter-vehicle separation) estimated at time t for time $t + \tau$.

Except the way previous equation 25 has been generated, it is evident that the ACC-oriented car-following approach proposed here is based on a simple time-discrete linear model, able to relate the instantaneous speeds of the leader and the follower and their spacing with the target variation of spacing the follower desires for next time-step.

The choice of managing the equations in such a way to reproduce the spacing instead of the acceleration (as more usual in car-following) is due to the application of the model to the ACC field. In ACC applications it is common to directly control

the headway (and then the spacing for a given speed). Controlling the spacing constitutes an advantage, in fact it assumes that the speed is almost perfectly reproduced (due to an even more accurate reproduction of acceleration), but for 1 or 2 seconds the actuated speed is only slightly wrong. Assume that, after that, the speed is again reproduced with no errors. The few seconds of the wrong speed have induced erroneous displacement (with respect to the one the model would have imposed) and then, given the trajectory of the leader, an error in the spacing. This error does not further increase when the speed is recovered, but it will never be corrected in the case the goal is to reproduce speed (or acceleration). This does not happen if the spacing is directly controlled, errors in terms of spacing can be recovered. Moreover, if the time series is correct in terms of spacing (and so is vehicle advancement, given the leader's trajectory), it is even more correct in terms of spacing derivatives (speed and acceleration).

Thus, equation 25 can be managed in order to control, in car-following conditions, the dynamics of the follower.

First of all, it should be noted that the condition for updating the leader's kinematics is:

$S_{n-1}^{t} = \Delta x_n^t + S_n^t$ and $v_{n-1}^{t} = \Delta v_n^t + v_n^t$

thus, to reach the target spacing the following vehicle computes at time step t a target position increment for time step $t + \tau$:

$$\Delta S_n^{t,t+\tau} = \bar{S}_n^{t+\tau} - S_n^t = \bar{S}_{n-1}^{t+\tau} - \Delta\xi_n^{t,t+\tau} - S_n^t = S_{n-1}^t + \Delta S_{n-1}^{t,t+\tau} - \Delta\xi_n^{t,t+\tau} - S_n^t =$$
$$\Delta S_{n-1}^{t,t+\tau} - \Delta\xi_n^{t,t+\tau} = \Delta S_{n-1}^{t,t+\tau} + \Delta x_n^t - [k_0 + k_1\Delta x_n^t + k_2\Delta v_n^t + k_3 v_n^t] \qquad 26)$$

where:

- $\bar{S}_n^{t+\tau}$ is an estimate of the position the follower will reach at time $t + \tau$;
- $\bar{S}_{n-1}^{t+\tau}$ is an estimate of the position the leader will reach at time $t + \tau$;
- and, consistently, $\Delta S_{n-1}^{t,t+\tau}$ is an estimate of the space driven by the leader from time *t* to time $t + \tau$.

In particular, the $\Delta S_{n-1}^{t,t+\tau}$ estimates at time step *t* the distance driven by the leader in the next future by considering a uniformly accelerated motion equation:

$$\Delta S_{n-1}^{t,t+\tau} = \tau v_{n-1}^t + \dot{v}_{n-1}^t \frac{\tau^2}{2}$$

The controlled vehicle will actually apply the driven distance increment computed $\Delta S_n^{t,t+\tau}$; it is worth noting that in the equation for the evaluation of $\Delta S_n^{t,t+\tau}$, the driven distance increment by the leader has been estimated, then the actual driven distance increment at time $t + \tau$ will differ from the target one by a

quantity *Err*. This is the error in estimating the leader progression, deliberately introduced in the model because of the uniformly accelerated motion. Formally:

$$Err^{t+\tau} = \Delta\xi_n^{t,t+\tau} - (\Delta x_n^{t+\tau} - \Delta x_n^t) = \bar{S}_{n-1}^{t+\tau} - S_{n-1}^{t+\tau} = \Delta S_{n-1}^{t,t+\tau} + S_{n-1}^t - S_{n-1}^{t+\tau}$$

From a modelling point of view, the error given by these approximation is not propagated because at each time step the spacing on which equation 25) is based is refreshed according to the real (measured) value Δx_n^t and the position of the leader is refreshed by using the given conditions.

The given model represents a stimulus-response model similar to those defined in Section1, even if here the response is rearranged in such a way that it coincides with the target variation of the spacing.

The model can also be specified for the equilibrium conditions, that are:

i) the leader as a constant speed, then the leader's position is updated using the law $\Delta S_{n-1}^{t,t+\tau} = \tau v_{n-1}^t$;
ii) the follower has the same speed of the leader, that is the one of equilibrium $v_{n-1}^t = v_n^t = v_n^*$;
iii) the actual spacing is the equilibrium one Δx_n^*, then the $\Delta\xi_n^{t,t+\tau} = 0$.

When the model is evaluated in equilibrium conditions

$$k_0 + k_1\Delta x_n^* + k_3 v_n^* = 0 \qquad 27)$$

a function that describes the equilibrium pairs (v_n^*, Δx_n^*) can be derived, that is:

$$\Delta x_n^* = -\frac{k_0}{k_1} - \frac{k_3}{k_1} v_n^* \qquad 28)$$

In other words, when the stimulus related to the relative speed is null, a car-following dynamics still can be observed (the response is not null); this happens when the actual spacing is not suitable for the speed at which the vehicles cruise (previous conditions *i* and *ii* are respected, but not *iii*):

$$\Delta\xi_n^{t,t+\tau} = k_0 + k_1\Delta x_n^t + k_3 v_n^* \qquad 29)$$

However, if the system satisfies all the three previous conditions, then it is at equilibrium and the spacing no longer changes. This phenomenon fits the expectations and confirms that the variables employed have been correctly identified. It is worth noting that the equilibrium function implicitly states the admissibility of parameters *k* of the model. It has to be ensured that for any feasible (non-negative) speed v* a feasible (non-negative) value of Δx* can be obtained. Moreover, it is expected that the regime spacing increases according to the regime speed. In practice, the (linear) curve Δx* = Δx(v*) has to be a non-decreasing and non-negative function. Sufficient conditions for that are $-\frac{k_0}{k_1} > 0$ and $-\frac{k_3}{k_1} > 0$. The two relationship above could be assumed as a constraint during the calibration of the model.

Some early versions of the ACC logic proposed here were presented in Simonelli et al. (2009) and Bifulco et al. (2008) and were respectively based on pure GPS data (properly corrected for un-biasing) and model-generated data, based on parameters accurately calibrated by using GPS trajectories. Unfortunately, for pure GPS data heavy-filtering and consistency-reaching procedures are required so that, given the extreme accuracy needed for ACC applications, few minutes (1 to 3) of useful trajectory were available for each of the eight trajectories collected. Moreover, a sizeable part of each trajectory was used for calibration and just a small part was available for validation. In the case of model-generated trajectories, the parameters of a standard Gipps (1981) model were accurately calibrated against real-world data. The obtained model was then used to generate (given a long GPS-revealed trajectory of the sole leader) a car-following trajectory. In this second case the trajectory obtained was long enough but perhaps too smooth and synthetic.

However, the extreme accuracy of the proposed regression in reproducing Gipps-produced synthetic data (in more than 90% of cases the discrepancy with the Gipps trajectory was less than 10%) indirectly proves the suitability of the linear approach or, at least, that its performance is comparable with that of widely accepted non-linear car-following models.

Application of a linear model in order to reproduce the observed spacing is justified by previous experience discussed in Bifulco et al. (2008), to which the reader should refer for details. The advantage of using more-than-linear formulation for the regressive model was estimated at 9% in terms of better RMSE of the simulated vs. observed spacing. Similarly, the advantage obtained by an even more flexible regression model based on artificial neural networks was measured at 15%. These advantages are not enough, in the authors' opinion, to forgo the great efficiency of the linear approach, especially in a case where real-time and on-demand estimation of the parameters is required.

Previous investigations concerned also the identification of the more appropriate value of τ. This has been chosen at a value of 0.6 seconds, then this value has been used also for analyses of the model reported in the following Sections.

4.1.2 Calibration of the model with respect to observed data

The linear model has been calibrated with respect to data obtained from the First Italian experiment (Section 2.1). The value of the obtained parameters, as well as the computed R-square and F Test results have been reported in the next *Table XIV*

Table XIV - The results of the calibration of the linear model

Driving Session	Characteristic set				Statistics	
	k_0	k_1	k_2	k_3	R^2	*F Test*
1	0,0759	-0,0056	0,5844	0,0013	0,963	4130,6
2	0,1053	-0,0069	0,6204	0,0007	0,788	2512,0
3	0,0558	-0,0090	0,5902	0,0047	0,954	3774,8
4	0,0254	-0,0018	0,6000	0,0006	0,918	2409,4
5	0,1275	-0,0018	0,5577	-0,0050	0,922	5074,8
6	0,0884	-0,0014	0,5881	-0,0022	0,944	5592,2
7	0,1780	-0,0022	0,5820	-0,0050	0,982	13609,2
8	0,1034	-0,0046	0,5768	-0,0030	0,962	4332,3
9	-0,0897	0,0031	0,5906	0,0014	0,926	1609,0
10	0,0133	-0,0024	0,5929	0,0018	0,975	9168,1
11	0,0556	-0,0104	0,5643	0,0029	0,927	6351,2
12	0,0636	-0,0076	0,5885	0,0043	0,777	690,7
13	0,0551	-0,0011	0,5697	-0,0016	0,942	5208,2

The model shows a very good fit and values of the parameters do not appear too much dispersed; this can be better observed from next Figure 44, where the box-and-whisker plot of the four parameters have been depicted.

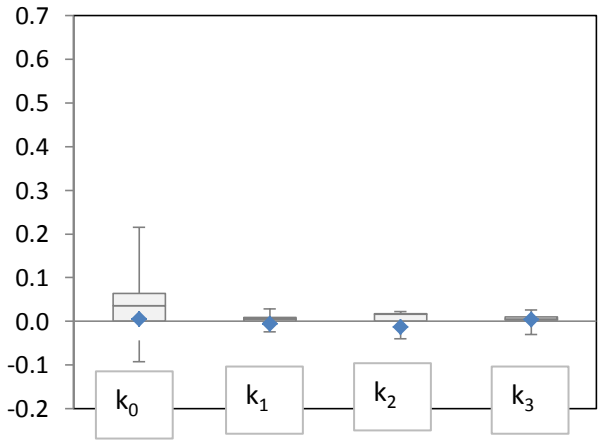

Figure 44 - The box-and-whisker plot depicted for the parameter of the linear model

It is worth noting that the parameter with the most variability is k_0 Instead,. k_1 and k_3 have a very small mean, but their contribute is not negligible because they are multiplied for the two biggest variables of the process, that are respectively the spacing and the follower's speed.

Values of the three parameters have also an impact on the *equilibrium function* introduced in the previous Section (equation 28).

Results of this computation have been reported in the next Table XV, together with the p-values evaluated in order to test the significance of the computed parameters.

Table XV - Analysis of the parameters with respect to their significance and equilibrium properties

Driving Session	p-values				$-\frac{k_0}{k_1}$	$-\frac{k_3}{k_1}$
	k_0	k_1	k_2	k_3		
1	0,004	0,000	0,000	*0,585*	13,49	*0,23*
2	0,000	0,000	0,000	*0,678*	15,34	*0,10*
3	0,000	0,000	0,000	0,000	6,22	0,52
4	*0,290*	0,003	0,000	*0,657*	*13,76*	*0,32*
5	0,000	0,001	0,000	0,001	71,01	-2,79
6	0,009	*0,054*	0,000	*0,385*	62,61	*-1,53*
7	0,000	0,000	0,000	0,003	79,64	-2,24
8	0,000	0,000	0,000	0,034	22,69	-0,66
9	*0,368*	0,001	0,000	*0,790*	*28,68*	*-0,45*
10	*0,530*	0,000	0,000	*0,154*	5,64	*0,75*
11	0,001	0,000	0,000	0,003	5,36	0,28
12	*0,454*	0,000	0,000	*0,439*	*8,34*	*0,56*
13	*0,068*	0,020	0,000	*0,320*	*51,42*	*-1,45*

Values in italics and underlined represent p-values greater than 0.05 (the chosen level of significance), they correspond to estimated parameters with a potentially random value; for this reason the corresponding calculated value has been highlighted by using italics too.

However, the $-\frac{k_0}{k_1}$ is always greater than zero, therefore the model admits the presence of a minimum spacing, even if this value is very dispersed between trajectories. In the case of the second term $-\frac{k_3}{k_1}$ results are very controversial. It seems that for several trajectories the model imposes spacing values that decrease when the speeds increase. This circumstance is in contrast with what is assumed as *rational*, but it has to be taken into account that model responses are conditioned by observed behaviours; then an *irrational* response of the model could have been conditioned by the observation of *irrational* behaviours (it should be remembered that the observed behavior represent only a sample of the behaviour of the driver, then it could represent a particular case).

4.1.3 Consistency between linear model and behavioural paradigms

The obtained parameter sets of the linear model have been tested in a unique (synthetic) situation in order to observe trend differences. The situation is identified by a leader's constant speed of 25 m/s and an initial conditions of 30m for the spacing and -2.5 m/s for the relative speed. At each set of parameters is associated a different desired equilibrium condition, it can be computed from the estimated parameters. Responses of five parameter sets (those associated with trajectories 1, 3, 10, 11 and 12) have been reported in the next Figure 45 in terms of phase portrait, opening and closing charts. The obtained model responses have a strong accordance with patterns introduced with respect to the revised Action Point Paradigm.

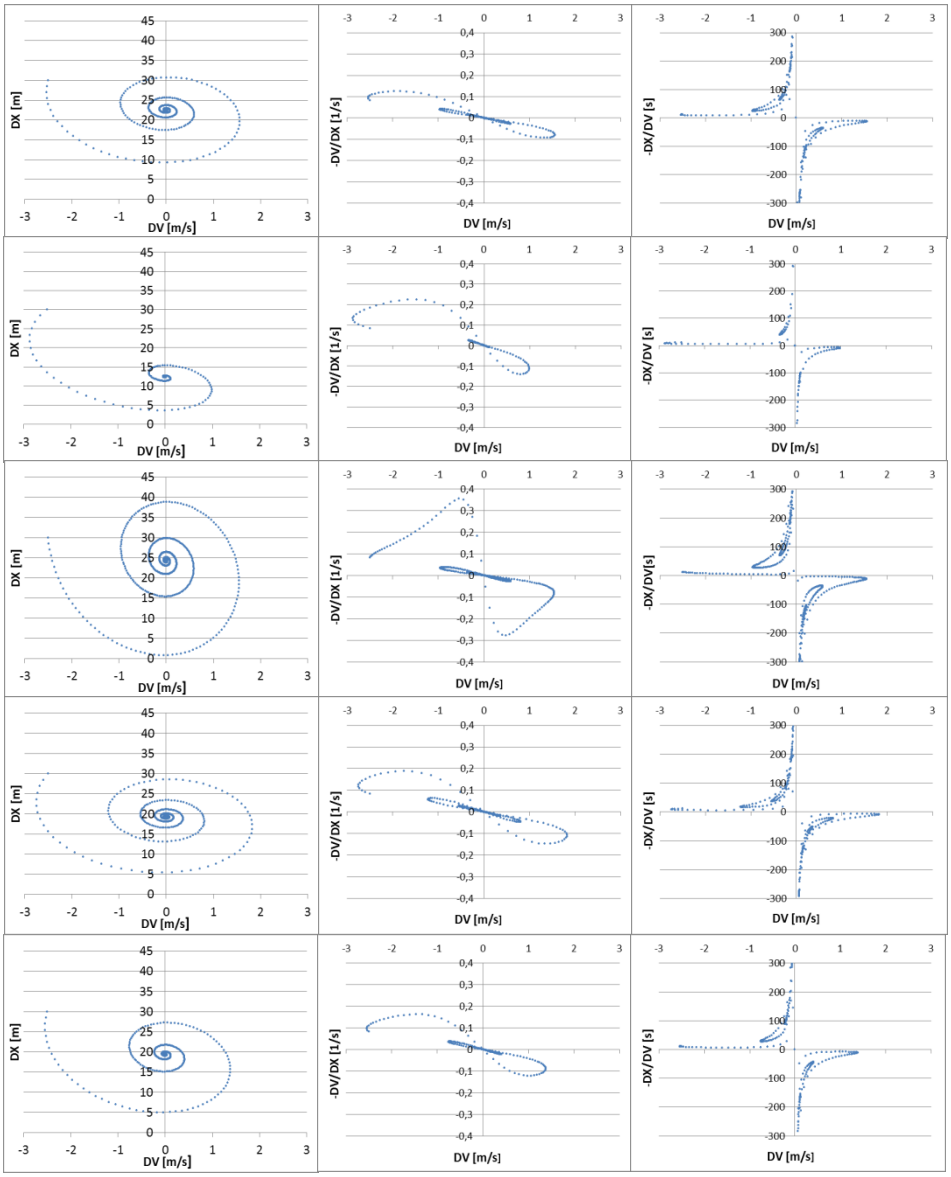

Figure 45 - A comparison between the responses of the linear model parameter sets of the trajectory 1, 3, 10, 11 and 12 in a unique (synthetic) situation. The initial condition is DX=25 m, DV=-2.5 m/s. The leader has a constant speed of 25 m/s.

Trajectories for which an *irrational* behavior has been obtained (5, 6, 7, 8, 9 and 13, as reported in *Table XV*) have been discarded from the analysis. Moreover also trajectories where $k_2 \geq 0.6$ (2 and 4) have not been reported, while in that case the stability conditions are not reached.

The obtained responses show an harmonic pattern. This is consistent with the responses shown by the state space model presented in Section 3.2 in the event of under-damped response. However, it should be noted that the state space model has been identified with respect to the same dataset and (except for trajectory 12) the model exhibits always an over-damped response. This represents a contradiction

between the calibrations of the two models. A better understanding of these points could represent an interesting issue of future studies, also considering that both the models well fit observed data.

4.2 Embedding the linear model into a fully adaptive cruise control

This section presents some crucial developments towards a human-like, fully-adaptive ACC system suitable for real-time and on-demand estimation and application, based on the linear model discussed in previous section 4.1.

The system is intended to be adopted in stand-alone mode and does not rely on vehicle-to-vehicle (v2v) communication. Of course, v2v communication is compatible with the framework here presented; it can be viewed as an alternative way for evaluating spacing and relative speed with respect to the leading vehicle. This could replace the use of radar/lidar or (rather) allow for the integration of more data sources. The effects on traffic flows of the market penetration of this system are not treated here and are left for future possible works.

The proposed modelling framework is composed by four layers:

- the first layer, the *sampler* is responsible for the main ACC control logic;
- the *profiler* is a key component which is asked to translate the driving behaviour produced by the sampler into admissible (continuous) kinematic profiles, suitable to be applied to the controlled vehicle;
- the third layer, the *tutor*, ensures that the reference driving trajectory obtained by using the profiler is ultimately safe, so that it can be applied by the last layer,
- the *performer* is in charge of actuation by controlling the vehicle actuators (e.g. the throttle, the brakes, etc.). Development and testing of the performer goes far beyond the scope of this research, then it is assumed that an effective and efficient performer already exists. For example, CarSim software (Mechanical Simulation Corporation; 2009) can be used for this purpose.

In this section the four-layer framework is briefly presented. The approach was explicitly conceived for ACC applications. It can be argued that it can be employed for other kinds of applications but here this opportunity is not discussed.

The inception idea is that the driver's behaviour in car-following conditions can be identified by means of the time-series of *spacing*, sampled at a given frequency (e.g. at 1 Hz). This is consistent with previous section, where it has been redefined the car-following model in terms of spacing dynamics. Computation of this sequence is the role of the *sampler*. Within the *sampler* the vehicle dynamics is

neglected, as it is the consistency among different kinematic variables (position, spacing, speed, acceleration, etc.).

The second modelling layer (the *profiler*) recovers the full (and consistent) representation of vehicle trajectory by adopting a time-continuous state-space approach. Of course, the *profiler* has to ensure that the resulting trajectory fits the points identified by the *sampler*; this is obtained by assuming these points as the *requests* supplied to the profiler. The profiler also checks whether these requests are actually admissible. Checking is based on general kinematic considerations and rough hypotheses about vehicle performance. For instance, if the *sampler* requests too high a variation of position to be satisfied with an admissible acceleration, the *profiler* limits the reached position consistently with a predefined maximum acceleration. The trajectory produced by the profiler is continuous, consistent and likely to be admissible; it represents a *reference* trajectory.

However, the *actual* trajectory can be different from the reference one given that it results from the actuation (throttle, brake, engine, etc.) performed by the vehicle mechanics and electronics, as well as from interaction with the road (slope, grip, etc.). The simulation of how the vehicle and its actuators are able to actually match the profiler-supplied reference trajectory pertains to the *performer*. Actually, development of a tool like the *performer* is a typical service for the automotive sector. Some commercial tools already exist to this aim (e.g. CarSim – mechanical Simulation Corporation, 2009). Hence the *performer* is here totally neglected and the assumption is made that such a tool is available and able to actuate the reference trajectory; on these assumptions are also based all results presented forward.

Between the *profiler* and the *performer*, the *tutor* is inserted; it ensures that safety conditions are satisfied. It computes the maximum allowed speed (or spacing, or position increment) compatible with the safety, revealed by applying a safety model to real-time (and high-frequency – much higher than the sampler) sensor measurements. The *performer* then tries to apply the lowest position increment suggested by the *profiler* or the *tutor*.

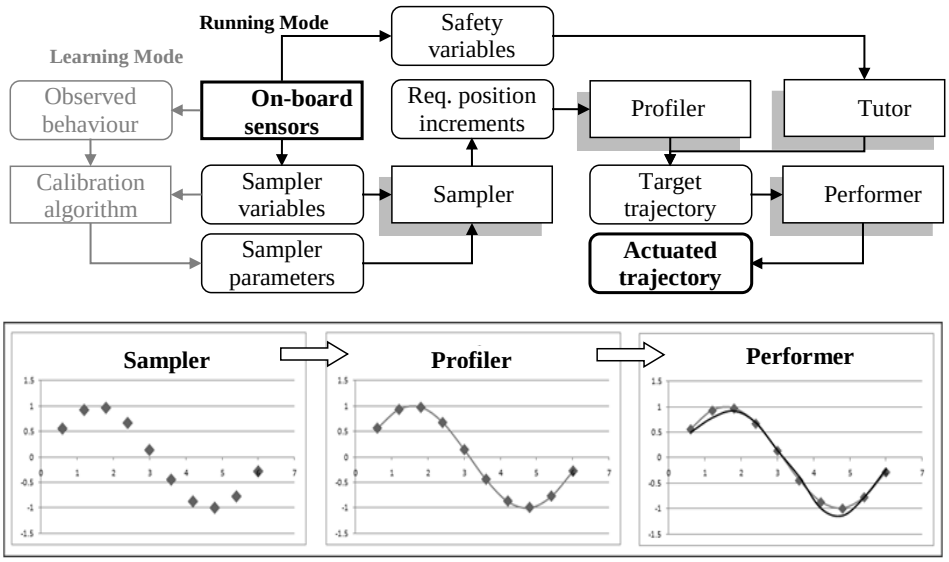

Figure 46 - The modelling architecture

As should be noted from Figure 46 the modelling architecture consists of two modes, the *running* and the *learning* ones. In particular the running mode, that concerns the actual application of the model to control the vehicle, has already been shown through the description of the four layers introduced previously, but a pre-requisite for the application of the algorithm in our modelling framework is the learning mode, that is strictly related to the concept of *fully adaptivity* of the proposed ACC. In fact, the nature of the fully adaptive approach excludes the calibration of a set of parameters common to all the trajectories, nor the calibration of the dispersion of these parameters. Rather, the parameters are intended to be calibrated for each single driver and for each single driving session (in real time and on demand), according to a learning-mode phase of the ACC system. It is worth noting that in the learning mode only parameters of the sampler are changed; in fact, variations of driving behaviours are interpreted in this approach with variations of the requests of the sampler consistent with the behaviour observed in the learning mode.

4.3 The car-following model for the human-like ACC

As said, the sampler is responsible for estimating a time-series for spacing. It is based on the car-following model described in previous section 4.1. From the time-series of spacing, a time-series of driven distances can be derived. It reproduces as closely as possible the sampling of the car-following trajectory that a driver would have applied in manual driving conditions. The adopted sampling frequency is in the order of magnitude of 1 Hz; this was chosen on the basis of some major considerations:

a) the typical reaction time of car-following models proposed in the literature is around 1 second; from that a sort of human-like refreshing frequency of 1 Hz can be argued; in other words, we assume that drivers habitually distinguish with a granularity no more detailed than 1 second (of course, if things go smoothly);
b) even if the human likeness of the trajectory is sampled at a 1 Hz frequency, the ACC system checks the safety at a much higher frequency (say, 10 Hz); this is the task assigned to the tutor; as a result, the system is able to react to stimuli, if dangerous, much more promptly than the driver (say, human likeness is excluded in the case of danger);
c) the time step between sampled points is a trade-off between opposite interests as expressed by the following points i) and ii);
    i. the car-following model implemented by the sampler is based on some approximate assumptions on how the leading vehicle moves; a shorter time step between two successive sampled points bounds the errors introduced by this approximation;
    ii. the car-following trajectory between two sampled points evolves according to the profiler; having fixed the sampled points, some optimisation can be done in the transition, according to some external objectives (e.g. reduction in consumption and/or pollutants); this is aided by a longer time step.

The sampler works with respect to two main traffic regimes: free-flow and car-following. The free-flow regime is where the ACC actually acts as a CCC and a pre-defined speed is applied. This could vary along the route, possibly being associated to location-aware (dynamic) speed regulation policies and on-board speed navigators. That said, the free-flow speed is not a modelling task in the context of this thesis and is treated as a known, fixed (constant within each time step) and exogenously given value. Of course, the desired position increment in the case of free-flow speed is easily computable. Consistently with all the previous of this thesis, the car-following regime is the main focus of the sampler.

It is worth noting again that no safety considerations are made in order to avoid collisions. Actually, given the capital importance of safety considerations, these are applied to the vehicle at a higher frequency and are superimposed upon any other consideration. For such a reason, safety and emergency considerations are not included as sampler tasks. Rather, they are postponed between the profiler and the performer and constitute the main task of the tutor.

From a theoretical point of view, finding a parametric driving behavior model here entails estimating a model able to reproduce and predict vehicle responses in

car-following conditions. The predicted vehicle is the *follower* in the car-following trajectory, also referred to as the *controlled* vehicle.

The estimation process for the behavioral model consists in finding the vector of modeling parameters that minimize the distance between the observed vehicle kinematics and the kinematics reproduced by the model. Formally:

- ***Ob*** is the observed kinematics of the controlled vehicle, with entries $Ob_{i,t}$, where *i* refers to a component of the observed vector and *t* is the time at which the observation is taken; the length of the observation is the estimation phase, from $t = t_0$ to $t = T$; the observed variables are also referred to as the *observed response*;
- $\boldsymbol{I^0}$ is the (known) initial condition of the (controlled) vehicle kinematics, with entries I^0_i, where *i* refers to a component of the observed kinematics (speed, travelled distance, etc.) at the initial observation time (t_0, when the estimation phase starts); typically, the initial conditions refer to the set of relevant kinematic variables, the observed response is typically a subset of the initial condition variables;
- ***U*** is the observed kinematics of the leading vehicle, with entries $U_{j,t}$, where *j* refers to a component of the observed stimuli vector (speed, spacing, acceleration of the leader, etc.) and $t>t_0$ is the time at which data are collected;
- ***M*** is the kinematics reproduced by the model, with entries $M_{i,t}$, where *i* refers to a component of the observed vector (the same components considered for ***Ob***) and $t>T$ is the time at which the model runs (the sampling time should be the same for sensor data collection and response observation); the reproduced variables are also referred to as the *reproduced response*.

From the observed kinematics of the controlled vehicle and those of the leading vehicle, the observed stimuli (***S***) vector can be computed; stimuli are variables like relative speeds, relative spacing, etc.:

$$\boldsymbol{S} = \mathbf{S}(\boldsymbol{Ob}, \boldsymbol{U}) \qquad 30)$$

The reproduced responses, once the initial conditions are known and the stimuli have been computed, depend on the vector of modeling parameters ($\boldsymbol{\beta}$), in formal terms:

$$\boldsymbol{M} = \mathbf{M}(\boldsymbol{\beta} / \boldsymbol{I^0}, \boldsymbol{S}) \qquad 31)$$

where $\mathbf{M}(\cdot)$ is the function (model) assumed to describe the observed behavior appropriately.

The vector of parameters $\boldsymbol{\beta}$ is the solution of an optimization problem formally defined by:

$$\boldsymbol{\beta} = \text{argopt} \, || \, \mathbf{M}(\boldsymbol{\beta} / \boldsymbol{P}, \boldsymbol{S}) - \boldsymbol{Ob} \, || \qquad 32)$$

where $\| \cdot \|$ represents a properly defined measure of distance between the responses observed and those reproduced.

A simple explicit formulation can be applied that minimises the distance between the model outputs and the observed outputs by solving an ordinary least square (OLS) problem:

$$\boldsymbol{\beta} = \left(\boldsymbol{\Gamma}^{\mathbf{T}} \, \boldsymbol{\Gamma}\right)^{-1} \boldsymbol{\Gamma}^{\mathbf{T}} \, \boldsymbol{\gamma} \qquad 33)$$

where

- Γ is the matrix enlisting in each column the values observed at each time step k for the independent variables, plus a first column of unitary values, accounting for the estimation of the intercept of the model (β_0);
- γ is the vector of all the observations of the dependent variables .

Several algorithms can be employed to solve the OLS problem. One of the most efficient for real-time applications is the recursive least squares (RLS) algorithm (Haykin, 2001); it is widely applied in many areas, such as real-time signal processing. In the general formulation it minimizes a weighted least squares cost function related to the input signal under the hypothesis that a new sample of signals is received at each iteration. Given the incremental nature of the algorithm, computation takes a very reasonable time even if a considerable amount of observed data is processed. Compared with most of its competitors, the RLS exhibits extremely fast convergence.

However, in-depth discussion of the algorithm or of its convergence and stability issues go well beyond the scope of this research; this may well be the subject of future works. The algorithm has been used in the following in a heuristic way and the stop criterion for terminating the estimation of the parameters was based on two conditions (occurring jointly):

- time is greater than 30 seconds;
- the objective function of the algorithm improves negligibly.

Of course, it is not guaranteed that the algorithm has reached stable solutions but some empirical evidence can be claimed by considering all the successfully performed calibrations (as it will be shown also in the discussion on the calibration results). Moreover, effectiveness of the algorithm can be empirically accepted if good fitting of the calibrated model against the observed data is evidenced a posteriori, as happens in all our cases.

A model that can be used for the sampler is the one introduced in Section 4.1.

In particular, if that model is considered as suitable, the theoretical equations underlying the sampler can be particularized as reported hereafter:

- the vector $\boldsymbol{Ob^t} = [S_n^t, v_n^t, \dot{v}_n^t]$;
- the vector $\boldsymbol{U^t} = [S_{n-1}^t, v_{n-1}^t, \dot{v}_{n-1}^t]$;
- the vector $\boldsymbol{S^t} = \boldsymbol{S^t}(\boldsymbol{Ob^t}, \boldsymbol{U^t}) = [\Delta x_n^t, \Delta v_n^t, v_n^t]$;
- the model $\boldsymbol{M}$ = $\mathbf{M}(\boldsymbol{\beta} / \boldsymbol{I^0}, \boldsymbol{S}) = k_0 + k_1 \Delta x_n^t + k_2 \Delta v_n^t + k_3 v_n^t = \Delta \xi_n^{t,t+\tau}$ and where the distance $\boldsymbol{\beta}$ = argopt $\| \mathbf{M}(\boldsymbol{\beta} / \boldsymbol{I^0}, \boldsymbol{S}) - \boldsymbol{Ob} \|$= = argopt $\| \mathbf{M}(\boldsymbol{\beta} / \boldsymbol{I^0}, \boldsymbol{S}) - \boldsymbol{Ob} \|$= argopt $\|\Delta x_n^t + \Delta \xi_n^{t,t+\tau} - \Delta x_n^{t+\tau}\|$.

It is worth noting that the vector of stimuli is composed by the relative speed and relative spacing, then, strictly speaking, both the actual positions of leader and follower than the speed of the leader are not necessary to be known.

4.4 The profiler

The sampler estimates at each time step *t* the distance that the controlled vehicle should drive in order to reach at time step $t + \tau$ a human-like target spacing. The responsibility of the profiler is to produce a time-continuous trajectory consistent with the requests of the sampler. This is done by representing the trajectory of the controlled vehicle (and not the controlled vehicle itself) as a state-space dynamic system evolving from time step t to time step $t + \tau$. This evolution is controlled (forced) in order to impose the distance requested to be covered according to the estimates of the sampler.

Within the profiler some of the variables introduced in the previous sections are redefined:

- t_0 is the time instant corresponding a generic instant in which the sampler is applied and gives its request;
- ΔT is the duration of the time step defined in the discrete-time approach adopted for the sampler; as a consequence, the profiler is in charge of producing a continuous trajectory in the time interval $[t_0, t_0+\Delta T]$ and the instant $t_0+\Delta T$ coincides with the time-instant in which the sampler is applied again and gives another request;
- $u = \Delta sF(k, k+1)$ is the driven distance the profiler should impose from t_0 to $t_0+\Delta T$, as supplied by the sampler; it is the instantaneous step-solicitation;
- Δs is the distance actually covered by the vehicle in the time interval $[t_0, t_0+\Delta T]$; it could prove different from the requested one (u);
- ΔV is the variation in speed actually attained in the time interval $[t_0, t_0+\Delta T]$;

- $x_1(t)$ is the instantaneous acceleration at a generic time instant $t \in [t_0, t_0+\Delta T]$; it represents the first state variable;
- $x_2(t)$ is the instantaneous jerk at a generic time instant $t \in [t_0, t_0+\Delta T]$; it represents the second state variable.

It is assumed that the trajectory of the vehicle can be described as a (linear, time-invariant in ΔT) dynamic system according to the following model:

$$\dot{x}_1(t) = \tilde{e}_1\, x_1(t) + \tilde{e}_2\, x_2(t) + \tilde{f}\, u$$
$$\dot{x}_2(t) = e_1\, x_1(t) + e_2\, x_2(t) + f\, u$$

Of course, the state variables have to respect the physical consistency between jerk and acceleration:

$$\dot{x}_1(t) = x_2(t)$$

One of the possible solutions that ensures consistency is:

$$\tilde{e}_1 = 0 \qquad \tilde{e}_2 = 1 \qquad \tilde{f} = 0$$

This is equivalent to rewriting the dynamic system in the form:

$$\dot{x}_1(t) = x_2(t)$$
$$\dot{x}_2(t) = e_1\, x_1(t) + e_2\, x_2(t) + f\, u$$

Or, by using a matrix notation:

$$\dot{\mathbf{x}}(t) = \mathbf{A}\, \mathbf{x}(t) + \mathbf{c}\, u$$

where

$$\mathbf{A} = \begin{bmatrix} 0 & 1 \\ e_1 & e_2 \end{bmatrix} \qquad \mathbf{c} = \begin{bmatrix} 0 \\ f \end{bmatrix} \qquad \mathbf{x}(t) = \begin{bmatrix} x_1(t) \\ x_2(t) \end{bmatrix}$$

As usual for dynamic systems, it is important that the model parameters ensure the stability of the system. This depends on the eigenvalues of matrix A:

$$\lambda_1 = \frac{1}{2}\left(e_2 - \sqrt{4\, e_1 + e_2^{\,2}} \right) \qquad 34)$$

$$\lambda_2 = \frac{1}{2}\left(e_2 + \sqrt{4\, e_1 + e_2^{\,2}} \right) \qquad 35)$$

In particular, the stability is ensured if the eigenvalues are real, distinct and negative; this enables the fixed point (regime) to be viewed as a so-called sink-node (in the gradient field). This is ensured if:

$e_1 < 0,\ e_2 < 0 \qquad e_2 > -4\, e_1$

Eigenvalues can be related to the so-called time constants (τ_1, τ_2) that can be used to compute (with excellent approximation) the so-called settling time (ts_1, ts_2),

defined as the time elapsing from the application of an instantaneous step input to the time at which the state variable has entered a δ bound around the final (fixed-point) value. In formal terms:

$$\tau_i = -\frac{1}{\lambda_i} \qquad \forall\, i \in \{1,2\}$$

$$ts_i \cong 2\,\tau_i \ln\left(\frac{1}{\varepsilon}\right) \quad \forall\, i \in \{1,2\}$$

This means that if, for instance, δ = 10% then $ts_i \cong 4.6\,\tau_i$ and if δ = 5% then $ts_i \cong 6\,\tau_i$

In practice:

$ts_i \cong \alpha\,\tau_i \;\forall\, i \in \{1,2\}$ where α∈[4.5, 6] for an attained system response varying in the range [90%, 95%] of the final response.

On the other hand, the settling times can be imposed to be equal to a predefined part of the whole transition period ΔT. This can be set as a function of two parameters (ω and ψ):

$ts_1 = \omega\,\Delta T \qquad \omega \in]0,1[$

$ts_2 = \psi\,\Delta T \qquad \psi \in]0,1[$

Finally, it results that:

$$\lambda_1 = -\frac{1}{\tau_1} = -\frac{1}{ts_1/\alpha} = -\frac{\alpha}{\omega\,\Delta T} = \frac{1}{2}\left(e_2 - \sqrt{4\,e_1 + e_2^{\,2}}\right)$$

$$\lambda_2 = -\frac{1}{\tau_2} = -\frac{1}{ts_2/\alpha} = -\frac{\alpha}{\psi\,\Delta T} = \frac{1}{2}\left(e_2 + \sqrt{4\,e_1 + e_2^{\,2}}\right)$$

It can be easily verified that previous equations are satisfied by:

$$e_1 = -\frac{\alpha^2}{\Delta T^2\,\psi\,\omega} \text{ and } e_2 = -\frac{\alpha\,(\psi+\omega)}{\Delta T\,\psi\,\omega} \qquad 36)$$

By comparing the previous values of e_1 and e_2 in conditions derived from equations 34 and 35, it can be noted for stability conditions that:

- $e_1<0$ and $e_2<0$, because $\psi\,\omega > 0$ and $\psi + \omega > 0$, being $\psi>0$ and $\omega>0$;
- $e_2^2 > -4\,e_1$ is ensured if $(\psi - \omega)^2>0$ that is if $\psi \neq \omega$; this can be verified using conditions in 36 in $e_2^2 + 4\,e_1$, thus obtaining
  $e_2^2 + 4\,e_1 = \varepsilon_2\,(\psi - \omega)^2$, where $\varepsilon_2 = \alpha^2 / (\Delta T^2\,\psi^2\,\omega^2)$.

It results that the stability of the trajectory is ensured by very mild assumptions on the parameters (ψ and ω) governing the settling time of the system. In practice, they just have to be admissible (values from 0 to 1) and distinct.

Stability is evaluated around the fixed point (the regime). Regime values for the state variables can be evaluated as:

$$\mathbf{0} = \mathbf{A}\,\mathbf{x}^{*} + \mathbf{c}\,u \quad \rightarrow \quad \mathbf{x}^{*} = -\mathbf{A}^{-1}\,\mathbf{c}\,u$$

where:

$$-\mathbf{A}^{-1}\,\mathbf{c}\,u = \begin{bmatrix} -f/e_1 \\ 0 \end{bmatrix}$$

It results that the jerk assumes at the fixed point a null value, while the acceleration is finite and assumes a value that depends on the step (u) requested by the sampler:

$$x_1^{*} = -f/e_1\,u \qquad x_2^{*} = 0 \tag{37}$$

Given the imposed stability of the system and assuming that the settling times have been properly set by means of parameters ψ and ω, the status of the system at time t0+ΔTt$_0$ + ΔT can be reasonably considered as being attained:

$$x_1(t_0 + \Delta T) = x_1^{*} = -f/e_1\,u$$

$$x_2(t_0 + \Delta T) = x_2^{*} = 0$$

Now, consider the variation of speed (Δv) in the time interval [t0, t0+ΔT]:

$$\Delta v = \int_{t_0}^{t_0+\Delta T} a(t)\,dt = \int_{t_0}^{t_0+\Delta T} x_1(t)\,dt = \int_{t_0}^{t_0+\Delta T} \left[\frac{1}{2}\left(\dot{x}_2(t) - e_2\; x_2(t) - f\; u\right)\right] dt =$$

$$= \int_{t_0}^{t_0+\Delta T} \left[\frac{1}{2}\left(\dot{x}_2(t) - e_2\; \dot{x}_1(t) - f\; u\right)\right] dt =$$

$$= \frac{1}{e_1}\left[x_2(t_0 + \Delta T) - x_2(t_0)\right] - \frac{e_2}{e_1}\left[x_1(t_0 + \Delta T) - x_1(t_0)\right] - \frac{f}{e_1} u\,\Delta T$$

$x_2(t_0) = 0$, because it represents the regime status of a previous time step: $t_0 = (t_0 - \Delta T) + \Delta T$

Then:

$$\Delta v = -\frac{e_2}{e_1}\left[x_1^{*} - x_1(t_0)\right] - \frac{f}{e_1} u\,\Delta T = -\frac{e_2}{e_1}\left[x_1^{*} - x_1(t_0)\right] + x_1^{*}\,\Delta T \tag{38}$$

The equation above, once x_1^* is known, allows the computation of the variation in speed imposed by the profiler when the step requested by the sampler is imposed. Now consider the actual variation of space (Δs) in the time interval [t0, t0+ΔT]:

$$\Delta s = \int_{t_0}^{t_0+\Delta T} v(t)\,dt$$

To compute it, the expression of the speed has to be derived:

$$v(t) = v(t_0) + \int_{t_0}^{t} a(z)\,dz = v(t_0) + \int_{t_0}^{t} x_1(z)\,dz = v(t_0) + \int_{t_0}^{t}\left[\frac{1}{e_1}\left(\dot{x}_2(z) - e_2\ x_2(z) - f\ u\right)\right]dz =$$

$$= v(t_0) + \int_{t_0}^{t}\left[\frac{1}{e_1}\left(\dot{x}_2(z) - e_2\ \dot{x}_1(z) - f\ u\right)\right]dz =$$

$$= v(t_0) + \frac{1}{e_1}\left(x_2(t) - x_2(t_0)\right) - \frac{e_2}{e_1}\left(x_1(t) - x_1(t_0)\right) - \frac{f}{e_1}u\,(t - t_0)$$

Therefore:

$$\Delta s = \int_{t_0}^{t_0+\Delta T} v(t)\,dt = \int_{t_0}^{t_0+\Delta T}\left[v(t_0) + \frac{1}{e_1}x_2(t) - \frac{e_2}{e_1}\left(x_1(t) - x_1(t_0)\right) - \frac{f}{e_1}u\,(t - t_0)\right]dt =$$

$$= \int_{t_0}^{t_0+\Delta T}\left[v(t_0) + \frac{1}{e_1}\dot{x}_1(t) - \frac{e_2}{e_1}x_1(t) + \frac{e_2}{e_1}x_1(t_0) - \frac{f}{e_1}u\,(t - t_0)\right]dt =$$

$$= v(t_0)\,\Delta T + \frac{1}{e_1}\int_{t_0}^{t_0+\Delta T}\dot{x}_1(t)\,dt - \frac{e_2}{e_1}\int_{t_0}^{t_0+\Delta T}x_1(t)\,dt + \frac{e_2}{e_1}x_1(t_0)\,\Delta T - \frac{f}{e_1}u\int_{t_0}^{t_0+\Delta T}(t - t_0)\,dt =$$

$$= v(t_0)\,\Delta T + \frac{1}{e_1}x_1^* - \frac{1}{e_1}x_1(t_0) - \frac{e_2}{e_1}\Delta v + \frac{e_2}{e_1}x_1(t_0)\,\Delta T + x_1^*\frac{\Delta T^2}{2}$$

Substituting the expression of Δv (equation 38), it is possible to obtain:

$$\Delta s = v(t_0)\,\Delta T + \frac{e_2}{e_1}x_1(t_0)\,\Delta T - \frac{\left({e_2}^2 + e_1\right)}{{e_1}^2}x_1(t_0) + x_1^*\left(\frac{\Delta T^2}{2} - \frac{e_2}{e_1}\Delta T + \frac{\left({e_2}^2 + e_1\right)}{{e_1}^2}\right) \qquad 39)$$

Solving with respect to x_1^* and considering that the aim of the profiler is to force the driven distance to the step requested by the sampler ($\Delta s = u$):

$$x_1^* = \frac{2\left[{e_1}^2\left(u - v(t_0)\,\Delta T\right) + {e_2}^2\ x_1(t_0) + e_1\ x_1(t_0)\left(1 - e_2\ \Delta T\right)\right]}{2\,{e_1}^2 + e_2\left(2 - 2\,e_1\ \Delta T + e_2\ \Delta T^2\right)} \qquad 40)$$

All the calculations stated above are applied by the profiler in the following way.

Step 1.

Fix values for settling time parameters ψ and ω, use admissible values ($\in$]0,1[), ensure stability ($\psi \neq \omega$) and, if appropriate, try to have mild transitions (e.g.: ψ, ω >0.70).

Step 2.

Compute parameters e_1 and e_2 from equations 36 and compute the regime acceleration (x_1^*) by using equation 40 that ensures the driven distance equals that requested by the sampler ($\Delta s = u$).

Step 3.

Check the resulting regime acceleration (x_1^*). Only if the resulting value is inadmissible and/or judged to be inappropriate (e.g.: $\|x1^*\| \geq 2$ m/s2) fix an appropriate value for x_1^* and compute by equation 39 the driven distance (Δs) the profiler will actually set (different from that – u – requested by the sampler).

Step 4.

Compute parameter f by solving from equation 37: $f = -x_1^* \, e_1 / \Delta s$

Step 5.

Run the profiler as a continuous state-space dynamic system from time t_0 to time $t_0+\Delta T$; the resulting trajectory is the output of the profiler; in the overall multilayer architecture this is the input for the tutor.

The output is formally expressed in terms of acceleration and jerk (state variables); if required, other variables describing the trajectory (e.g. speed, position, etc.) can be easily derived from the state variables by using standard integration techniques. Note that the main purpose of step 3 above is to ensure the development of a robust algorithm. In theory, the step requested by the sampler imitates a human-like behaviour, that is it should be intrinsically consistent (for example) with admissible accelerations. If this is not the case, it is due to local errors in estimating the human-like spacing to be imposed, for instance due to an instantaneous malfunctioning of the on-board sensors. The role of step 3 is to avoid the propagation of such an error over the controlled vehicle trajectory.

It is worth noting that in all the above considerations, there are still some degrees of freedom in fixing some of the parameters of the profiler. In particular, the values of the parameters (ψ and ω) can be somehow arbitrarily chosen. In the numerical applications related to this paper, discussed in section 5 below, they were set in order to obtain long settling times and support a smooth dynamics in terms of acceleration and jerking. Of course, smoothness is here intended as a pleasing

transition from the starting point to the final point requested by the sampler. Pleasing transitions are favoured not only by fairly high values of ψ and ω but also by the human likeness of the sampler (from which reasonable stimuli are expected for the profiler). Higher values for parameters ψ and ω could not only promote comfortable cruising but also a reduction in consumption and/or pollution. In future works, we will deal with the role of ψ and ω as well as making some formal in-depth considerations about their suitability for formal optimisation purposes.

4.5 The tutor

A simplified *tutor* module has also been included, essentially with the aim of overriding the trajectories provided by the profiler if unsafe. The simplified *tutor* implemented is not discussed here in detail.

In practice, it is based on the concept of safe emergency braking for both the leader and the follower. Safety is tested by the *tutor* at a very high frequency (the maximum technically allowed by the sensors and by the on-board trajectory actuators, i.e. 10 Hz). Due to both the high control frequency and the magnitude of the actual cruising speeds, any lag between detection and actuation can be considered negligible and the admissibility of the trajectory depends on the different maximum decelerations likely to be applied by the leading and following vehicle in emergency conditions. In the results shown below, the maximum deceleration of the follower is assumed to be 70% of that of the leader. Of course, more complex (and perhaps appropriate) approaches can be incorporated in the *tutor*. In future research, direct control of spacing also in the *tutor* may be tested, constraining it to a safe range; such an approach could be implemented parallel to the modelling sequence sampler-profiler and could be based, for instance, on the approach by Bageshwar et al. (2004) or Martinez and Canudas-De-Wit (2007). In any event, the smaller of the position increments suggested by the tutor or by the sampler+profiler is applied by the *performer*.

4.6 The performer

Implementation and application of the *performer* (which is the detailed representation of the internal vehicle dynamics and of vehicle interaction with the road) lie outside the scope of this thesis. In practice, the hypothesis is made that a *performer* is available and that it allows for the regulation of the actual vehicle trajectory around the reference one (produced by the profiler). It is worth noting that the characteristics of the *profiler* (and the *tutor*) are compatible with commercial simulation tools that can play the role of *performer*. As an example, refer to CarSim

(Mechanical Simulation Corporation, 2009) that can also be integrated within the adopted Simulink/Matlab environment.

4.7 Results

In order to test the proposed approach, trajectories collected in experiment described in Section 2.1 have been used. The first issue to be carried out for each trajectory concerns with the possibility to test it in the learning mode, that is to calibrate the sampler in the first part of the trajectory. Then the whole model is tested in the running mode.

Formally, it can be introduced $\boldsymbol{I}^{\mathbf{T}}$ as the (known) boundary conditions of the (controlled) kinematics of the vehicle at time $t = T$, when the running mode starts. The IV continues the data collection (***Ob*** and ***U***). Thus the reproduced stimulus ($\boldsymbol{S}^{\mathrm{C}}$) is:

$$\boldsymbol{S}^{\mathrm{C}} = \mathbf{S}(\boldsymbol{M}^{\mathrm{C}-}, \boldsymbol{U})$$

where, at any time $t > T$, $\boldsymbol{M}^{\mathrm{C}-}$ is the trajectory simulated for the controlled vehicle up to time $t - 1$; in fact in running mode the observed dynamic depends on the model. Thus:

$$\boldsymbol{M}^{\mathrm{C}} = \mathbf{M}(\boldsymbol{\beta} / \boldsymbol{I}^{\mathbf{T}}, \boldsymbol{S}^{\mathrm{C}}) = \mathbf{M}(\boldsymbol{\beta} / \boldsymbol{I}^{\mathbf{T}}, \mathbf{S}(\boldsymbol{M}^{\mathrm{C}-}, \boldsymbol{U}))$$

It is worth noting that the reproduced responses can only be computed by means of a dynamic simulation, given that at each time the reproduced responses up to the previous time steps have to be known.

For this purpose, the dynamic system composed by the two vehicles with their own kinematics has been modeled using Matlab-Simulink. It is worth noting that during the estimation process vectors ***U*** and ***Ob*** represent variables that could be read from the workspace and the dynamic process only regards the update of $\boldsymbol{\beta}$, while in the validation procedure $\boldsymbol{\beta}$ *is fixed,* $\boldsymbol{I}^{\mathbf{T}}$ is read from the workspace and $\boldsymbol{M}^{\mathrm{C}}$ is obtained as a result of the simulation.

The distance between the reproduced and observed kinematics is called the Validation Index (VI):

$$\mathrm{VI} = \| \boldsymbol{M}^{\mathrm{C}}, \boldsymbol{Ob} \| \qquad 41)$$

As in the estimation phase, the distance in (41) could be computed by using RMSE, MAPE or other suitable estimators. All previous studies have evidenced that the linear model for $\mathbf{M}(\cdot)$presented in previous Sections is not actually over-performed by more complicated approaches and that it is worth adopting in light of its great simplicity.

The comparison between modelled and observed data will be referred to one of the trajectories collected, randomly chosen and said to be the *current trajectory*;

however, to provide evidence of the general suitability and robustness of the method, the current trajectory will be compared with the others by using the envelop for the best and worst cases. This is not intended to draw general rules but only to investigate the sensitivity and robustness of the approach with respect to different sets of collected data.

Prior to calibrating the sampler, Pearson's tests were carried out to check the (linear) correlation between the independent variables of equation 27 and to exclude collinearity problems in parameter estimation. The tests evidenced a mild correlation among some variables, which should not give rise to practical problems. *Table XVI* below shows the Pearson's coefficients for the case of the observed values of the *current trajectory* to which we refer in this section when showing the results.

Table XVI - Pearson's test of correlation between the independent variables of the sampler

	Δx	Δv	v_F
Δx	1	0.0155	0.4399
Δv	0.0155	1	-0.1019
v_F	0.4399	-0.1019	1

Table XVII presents some results related to the calibration of the sampler. Estimation values and statistics are shown for the current trajectory (characterised by a good variety of the observed speed and spacing) but also the min, max, mean and standard deviation of the parameters over all estimated trajectories are shown, as well as the duration in seconds of the trajectory required by the calibration algorithm in the current trajectory, in the worst and best cases.

Table XVII - Calibration result

	Current trajectory	Other trajectories			
		min	max	mean	Std.Dev.
k_0	0.09064	0.002736	0.1844	0.05825	0.05743
k_1	-0.01634	-0.03032	0.02095	-0.009440	0.01520
k_2	0.5821	0.5444	0.6183	0.5738	0.02375
k_3	0.01165	-0.02826	0.02664	0.004439	0.01543
Calibration time (s)	44.4	30.6	52.2	39.5	6.95

It is worth noting that trajectories used here are the same of those used in Section 4.1.2; the difference here consists of calibration time, in that case the whole trajectories have been used, while in this only the firsts seconds. Then it could be interesting to compare calibration results in order to understand how much the learning-running approach is actually suitable. This has been done in the next where again a box-and-whisker plot of the difference for each parameter have been given.

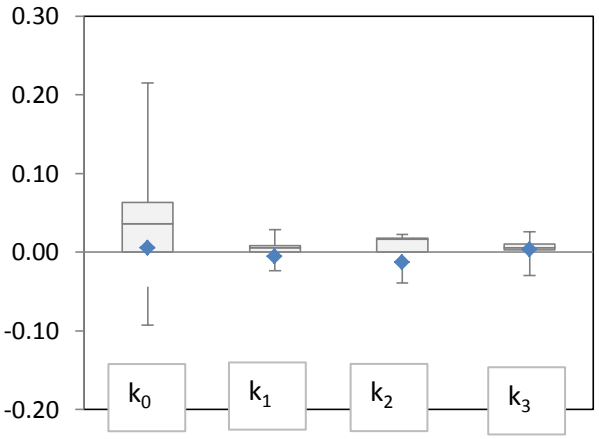

Figure 47 - The box-and-whisker plot of the difference in value of parameters in relationship to different calibration time

The main difference (however with a maximum of about 0.2) is found in the value of the constant term. Anyway all the means are more or less 0.

The results in terms of overall performance of the four-layer model are shown below; reference is made to the current trajectory but also the envelope of the worst and best performance is reported. In agreement with the approach proposed in other works based on experimental data collection (e.g. Marsden et al., 2001), comparison is made between the trajectory which would have been imposed by the ACC and that exhibited by the driver during manual driving. Figure 48 shows the ability of the sampler to reproduce the observed data. For the first 44.4 seconds the figure shows only the dark line representing the observed spacing (in metres). This part of the trajectory is required by the calibration algorithm (learning-mode phase) in order to estimate the parameters of the linear car-following model. After 44.4 seconds the dark curve plays the role of reference data, plotted until 900 seconds (15 minutes) together with estimated data (grey line). From the dark line in Figure 48, it can be seen that the current trajectory is representative of dense traffic conditions, the spacing between the vehicles ranges from about 12 to about 28 metres and the trajectory can be considered fairly variegated. The dark line in Figure 49 represents the observed speed (m/s) of the controlled vehicle. It is worth noting that as the observed speed increases (Figure 49) the spacing also increases (Figure 48), as expected. The dark line in Figure 49 ranges from 40 km/h (12 m/s) to 110 km/h (30 m/s) and confirms a variegated trajectory and the presence of dense traffic conditions.

Once the running mode starts (after 44.4 seconds), system evolution is based only on the sampler estimates and is not refreshed by observed data, that are used only for comparison purposes. Of course, in order to run the sampler also the trajectory of the leading vehicle is needed; this was obtained from observations and

represents a boundary condition for the sampler. The sampler-estimated spacing follows the observed one quite closely, confirming the human likeness of the proposed approach. From the sampler-estimated spacing the speed of the controlled vehicle can be easily computed; this is depicted by the grey line in Figure 49. The sampler-estimated speed agrees well with the observed speed. The reader should be aware that even if a satisfactory agreement with the observed spacing produces an almost perfect agreement of the speed, the reciprocal is not true. If the sampler were built to reproduce (for instance) speeds and not spacing, any error in this reproduction would have been recovered in terms of speed but not in terms of spacing due to integral error phenomena (already mentioned).

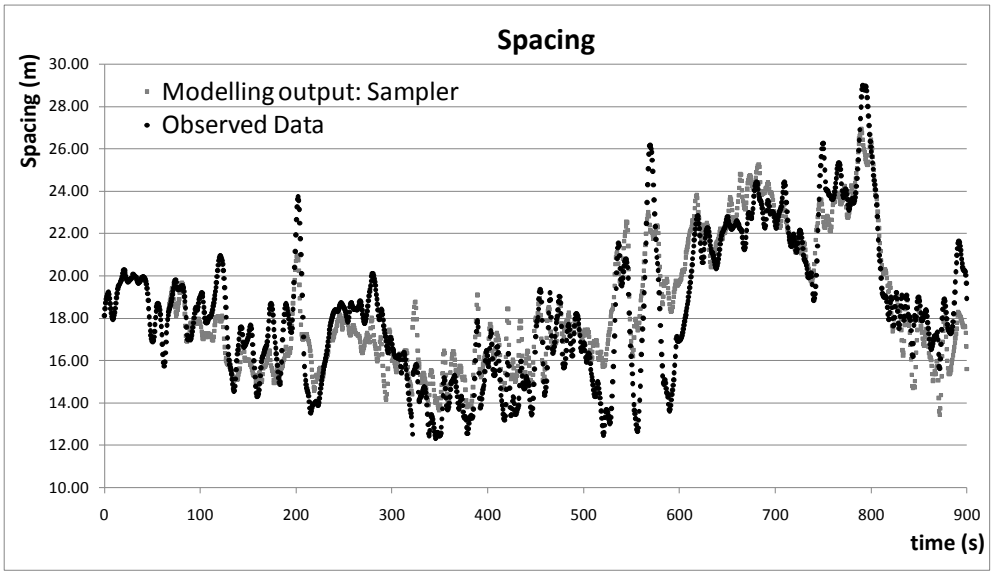

Figure 48 - Sampler performance: spacing

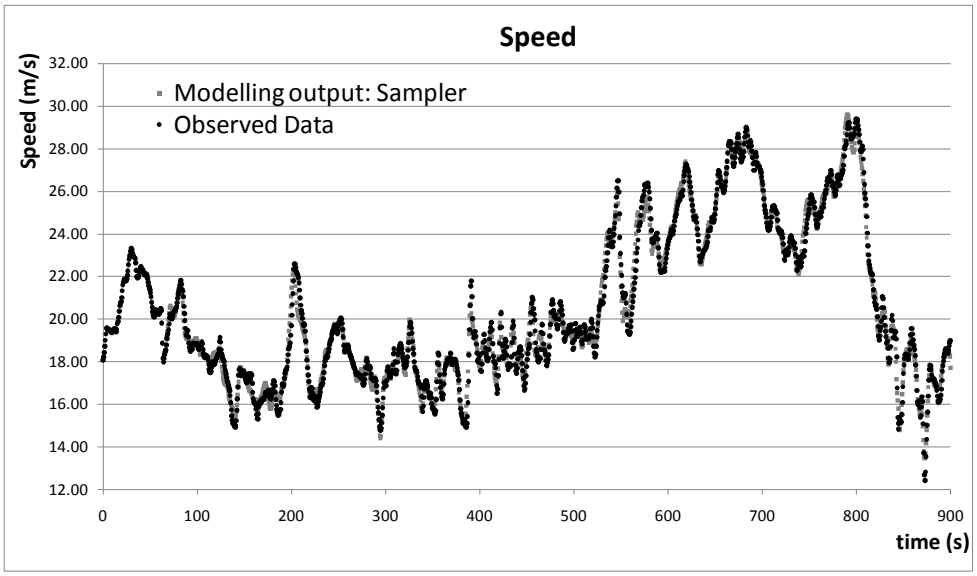

Figure 49 - Sampler performance: speed

Figure 50 extends the comparison to the results of the overall modelling platform (including the *profiler* and the *tutor*) but is restricted (for graphical representation) within a shorter interval (a little more than two minutes, from seconds 490 to 630) where the difference between the observed and estimated data is higher. In Figure 50, the observed data are represented by an interpolating continuous (dark) line just in order to enhance the clarity of the representation, but they have to be intended as plotted at a frequency of about 1 Hz, similarly to the *sampler* output (grey points). The *profiler*, instead, produces continuous data and the *tutor* produces data at quite a high frequency. Hence the grey curve that represents the result of the overall framework is continuous. The most interesting (and positive) phenomenon is that the *sampler* is able to recover estimation errors (such as after points 520 or 550 in Figure 50).

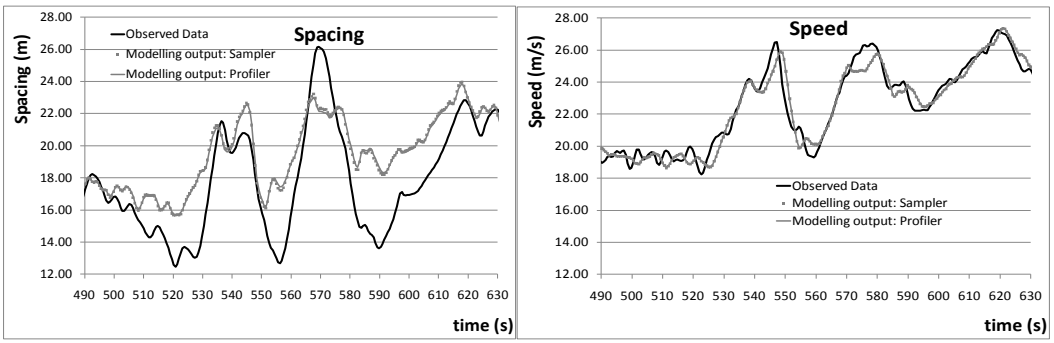

Figure 50 - Performance of the overall modeling framework: spacing and speed (details)

It should be noted that the *profiler* is built in order to fit the target spacing estimated by the *sampler*. The almost perfect overlapping of the grey points and the grey line (practically indistinguishable) on the left-hand side of Figure 50 shows that the *profiler* was appropriately constructed and that it works exactly as required (it is also evident that the *tutor* does not need to actually operate in this time interval).

The difference between the observed data and the trajectory resulting from the application of the proposed ACC can also be shown by means of the cumulative error distributions, as depicted in Figure 51 and Figure 52. The left-hand side of figure Figure 51 shows that the error made by the *sampler* in estimating the observed spacing is never greater than 77%: it is less than 20% in 60% of cases and in 40% of cases is less than 10%. Similarly, the right-hand side of figure 6 shows that the error in terms of speed reproduction is never greater than 15%, is less than 10% in 95% of cases, is less than 5% in about 80% of cases and in many cases is negligible. The different perception of errors in terms of spacing and speed should also be considered, evaluated in absolute terms. For instance, a 40% error with respect to a real spacing of 20 metres corresponds to an absolute error of 8 metres;

the same with respect to a speed of 20 m/s (72 km/h) corresponds to an absolute error of about 30 km/h. Whether a difference in spacing of 8 m with respect to the human-like one is more or less perceived by the driver (and perceived as more or less acceptable) than a difference in speed of 30 km/h should be evaluated.

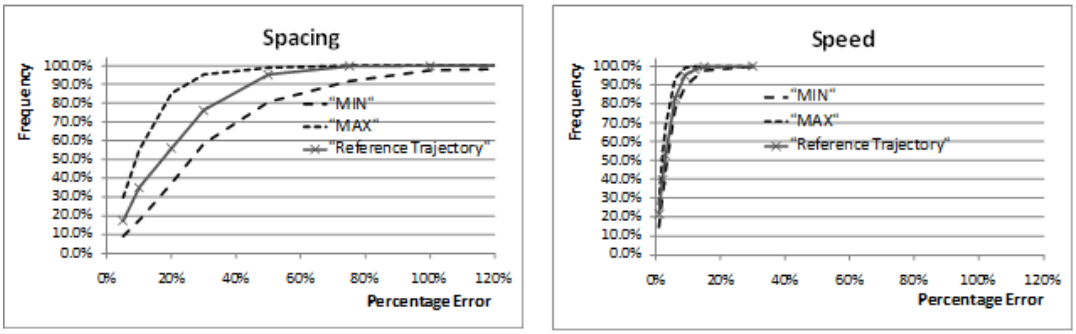

Figure 51 - Cumulative error, sampler vs. observed data: spacing and speed

Figure 52 shows the agreement of the continuous trajectory generated by the *profiler* with the discrete points estimated by the *sampler*; it is computed on the whole running mode part of the trajectory and not only on the time interval shown in figure 5. The agreement is almost perfect for spacing and very good for speed (in almost all cases the discrepancy is less than 10% and in 80% of cases less than 3%).

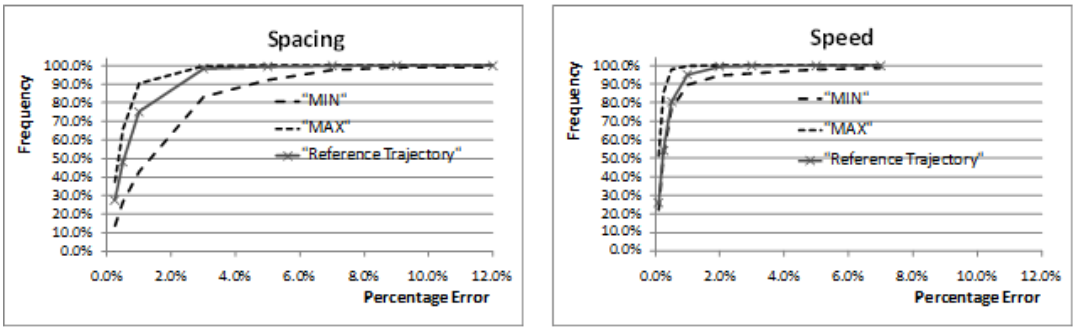

Figure 52 - Cumulative error, profiler vs sampler: spacing and speed

As a conclusive remark on comparison, the proposed framework is fairly satisfactory with respect to human likeness and, given that it can be easily calibrated in real time and on demand for different drivers, different contexts and/or different driving sessions, it can be judged to be fully adaptive.

The accordance of the reproduced responses with observed ones guarantees that also other variables of common interest, such as headway and/or adopted TTC, have similar pattern when computed both on the observed data and on the response of the model. Some examples for what concerns the Revised AP Paradigm, using the Opening Chart, are given in the following:

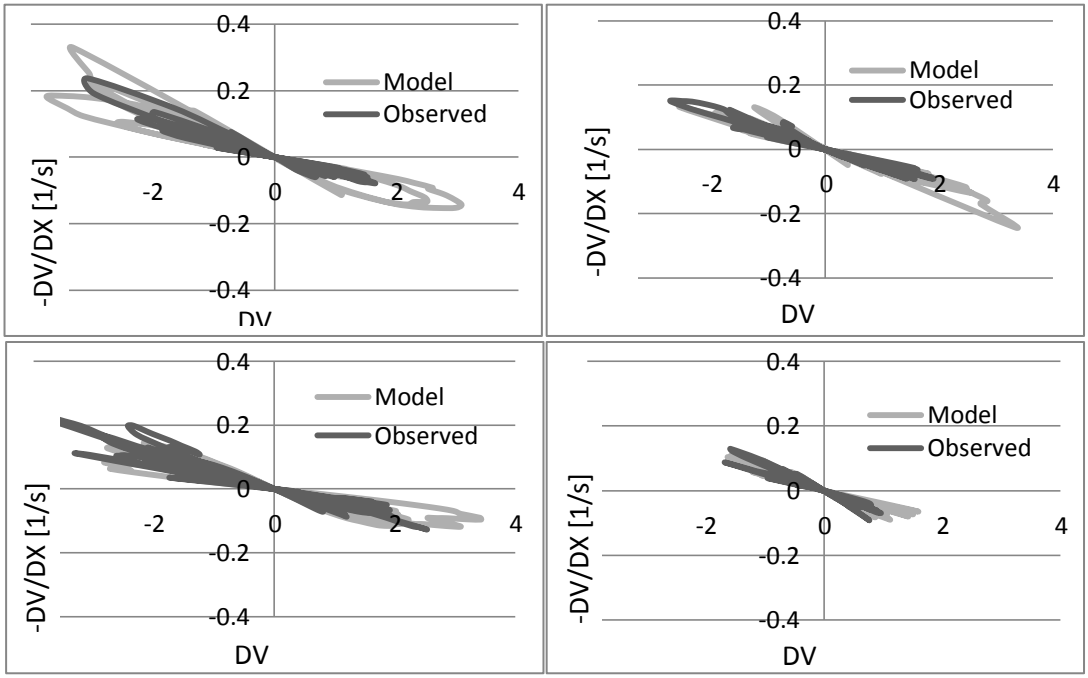

Figure 53 - The opening chart depicted with respect to several responses of the ACC and compared with the observed patterns

The Figure shows the opening charts depicted for four trajectories (randomly selected between the thirteen considered) and for both the observed and reproduced behaviours; the observed pattern is in dark grey, the reproduced is lighter. Unavoidably differences can be found even here, but what is interesting is that the slope of both patterns (for all the cases) is very similar; it is worth noting that this term represent the main parameter of the regression curves given in Table VI of Section 3.1.2.

Conclusion

The works described in this thesis have been based on experimental data of car following behaviour collected in Italy and United Kingdom by means of an instrumented vehicle.

For what concerns the theoretical part of the thesis, analyses of collected data in the frame of a revised action point paradigm have shown that observed patterns are consistent with those discussed elsewhere (Brackstone et. al., 2002). This suggests that the action point paradigm is able to reproduce consistent results when applied to different data sets. However, from the collected data it is observed that although the observed action points defined with respect to the relative velocity (OPDV and CLDV) fit the existing paradigm, the observed action points defined with respect to spacing (SDX and ABX) are more problematic. This has suggested that a reinterpretation of the action point paradigm is needed only in terms of relative velocities, and this has been presented and expanded. It has been shown that this revised version of the paradigm is more compliant with original studies related to Action Point models (refer to Section 1 for more details).

The resulting process is internally consistent, and fits observed data, also leading to consistent figures for other variables such as time-headways and times-to-collision. In particular, time-to-collision and inverse of time-to-collision can be interpreted in terms of *closing and opening waves*, which may be used to describe patterns in the distribution of action points.

An engineering model has been proposed too, developed in the form of a dynamic-system. This approach can be considered as a consolidated practice in order to describe a car following process. Indeed, the general car-following model given by Wilson has been particularized and framed within a state-space (continuous) model. The analytical framework developed allows for a simple, but not simplistic, model for car-following, depending on only a few parameters. The main parameter is the desired spacing (space headway), computed at the equilibrium, that is when the follower has attained a satisfactory spacing with the leader and has no residual stimuli for changing the dynamics of the vehicle.

The general response of the proposed state-space model can be described as a *step* response in the event that the leader has a constant speed. The bias reproduced in the model by non-constant leader's speed can be incorporated in the model, but it is not possible in this case to derive an analytical solution of the general response, at least if it is not proposed a proxy function for the leader's speed. However, in this more general case it is still possible to use the model in simulation and the obtained

behaviour is similar to the one evidenced by observed car-following data, once the model is properly identified.

A formal relationship can be established between the proposed state-space model and the Action-Point paradigm. Thanks to this relationship, some necessary and sufficient analytical conditions for finding APs from the proposed state-space model can be given, these hold in the event of constant leader's speed.

An empirical procedure introduced has been verified to be consistent with the analytical solutions. In the event of non-constant leader's speed, the analytical conditions are only necessary and no longer sufficient, thus they can't be used in order to identify APs and, in this case, empirical procedures are needed.

The relationship between the state-space model and the APs can be exploited in the reverse way. Once APs have been identified by means of any suitable empirical procedure, the desired equilibrium spacing can be estimated, which represents one of the main inputs required for the identification of the state-space model.

The overall framework has been confirmed with good evidence by observed data, independently collected in Italy and in United Kingdom. Application on real-world data has also shown that the estimation of the inputs and of the parameters of the state-space model is a suitable task. Moreover, the analytical structure of the state-space approach allows for understanding in which cases (and why) the observed behaviours deviate from the predicted ones.

Finally, a linear model has been derived again from the general formulation of Wilson. The model has been considered suitable in order to be applied in a *fully-adaptive* Cruise Control. The control logic behind the ACC was designed to be fully-adaptive, in the sense that it can be easily adapted to different drivers and/or different driving contexts, it can be calibrated on demand by just driving for a few minutes and, finally, it reproduces the behaviour the driver would have had (human likeness). The possibility of calibrating and applying the developed framework in real time and on demand is strongly associated with the linear architecture of the embedded car-following model. Despite the simple linear approach the results are very satisfactory, thus confirming the previous findings by Bifulco et al. (2008) and Simonelli et al. (2009), as well as some evidence in the literature, where simpler models outperform (especially in validation) more complex ones. The linear model is shown to be consistent with the revised Action Point paradigm, as well as with the proposed state-space model. However, with respect to the latest, the linear model produces as a phase portrait a typical harmonic oscillator shape; this is consistent with the proposed state-space model only in case of under-damped results of the calibration, that happens on real data in few cases. The inconsistency in the calibration of the linear and the state-space model should be investigated in future works.

The developed framework for the ACC system was structured into four layers: the *sampler*, the *profiler*, the *tutor* and the *performer*. The *sampler* is responsible for establishing the ACC control logic, the *profiler* is intended to transform the control logic into a continuous kinematic profile to be followed by the controlled vehicle, the *tutor* is in charge of ensuring the ultimate safety of the vehicle's kinematics, and the *performer* is in charge of applying the reference trajectory by using the vehicle's on board actuators (e.g. brakes, throttle, etc.) and by interacting with the internal dynamics of the vehicle and with the road. The proposed modelling framework was implemented in a Simulink/Matlab environment in order to release a standard implementation suitable in the future for possible fast-prototyping.

In the proposed ACC-oriented car-following formulation the stimulus towards spacing adjustment not only depends on the relative speed difference but also on the consistency between the current spacing and the cruising speed. This effect is somehow embedded in the value of the parameters of the proposed linear model. In particular, future studies could investigate whether an appropriate combination of linear model parameters could represent a sort of footprint of the driver's driving style. Even if the proposed modelling framework could well be adapted to a wider range of applications, including traffic simulation, it is developed and presented herein with specific reference to the case of ACC. However, ACC applications require that some strict requirements in terms of real-time applicability be satisfied and a major part of our research effort was devoted to precisely that. The authors' perception is that preparing answers to such real-time issues is also relevant to non-ACC applications, given that an increasing number of traffic problems need to be solved nowadays in real-time (or fast-time) contexts. However, extension of the approach to non-ACC oriented applications is another task for future research.

Future experiments should also fill some gap of the current research.

In this thesis the parameters of the models have been estimated with the aim to fit observed data. This has allowed for modelling validation and for demonstration of the suitability of proposed models. However, an analysis of the dispersion of obtained parameters across a significant population of drivers could be of great help for understanding the dispersion of driving behaviours or for clustering them with respect to the driving style. This also applies to the linear regressions associated with the opening and closing charts of the revised AP theory.

For what concerns the developed ACC logic, a comparison of the kinematic imposed this model with conventional/commercial versions of the ACC would have been opportune. Unfortunately, the exact logics used by manufacturers (e.g. Bosch) are not reported and instrumented vehicles equipped with ACC were not available (it would have required extra funding).

Finally this thesis lacks of an analysis of stability properties of the proposed models. Investigate on this issue will give the possibility to evaluate stability of observed behaviours and to put in place strategies aimed at obtaining a more correct calibration; this seems a natural outlet in order to design actual ADAS.

References

Aron, M. (1988). Car following in an urban network: simulation and experiments. In *Proceedings of Seminar D, 16th PTRC Meeting*, 27‑39.

Bageshwar, V.L., Garard, W. L., & Rajamani, R., 2004. Model predictive control of transitional maneuvers for adaptive cruise control vehicles, *IEEE Transaction on Vehicular Technology*, 53(5), 1573-1585.

Bando, M., Hasebe, K., Nakayama, A., Shibata, A., and Sugiyama, Y. (1995) Dynamic model of traffic congestion and numerical simulation. *Physical Review E*, vol. 51, 1035-1042

Barbosa, L. (1961) Studies on Traffic Flow Models. Reports No. 202A-1. The Ohio State University Antenna Laboratory

Benekohal, R., F. and Treiterer, J. (1989) Carsim: car following model for simulation of traffic in normal and stop and go conditions. *Transportation Research Records*, vol. 1194, 99-111

Bevrani, K. and Chung, E. (2011) An examination of the microscopic simulation models to identify traffic safety indicators. *International Journal of Intelligent Transportation Systems Research* Available from 28th December 2011 before print publication. DOI: 10.1007/s13177-011-0042-0.

Bifulco G.N., Simonelli F., & Di Pace R. 2008, Experiments toward a human-like Adaptive Cruise Control. In: 2008 IEEE Intelligent Vehicles Symposium, pp. 919-924.

Bifulco, G., N., Pariota, L., Simonelli, F. and Di Pace, R. (2011) Real time smoothing of car-following data through sensor fusion techniques, *Procedia - Social and Behavioral Sciences*, vol. 20, 524-535.

Bishop, R. (2000) A Survey of Intelligent Vehicle Applications Worldwide, In: *Proceedings of The IEEE Intelligent Vehicle Symposium*, 2000.

Bonsall, P., Liu, R. and Young, W. (2005) Modelling safety related driving behavior – impact of parameter values. *Transportation research Part A: Policy and Practice*, 39, 425-444.

Boyce, T. E., & Geller, E. S. (2002). An instrumented vehicle assessment of problem behavior and driving style: Do younger males take more risks?. *Accident Analysis and Prevention*, vol. 34(1), 51-64.

Brackstone, M. and McDonald, M. (1999) Car following : a historical review. *Transportation Research Part F: Traffic Psychology and Behaviour*, vol. 2(4), 181-196.

Brackstone, M., Sultan, B. and McDonald, M. (2002) Motorway driver behaviour: studies on car following. *Transportation Research Part F: Traffic Psychology and Behaviour, vol.* 5**,** 31-46

Brackstone, M.,Waterson, B. and McDonald, M. (2009) Determinants of following headway in congested traffic. *Transportation Research Part F: Traffic Psychology and Behaviour, vol.* 12**,** 131-142

Brockfeld E., Kuhne R.D., & Wagner P., 2005. Calibration and validation of microscopic traffic flow models. *Transportation Research Records*, 1934, 179-187.

CarSim 8: Math Models. Mathematical Simulation Corporation, viewed 29 June 2011. http://www.carsim.com/

Ceder, A., and May, Jr., A. D. (1976). Further evaluation of single and two regime traffic flow models. *Transportation Research Record*, vol. 567, 1‑30

Chakroborty, P. and Kikuchi, S. (1999). Evaluation of the General Motors based Car-Following Models and a Proposed Fuzzy Inference Model. *Transportation Research Part C*, vol. 7(4), 209-235.

Chandler, R., E., Herman, R. and Montroll, E., W. (1958). Traffic dynamics: studies in car-following. *Operations Research*, vol. 6, 165-184.

Ervin, R. D., (2005). *Automotive collision avoidance system field operational test methodology and results*, 2005. DOT HS 809 900. University of Michigan, Ann Arbor, Transportation Research Institute.

Evans, L., and Rothery, R. (1977) Perceptual thresholds in car following – a recent comparison. *Transportation Science*, vol. 11(1), 60-72.

Fancher, P., S. and Bareket, Z. (1998) Evolving model for studying driver-vehicle system performance in longitudinal control of headway. *Transportation Research Record*, vol. 1631, 13-19.

Fancher, P., Ervin, R. D., Sayer, J., Hagan, M., Bogard, S., Bareket, Z., Mefford, M., and Haugan, J., (1998). *Intelligent cruise control field operational test - final report*, July 1998. DOT HS 808 849. NTIS, Springfield, Virginia 22161, USA.

Fritzsche, H-T. (1994). A model for traffic simulation. *Transportation Engineering Contribution*, vol. 5, 317–321.

Gazis, D. C., Herman, R. and Potts, R. B. (1959) Car-following theory of steady-state traffic flow. *Operations Research*, vol. 7**,** 499-505.

Gazis, R., Herman, R. and Rothery, R., W. (1961). Nonlinear follow the leader models of traffic flow. *Operations Research*, vol. 9, 545-567.

Gettman, D. and Head, L. (2003) Surrogate Safety Measures from Traffic Simulation Models, Final Report Federal Highway Administration, http://www.fhwa.dot.gov/publications/research/safety/03050/index.cfm

Gipps, P., G. (1981) A behavioural car-following model for computer simulation. *Transportation Research Part B: Methodological*, *vol.* 15**,** 105-111

Goodrich, M. A., Boer, E. R. and Inoue, H. (1999). A model of human brake initiation behavior with implications for ACC design. In *Proceedings of International Conference on Intelligent Transportation Systems* (ITSC99), 5-8 October. Tokyo.

Gray, R., and Regan, D. (1998). Accuracy of estimating time to collision using binocular and monocular information. *Vision Research*, 38, 499-512

Gurusinghe, G.S., Nakatsuji, T., Yoichi, A., & Prakash, R., 2002. Multiple car-following data with real-time kinematic Global Positioning System, *Transportation Research Records*, 1802, 166-180.

Hamdar, S. H. and Mahmassani, H. S. (2008) Driver car-following behavior: From discrete event process to continuous set of episodes. *Transportation Research Board 87th Annual Meeting, preprint CD-ROM*

Harms, L., and Patten, C. (2003). Peripheral detection task as a measure of driver distraction. A study of memory-based versus system-based navigation in a built-up area. *Transportation Research Part F: Traffic Psychology and Behaviour*, vol. 6, 23-26.

Helly, W. (1958). Simulation of Bottlenecks in Single Lane Traffic Flow. In *Proceedings of the Symposium on Theory of Traffic Flow*, Research Laboratories, General Motors, 207-238. New York: Elsevier

Heyes, M., P. and Ashworth, R. (1972). Further research on car following models. *Transportation Research*, vol. 6, 287-291.

Hoefs, D.H. (1972). *Entwicklung einer Messmethode uber den Bewegungsablauf des Kolonnenverrkehrs*. Universitat (TH) Karlsruhe, German

Hoffmann, E., R. and Mortimer, R., G. (1996). Scaling of relative velocity between vehicles. *Accident Analysis and Prevention*, vol. 28 (4), 415-421.

Hoogendoorn, S., Hoogendoorn, R., G. and Daamen, W. (2011). Wiedemann Revisited: New Trajectory Filtering Technique and Its Implications for Car-Following Modeling. *Transportation Research Record*, vol. 2260, 152-162.

Kesting, A., Treiber, M., Schonof, M., and Helbing, D., (2008). Adaptive cruise control design for active congestion avoidance. *Transportation Research Part C:emerging technologies*, 16(6), 668-683.

Kesting, A. (2008) Microscopic Modelling of Human and Automated Driving: Towards Traffic-Adaptive Cruise Control. Ph.D. Thesis, University of Dresden

Kometani, E. and Sasaki, T. (1958). On the stability of traffic flow. *Journal of Operations Research Japan*, vol. 2, 11-26.

Kometani, E. and Sasaki, T. (1959). Dynamic behaviour of traffic with a nonlinear spacing-speed relationship. In Proceedings of the Symposium on Theory of Traffic Flow, Research Laboratories, General Motors, pp. 105-119.

Ljung, L., (1987). System Identification: Theory for the User. Prentice-Hall, Englewood Cliffs.

Ma., X. & Andreasson, I. 2005, Dynamic car following data collection and noise cancellation based on the Kalman smoothing. In: *2005 IEEE International Conference on Vehicular Electronics and Safety*, pp. 35-41.

Marsden, G., McDonald, M., & Brackstone, M., 2001. Towards an understanding of adaptive cruise control. *Transportation Research Part C*, 9 (1), 33-51

Marsden, G., McDonald, M. and Brackstone, M. (2003) A Comparative Assessment of Driving Behaviours at Three Sites. *European Journal of Transportation and Infrastructure Research*, vol. 3(1), 5-20.

Martinez, J. J. & Canudas-De-Wit, C., 2007. A safe longitudinal control for adaptive cruise control and stop-and-go scenarios, *IEEE Transaction on Control Systems Technology*, 15(2), 246-258.

May, A., D., Jr. and Keller, H., E., M. (1967). Non integer car following models. *Highway Research Record*, vol. 199, 19-32.

McCall, J., C., Achler, O. and Trivedi, M., M. (2004). Design of an Instrumented Vehicle Test Bed for Developing a Human Centered Driver Support System. In *Proceedings of the IEEE Intelligent Vehicles Symposium*

McDonald, M., Brackstone, M., Sultan, B. and Roach, C. (1999). Close Following on the Motorway: Initial Findings of an Instrumented Vehicle Study. In *Proceedings Vision in Vehicles Conference VII*, 381-389. Elsevier, Netherlands.

McLaughlin, S.,B., Hankey, J., M. and Dingus, T., A. (2008) A method for evaluating collision avoidance systems using naturalistic driving data, *Accident Analysis & Prevention*, vol. 40 (1), 8–16.

Michaels, R.M. (1963). Perceptual factors in car following. In *Proceedings of the Second International Symposium on the Theory of Road Traffic Flow*, 44‑59. Paris: OECD

Minderhoud, M.M. and Bovy, P.H.L. (2001) Extended time-to-collision measures for road traffic safety assessment. *Accident Analysis and Prevention*, vol. 33, 89‑97

Montella, A. (2010) A comparative analysis of hotspot identification methods. *Accident Analysis and Prevention*, vol. 42(2), 571-581.

Montroll, E.W. (1959). Acceleration and clustering tendancy of vehicular traffic. In *Proceedings of the Symposium on Theory of Traffic Flow*, Research Laboratories, General Motors 147‑157. New York: Elsevier

Moon, S. and Yi, K., (2008). Human driving data-based design of a vehicle adaptive cruise control algorithm. *Vehicle System Dynamics*, 46 (8), 661-690

Newell, G., F. (2002) A simplified car-following theory: a lower order model. *Transportation Research part B: Methodological*, vol. 36(3), 195-205.

NGSIM: Next Generation Simulation. FHWA, U.S. Department of Transportation. http://ops.fhwa.dot.gov/trafficanalysistools/ngsim.htm Accessed Jan 14, 2013.

Oh, C., Hong, S. and Park, J. (2009) Analysis of Driver Behavior in Response to Variable Message Signs Using In-Vehicle Differential Global Positioning System Data, Proceedings of *88th Transportation Research Board Annual Meeting (TRB)*, National Research Council, Washington, D.C., January 2009.

Ossen, S. & Hoogendoorn, S.P., 2010. Heterogeneity in car-following behavior: theory and empirics. *Transportation Research Part C*, 19 (2), 182-195.

Ozaki, H. (1993). Reaction and anticipation in the car following behaviour. In *Proceedings of the 13th International Symposium on Traffic and Transportation Theory* 349‑366.

Pérez Zuriaga, A., M., García, A. , Camacho Torregrosa, F., J., and D'Attoma, P. (2000) Modeling operating speed and deceleration on two-lane rural roads with global positioning system data, *Transportation Research Record*, vol. 2171, 11-20.

Punzo, V. & Simonelli F., 2005. Analysis and comparison of car-following models using real traffic microscopic data. *Transportation Research Records*, 1934, 42-54.

Ranjitkar, P., Nakatsuji, T., & Asano, M., 2004. Perfomance Evaluation of microscopic traffic flow models using test track data. *Transportation Research Records*, 1876, 90-100.

Ranjitkar, P., Nakatsuji, T., & Kawamua, A., 2005. Car-following models: an experiment based benchmarking. *Journal of Eastern Asia Society for Transport Studies*, 6, 1582-1596.

Reichart, G., Haller, R., & Naab, K., 1997. Driver assistance: BMW solutions for the future of individual mobility, In: *Proceedings of the Fourth World Congress on ITS*. Berlin, Germany

Simonelli F., Bifulco, G. N., De Martinis, V., & Punzo, V., 2009, Human-like adaptive cruise control systems through a learning machine approach. In: Avineri, E., Köppen, M., Sunitiyoso, Y., Dahal, K. and Roy, R. (Eds.) Applications of soft computing: updating the state of art, Springer - Berlin, pp. 240-249.

Tarko, A., Davis, G., Saunier, N., Sayed, T. and Washington, S. (2009) Surrogate measures of safety, White paper, ANB20(3) Subcommittee on Surrogate Measures of Safety.

Thiemann, C., Treiber, M. and Kesting, A. (2008) Estimating acceleration and lane-changing dynamics from next generation simulation trajectory data. *Transportation Research Record*, **2088**, 90-101.

Todosoiev, E., P. (1963) The Action Point Model of the Driver Vehicle System. Report No. 202A-3. The Ohio State University, Engineering Experiment Station, Columbus, Ohio

Toledo, T. (2007) Driving Behavious: Models and Challenges (2007) *Transport Reviews*, vol. 27(1), 65-84.

Toledo, T., Koutsopoulos, H., N., and Ben-Akiva, M. (2009). Estimation of an integrated driving behavior model. *Transportation Research Part C: Emerging Technologies*, vol. 17(4), 365-380.

Treiber, M., Hennecke, A., and Helbing, D. (2000) Congested Traffic states in empirical observations and microscopic simulations. *Physical Review E*, vol. 62, 1805-1824.

Treiber, M., Kesting, A., and Helbing, D. (2006) Delays, inaccuracies and anticipation in microscopic traffic models. *Physica A*, vol. 360, 71-88

Treiterer, J. and Myers, J. A. (1974). The hysteresis phenomenon in traffic flow. In *Proceedings of the Sixth International Symposium on Transportation and Traffic Theory*, Sydney, 13‑38

Tripodi, A. (2007) Applicazione della teoria dei sistemi dinamici non lineari nei modelli microscopici di traffico. Ph.D. Thesis, University of Naples Federico II

Van der Heijden, R.E.C.M. and Marchau, V.A.M.J. (2005) Intelligent transportation systems (ITS) and driving behavior: setting the agenda. Systems, Man and Cybernetics, 2004 IEEE International Conference, vol. 4, ISSN 1062-922X, ISBN 0 7803 8566 7. pp. 4003-4010.

Viti, F., Hoogendoorn, S. P., Alkim, T. P., and Bootsma, G., (2008). Driving behavior interaction with ACC: results from a Field Operational Test in the Netherlands. In: Proceedings of *2008 IEEE Intelligent Vehicle Symposium*. Eindhoven, Netherlands.

Wagner, P. (2011). A time-discrete harmonic oscillator model of human car-following. *European Physical Journal B*, 84 (4), 713-718.

Ward, J., A. (2009) Heterogeneity, Lane Changing and Instability in Traffic: A mathematical Approach. Ph.D. Thesis, University of Bristol

Warren, W. H. (1995). Self-motion: visual perception and visual control. In W. Epstein, & S. Rogers, Perception of space and motion (pp. 263-312). San Diego, CA: Academic Press.

Weber-Fechner Law. http://en.wikipedia.org/wiki/Weber%E2%80%93Fechner_law. Accessed Jan 14 2913

Wiedemann, R. (1974) Simulation des Strassenverkehrsflusses Tech. Rep. Institut für Verkehrswesen. Universität Karlsruhe, Heft 8 der Schriftenreihe des IfV (in German).

Wiedemann, R., and Reiter, U. (1992). *Microscopic traffic simulation: the simulation system MISSION, background and actual state, CEC Project ICARUS (V1052)*, Final Report, vol. 2, Appendix A. Brussels: CEC

Wilson, R. E. (2008). Mechanism for spatiotemporal pattern formation in highway traffic models. *Philosophical Transactions of the Royal Society part A*, vol. 366, 2017-2032

Wu, J., Brackstone, M., & McDonald, M., 2003. The validation of a microscopic simulation model: a methodological case study. *Transportation Research Part C*, 11 (6), 463-479.

Yi, K. and Moon, S. (Ed.), (2004). A Driver-adaptive stop-and-go cruise control strategy. In: *2004 IEEE International Conference on Networking, Sensing & Control*, 601-606.

Yan, X., Abdel-Aty, M., Radwan, E., Wang, X. and Chilakapati, P. (2008) Validating a driving simulator using surrogate safety measures, *Accident Analysis & Prevention*, Vol. 40 (1), 274-288

Zhang, H., M. (1999) A mathematical theory of traffic hysteresis. *Transportation Research part B: Methodological*, vol. 33(1), 1-23.

Zheng, P. and McDonald, M., (2005). Manual vs. adaptive cruise control – Can driver's expectation be matched? *Transportation Research Part C*, 13 (5-6), 421-431.

Appendix A – Information fusion for car-following data

The smoothing procedure to filter raw sensor described in this Section derives from experiment described in Bifulco et al. (2011), to which the reader can refer for more details.

The basic idea is to use a Kalman filter in order to smooth sensors-measured data. Smoothing of raw data in order to obtain useful time-series could be made (Gurushinghe et al., 2002) independently for time-series related to different variables at hand (speeds, spacing among vehicles, etc.). However, the use of the Kalman filter technique ensures the consistency among different measures related to the same physical phenomenon. This can be obtained thanks to the state space model underlined by the Kalman approach.

It is assumed here that the kinematic variables of the leading vehicle and the follower obey to a physical phenomenon. In particular the hypothesis is that the vehicles move from any discrete time (k-1) to the successive one (k) with uniform acceleration motion. In formal terms:

$$s_i(k+1) = s_i(k) + v_i(k)\,T + 0.5\,a_i(k)\,T^2 \quad (42)$$

$$v_i(k+1) = v_i(k) + a_i(k)\,T \quad (43)$$

where:

- i, is the generic vehicle, in our car following context $i \in \{F, L\}$, where F identify the follower and L the leading vehicle;
- s_i, is the total traveled distance by vehicle i starting from an arbitrary initial point (the same for all vehicles);
- v_i, is the speed in the direction of the motion;
- a_i, is the acceleration in the direction of the motion;
- T, is the (fixed) time step elapsed from k to k+1.

In order to complete the dynamic model which is beside the Kalman approach, an hypothesis is needed on the acceleration dynamic; the approach here is to assume a random walk model for it.

Under the previous hypotheses the state vector of the dynamic system composed by the two vehicles in car-following conditions can be assumed as $\mathbf{X}^T = [s_F, s_L, v_F, v_L, a_F, a_L]$ and the state space model can then be written as:

$$\mathbf{X}(k+1) = \mathbf{A}\,\mathbf{X}(k) + \boldsymbol{\xi}(k) \quad (44)$$

Where no control input has been considered and where $\mathbf{A}$ is the state transition matrix and $\boldsymbol{\xi}$ the process error vector.

In particular, according with equations 42) and 43) (written for both the follower and the leader) and the random walk hypothesis for the accelerations:

$$\mathbf{A} = \begin{bmatrix} 1 & T & 0.5\cdot T^2 & 0 & 0 & 0 \\ 0 & 0 & 0 & 1 & T & 0.5\cdot T^2 \\ 0 & 1 & T & 0 & 0 & 0 \\ 0 & 0 & 0 & 0 & 1 & T \\ 0 & 0 & 1 & 0 & 0 & 0 \\ 0 & 0 & 0 & 0 & 0 & 1 \end{bmatrix}, \quad \boldsymbol{\xi}^T = [\xi_{sF}, \xi_{sL}, \xi_{VF}, \xi_{VL}, \xi_{aF}, \xi_{aL}]$$

Where:

- ξ_{sF}, ξ_{sL}, ξ_{VF} and ξ_{VL} are withe (zero-mean) noises. They take into account the approximations introduced on the positioning of the vehicles and on the velocities, including the ones deriving from the approximated uniformly accelerated motion hypothesis;
- ξ_{aF} and ξ_{aL} represents the random walking of accelerations (white noises too).

The elements of vector $\boldsymbol{\xi}$ are here considered as independently distributed Gauss variables with zero mean. The dispersion matrix (process noise covariance matrix) of $\boldsymbol{\xi}$ is denoted as **Q** and, because of independence, is assumed to be diagonal.

The kinematics of the vehicle is assumed to also be instantaneously measurable by means of on-board sensors. This happen for both the following and the leading vehicle. In particular, the following vehicle is assumed to be the controlled one, on which the Kalman filter is applied by an on-board ECU (Electronic Control Unit) also responsible for the application of the more general ADAS/ACC system. The controlled vehicle is assumed to be equipped at least by a radar, able to measure the relative spacing and velocity with respect to the leading vehicle. Likely, the vehicle is also equipped by a WSS, able to measure the velocity in the direction of the motion.

In the state space model of equation 44) and matrix **A** the position is not identified by means of global positioning coordinates; rather, it is identified by means of the total travelled distance (from an arbitrary origin) which is not a straight measurement for GPS sensors.

In our case, the complete measurement vector is:

$\mathbf{z}^T = [\mathbf{zr}^T, vw_F]$

where

- $\mathbf{zr}^T = [\Delta s, \Delta v]$

- and where Δs and Δv and relative spacing and speed measured by the radar and vw_F is the velocity measured by the WWS.

The complete matrix that relates the measurement to the state variables is then:

$$H=\begin{bmatrix} -1 & 0 & 0 & 1 & 0 & 0 \\ 0 & -1 & 0 & 0 & 1 & 0 \\ 0 & 1 & 0 & 0 & 0 & 0 \end{bmatrix}$$

The instantaneous measurement equation required by the filter can then be expressed by:

$\mathbf{z}(k) = \mathbf{H}\,\mathbf{X}(k) + \zeta(k)$

- where ζ is the vector of measurement errors, here assumed to be distributed as a multivariate normal with zero mean and independent components. The dispersion matrix associated to ζ is denoted by **R**. It is diagonal because of the independence hypothesis and the values of the variances depends on the measurement.

The vector of the measurements plays with its complete form only if all sensors are available. Otherwise, only some components of the complete vector **z** have to be considered, as well as only the corresponding sub-matrices composing matrix **H**.

Appendix B – Empirical procedure for APs selection

The selection of APs from on field data has been based on the procedure reported in Brackstone et al. (2002) to which the reader can refer for more details.

The starting point is represented by the observed spiral plot (the plot of the relative speed against the spacing).

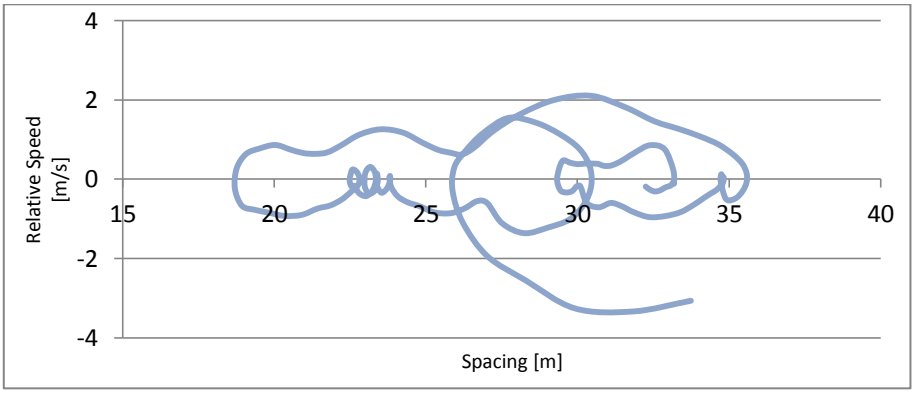

Figure 54 - An observed spiral plot

The observed trajectory is divided in semi-spirals; each semi-spiral is represented by the portion of trajectory between two consecutive points where the relative speed is null.

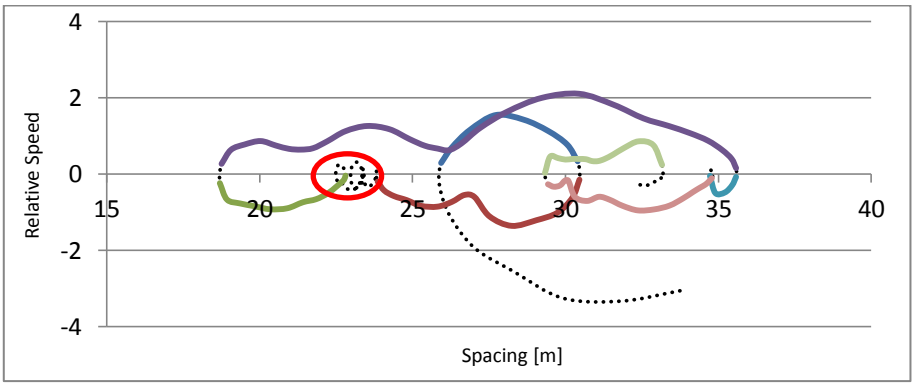

Figure 55 - The selected semi-spirals

As evidenced in Figure 55 not all the semi-spirals are selected in the procedure, in fact some criteria have to be respected, that are:

- a subjective cut-off in leader's acceleration is imposed, that conducts to an elimination of any semi-spirals where the absolute value of the lead vehicle acceleration greater than 0.6 m/s^2 is observed; this allows to presume that the relative motion of the follower is not overly effected by large fluctuations in leader's speed and that close-following conditions are observed;

- a minimum time-duration as well as a minimum length of the semi-spiral (expressed as the observed change in spacing of the semi-spiral) are required, that are respectively 2s and 1m; the reason behind this is to discharge *mini-spirals* that results from traffic fluctuations and not from actual adjustment of the driver to the behaviour of the vehicle in front (an example for this has been evidenced with a red circle in Figure 55).

The smaller and the bigger values of spacing of each semi-spiral represent respectively an ABX and an SDX points.

For the selection of CLDV and OPDV a similar procedure is used, in fact CLDV and OPDV represent respectively the point of the semi-spiral with the lower value of relative speed (when the follower decreases the distance and semi-spiral goes from SDX to ABX) and the one with greater value of relative speed. Moreover, in this case, a further step is added:

- a cut-off threshold for the selection of action points is imposed, where the rate between the magnitude of relative speed and the spacing exceeds the value 0.01. The principal reason behind this is to exclude any points where an action is taken without the drivers' perception of the relative speed. In essence this threshold describes the minimum relative speed that a driver is able to detect and use in the decision making process.

An example of the result of this procedure has been shown in the next Figure, where it has been applied one of the trajectory collected in the experiment described in Section 2.1.

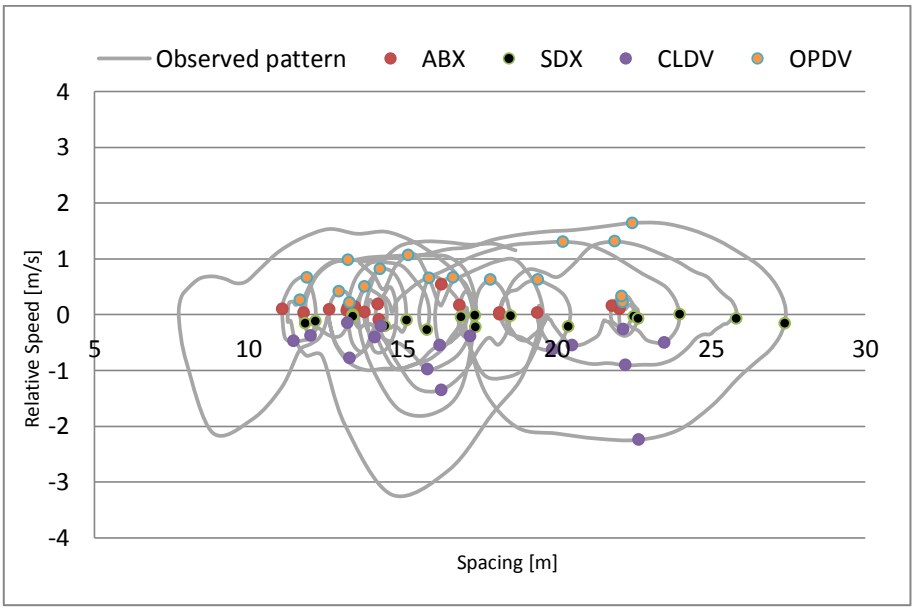

Figure 56 - An example of the results of the procedure once applied to one of the collected trajectory

Appendix C – Validation of the empirical procedures for APs

In order to validate the estimates made by the Brackstone et al. (2002) procedure, it was applied to the ad-hoc data shown in Figure 29, for which the results are known. Table XVIII below shows that the same points obtainable (in this case) in the analytical way (or graphically by Figure 30) can be also obtained by the procedure. As a consequence, the procedure will be considered as accurate and can be used for the practical identification of APs.

Table XVIII. Validating the Brackstone's procedure for APs with known (analytical) data

AP	Δx (m)	Δv_n (m/s)	v_n (m/s)	a_n (m/s^2)
SDX	34.98	0.00	30.00	0.11
	30.54	0.00	30.00	0.01
ABX	14.87	0.00	30.00	-0.34
	28.36	0.00	30.00	-0.04
CLDV	49.84	-4.46	34.46	0.00
	32.15	-0.48	30.48	0.00
OPDV	23.48	1.47	28.53	0.00
	29.29	0.16	29.84	0.00

Next Figure 57 shows a typical phase portrait for realistic data; it has been obtained stressing the example model presented in Figure 25 with the additional input coming from the leader's trajectory presented in Figure 26.

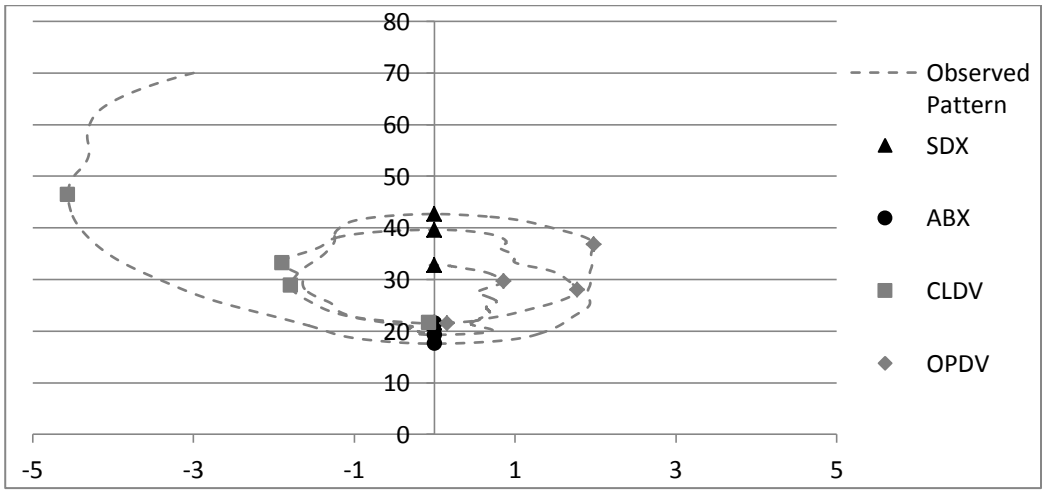

Figure 57 - Car-following spirals in case of real data: the leader's behaviour un-stabilises the system and several spirals are often reinitialised

The points obtained in this case have been summarized in Table XIX.

Table XIX - Action points obtained in the general case

AP	Δx (m)	Δv_n (m/s)	v_n (m/s)	a_n (m/s^2)
SDX	42,69	0,00	33,38	0,29
	39,64	0,00	31,69	0,22
	21,65	0,00	29,30	-0,19
	32,80	0,00	28,88	0,06
ABX	17,59	0,00	30,73	-0,28
	19,30	0,00	30,07	-0,24
	21,43	0,00	29,72	-0,19
	21,57	0,00	28,98	-0,19
CLDV	46,39	-4,56	34,35	-0,09
	28,88	-1,79	33,83	-0,20
	33,18	-1,89	31,94	-0,12
	21,61	-0,07	29,15	-0,20
OPDV	36,79	1,98	31,48	0,35
	28,00	1,77	29,13	0,13
	21,53	0,16	29,53	-0,17
	29,69	0,86	28,30	0,08

It is worth noting that selected APs respect the necessary conditions.

Appendix D – Estimation of the desired spacing by APs

Another important point to be addressed concerns the determination of the desired spacing (Δx_n^*), that is one of the crucial parameters of the state-space model, as a well as a crucial parameter of the drivers' behaviour. AP theory is useful for the purpose, in fact given the OPDVs and CLDVs a linear regression in the $\Delta x_n^t, \Delta v_n^t$ plane can be evaluated:

$$\Delta x_n^t = c\Delta v_n^t + d$$

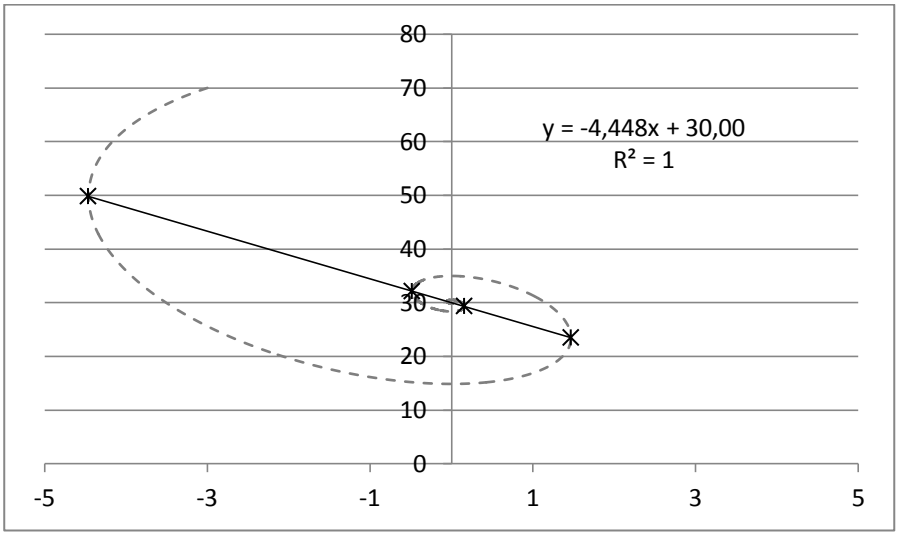

Figure 58 - Identification of the desired spacing in car-following (30 m, in the example)

Figure 58 shows the statements in the event of deterministically produced (example-oriented) data, with known Δx_n^* equal to 30 (m). It is observed that using the linear regression evaluated for $\Delta v_n^t = 0$, the Δx_n^* is obtained (in practice Δx_n^* is represented by the fixed term of the equation).

Considering the chart depicted in Figure 57, averaging over the CLDVs and OPDVs (reported in Table XIX), the obtained regression line is in that case:

$$\Delta x_n^t = -1{,}985\Delta v_n^t + 29{,}88$$

Even if the model response is perturbed by the leader's kinematic, a good estimation of the Δx_n^* can be obtained. In fact setting $\Delta v_n^t = 0$, it is obtained $\Delta x_n^* = 29{,}88 \approx 30$.

This method could be so used to obtain an estimation of Δx_n^* from observed car following data.

An interesting application of this procedure has been reported hereafter.

Experiments described Section 2.3 (point ii) give the possibility to observe trajectories with very low stimuli that allow to observe patterns with a very shape

behaviour (for an example refer to Figure 37). Evaluating the desired spacing in those trajectories an explanation of the dependency of the desired spacing from the actual speed can be investigated. As an example in the next Figure 59results of this methodology applied to trajectories described in Table XII have been plot with respect to leader's speed.

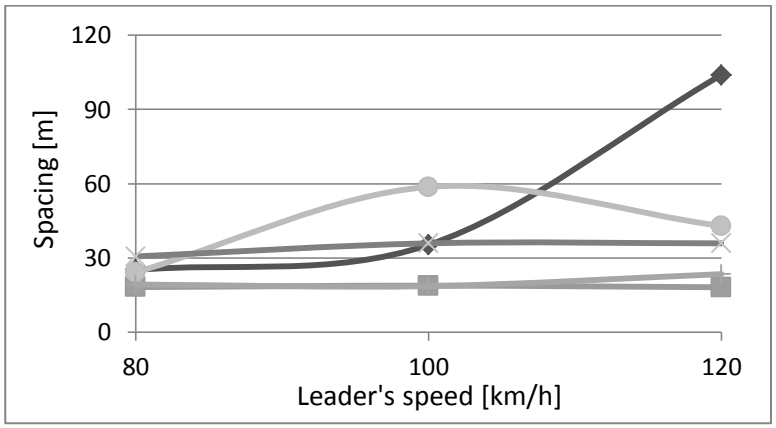

Figure 59 - An example of the dependency of the desired spacing from the actual speed

The given example does not give any significant representation of the phenomena, but has been showed only in order to stimulate the discussion with reference to this point and this *indirect* usage of experiments in Section 2.3 (point ii). Obviously this issue is not covered in the ambit of this thesis and will be left to further investigations.